IQGAP1 AS A MEDIATOR OF RAC1 P29S-DRIVEN MELANOMAGENESIS

Jaclyn C. Retallick

Department of Biochemistry

Goodman Cancer Research Centre

McGill University, Montreal

December 2020

A thesis submitted to McGill University in partial fulfillment

of the requirements of the degree of

Master of Science

Table of Contents

Abstract

Mutated in 5-10 % of cutaneous melanoma, RAC1 P29S is a fast-cycling GTPase that increases cellular migration *in vitro* while mediating metastasis *in vivo*. Still, how RAC1 P29S drives this behaviour remains unclear. Recent studies have suggested that enhanced actin polymerization and a unique phenotype of extended lamellipodia mediate a proliferative advantage associated with RAC1 P29S. Our lab has identified IQGAP1—a scaffold protein and actin remodeling regulator—as highly enriched in association with RAC1 P29S. On the basis of its involvement in cytoskeletal remodeling and proliferative signaling, we suspected that IQGAP1 may serve a pivotal role in the enhanced migratory phenotypes associated with RAC1 P29S. We hypothesized that if IQGAP1 is important for RAC1 P29S-driven migration and oncogenic signaling, then knocking down IQGAP1 would reduce RAC1 P29S-related activities. To interrogate this relationship, we performed reciprocal co-immunoprecipitation to validate the complex between IQGAP1 and RAC1 P29S, then isolated the active fraction of RAC1 P29S following siRNA-mediated IQGAP1 knockdown to reveal a stabilizing effect of IQGAP1 on the RAC1 P29S active state. In immortalized melanocytes expressing exogenous GFP, RAC1 WT, or RAC1 P29S, we probed the IFN response pathway, which has been upregulated in RAC1 P29S xenograft tumours, to reveal a complex regulatory role for IQGAP1 in RAC1 P29S signaling. Finally, we performed a series of proliferation and time-lapse random migration assays coupled with siRNA-mediated IQGAP1 knockdown. These conditions did not expose a great effect of IQGAP1 on proliferation; however, IQGAP1 knockdown consistently decreased the migration of melanocytes expressing RAC1 P29S. These results indicate a conserved role for IQGAP1 as a mediator of RAC1 P29S-driven melanomagenesis and suggest a greater involvement of IQGAP1 in the aggressively malignant character of RAC1 P29S-mutant melanoma. A thorough understanding of the mediatory role of IQGAP1 may guide the development of tools to disrupt RAC1 P29S contributions to melanomagenesis and improve treatments available for RAC1 P29S melanoma.

Résumé

Muté dans 5 à 10 % des mélanomes cutanés, RAC1 P29S est une mutant GTPase à cycle rapide qui augmente la migration cellulaire *in vitro* tout en médiant les métastases *in vivo*. Pourtant, la façon dont RAC1 P29S suscite ces phénotypes reste incertaine. Des études récentes ont suggéré que la polymérisation améliorée de l'actine et un phénotype unique de lamellipodes étendus médient un avantage prolifératif associé à RAC1 P29S. Notre laboratoire a identifié IQGAP1 – une protéine d'échafaudage et un régulateur de remodelage de l'actine – comme un partenaire de liaison hautement enrichi de RAC1 P29S par rapport à RAC1 de type sauvage. Sur la base de son implication dans le remodelage du cytosquelette et la signalisation prolifération, nous avons soupçonné que IQGAP1 peut jouer un rôle pivot dans les phénotypes migrateurs associés à RAC1 P29S. Nous avons émis l'hypothèse que si IQGAP1 est important pour la migration et la signalisation oncogénique pilotées par RAC1 P29S, puis knock-down de l'expression d'IQGAP1 réduira l'activité de RAC1. Pour interroger cette relation, nous avons effectué une co-immunoprécipitation réciproque pour valider l'interaction entre IQGAP1 et RAC1 P29S, suivi par un pull-down de la fraction de RAC1 P29S chargée en GTP lors d'un knockdown d'IQGAP1 médié par siRNA pour révéler s'il existe un effet stabilisateur de IQGAP1 sur l'état actif de RAC1 P29S. Dans les mélanocytes immortalisés avec surexpression exogène de GFP, RAC1 WT ou RAC1 P29S, nous avons examiné les voies de réponse IFN, qui sont régulées à la hausse dans les tumeurs de xénogreffe RAC1 P29S, pour révéler un rôle régulateur complexe de IQGAP1 sur la signalisation de RAC1 P29S. Enfin, nous avons effectué une série d'essais de prolifération et d'expériences de migration aléatoire time-lapse couplées avec knockdown d'IQGAP1 médiée par siRNA. Ces conditions n'ont pas révélé un grand effet d'IQGAP1 sur la prolifération ; cependant, le knockdown d'IQGAP1 a spécifiquement diminué la migration des mélanocytes exprimant RAC1 P29S. Ces résultats indiquent un rôle conservé pour IQGAP1 en tant que médiateur de la mélanomagenèse induite par RAC1 P29S et suggèrent une plus grande implication d'IQGAP1 dans le caractère agressivement malin du mélanome mutant RAC1 P29S. Une compréhension approfondie du rôle médiateur de l'IQGAP1 peut guider le développement futur de thérapies pour perturber les contributions de RAC1 P29S à la mélanomagenèse et améliorer le pronostic des patients atteints de mélanome RAC1 P29S.

Acknowledgments

I would like to thank my supervisor, Dr. Ian Watson, for offering me the incredible opportunity to pursue my graduate studies in his lab. The training and guidance I have received have greatly contributed to my growth as a scientist and as an individual beyond the lab. I have been fortunate to work on an exciting project that has very recently gained more widespread interest, and the rapidly expanding literature base has offered a valuable chance to integrate the latest international discoveries into the design of relevant, meaningful investigations. My experiences in this lab have immensely stimulated my ability to think critically and my independence as a researcher. I also thank my research advisory committee, Drs. Luke McCaffrey, Nicole Beauchemin, and Natalie Lamarche-Vane. It is immeasurably helpful to hear from other perspectives in regards to one's work, and I highly appreciate your thoughtful feedback and guidance.

I am very grateful to my past and present compatriots in the Watson lab. Not only are they exceptional scientists who are impassioned by their research, but their abundance of kindness and warmth fosters a dynamic, cooperative, and inclusive academic environment that keeps motivation high amid any obstacles that arise. Additionally, I would like to declare the specific contributions of Dr. Mathieu Lajoie to this manuscript, who kindly provided the frequency of RAC1 P29S within the 1000-exome dataset and compiled the RAC1 somatic mutation data from the TCGA-SKCM and 1000-exome datasets to produce the corresponding graphic shown in Figure 3.

I also received assistance from Miss Rebecca Deagle (MSc) of the McCaffrey lab, who coordinated setup of the confocal microscope for the image acquisition component of the random migration assays. She additionally demonstrated the basics of manual tracking when we were first getting the migration experiments up and running. I am very grateful for her enthusiasm and mentorship concerning microscopy and migration.

Furthermore, I would like to acknowledge the support I have received for my research project internally from the Faculty of Medicine and externally from the Natural Sciences and Engineering Research Council of Canada (NSERC). I am very fortunate to have been selected for scholarships from these sources, which have contributed tremendously to the funding of my graduate studies.

Finally, I would particularly like to thank Mr. Jeff Retallick (MSc) for his diligent editorial help on this thesis, and I must express my overwhelming gratitude to Cora Jackson (MA) and Amy Jackson for their swift proofreading at the eleventh hour. Furthermore, I would be remiss not to extend a special thank-you to all my loving family, dearest friends, and my beloved partner. The past two years have been filled with many highs and lows, and these precious people have held me up through even the most challenging of times. Their relentless support, encouragement, and strength have been the wind under the wings of this woman of science, and I thank them to infinity and beyond.

List of Figures

List of Tables

List of Abbreviations

ABI2: Abl Interactor 2
ABR: Active breakpoint cluster region-related protein
AID: Auto-inhibitory domain
AKT: Protein kinase B
AP-1: Activator protein-1
APC: Adenomatous polyposis coli
ARP2/3: Actin-related protein 2/3 complex
ATP: Adenosine triphosphate
AURKA: Aurora kinase A
AXIN: Axis inhibitor
BCL-2: B-cell lymphoma 2
BCR: Breakpoint cluster region protein
BRAF: B-Raf serine/threonine kinase
BRAFi: B-Raf inhibition
BSA: Bovine serum albumin
CDC42: Cell division cycle 42
CK1α: Casein kinase 1α
CLIP170: Cytoplasmic linker protein of 170 kDa
COSMIC: Catalogue of somatic mutations in cancer
CTLA-4: Cytotoxic T-lymphocyte protein 4
CYBA: Cytochrome b-245 alpha chain
CYBB: Cytochrome b-245 beta chain
Dbl: Diffuse B-cell lymphoma
DH: Dbl-homology
DHR1/2: DOCK-homology region 1/2
DMEM: Dulbecco's modified Eagle's medium
DOCK: Dedicator of cytokinesis
DVL: Disheveled
ECM: Extracellular matrix
EMT: Epithelial-to-mesenchymal transition
ER: Estrogen receptor
ERK1/2: Mitogen-activated protein kinase 1/2; extracellular signal-regulated kinase 1/2
ETS1: Ets proto-oncogene 1
F-actin: Filamentous actin
FAK: Focal adhesion kinase
FBS: Fetal bovine serum
FDA: Food and Drug Administration
FER: Fer tyrosine kinase
FZD: Frizzled
G-actin: Globular actin
GAP: GTPase-activating protein
GDI: Guanine nucleotide dissociation inhibitor
GEF: Guanine nucleotide exchange factor
GLUT4: Glucose transporter 4
GoF: Gain-of-function
GPCR: G-protein-coupled receptors
GRD: Ras GAP-related domain
GSEA: Gene set enrichment analysis
GSK3: Glycogen synthase kinase-3
GDP: Guanosine-5'-diphosphate

GTP: Guanosine-5'-triphosphate
GTPase: Monomeric G-protein
HACE1: HECT domain and ankyrin repeat containing E3 ubiquitin-protein ligase 1
HMEL: pMEL-BRAF V600E immortalized melanocytes
HPSC300: Hematopoietic stem/progenitor cell protein 300
IAP: Inhibitor of apoptosis protein
ICB: Immune checkpoint blockade
IFN-γ: Interferon-γ
IL-2: Interleukin-2
IQGAP1: IQ motif-containing GTPase-activating protein 1
JNK: c-Jun N-terminal kinase
JUN: c-Jun transcription factor
LEF: Lymphoid enhancer factor
LGR5: Leucine-rich repeat-containing G-protein coupled receptor 5
LIMK: LIM kinases
LoF: Loss-of-function
LPA: Lysophosphatidic acid
LRP5/6: Low-density lipoprotein receptor-related protein 5/6
mAb: Monoclonal antibody
MAP3K: MAP kinase kinase kinase
MAPK: Mitogen-activated protein kinase
MAPKi: Mitogen-activated protein kinase inhibition
MEK1/2: Mitogen-activated protein kinase kinase 1/2
MEKi: Mitogen-activated protein kinase kinase inhibition
MITF: Melanocyte-inducing transcription factor
MLK3: Mixed-lineage kinase 3
MMP: Matrix metalloprotease
MRTF: Myocardin-related transcription factor
mTOR: Mammalian target of rapamycin
mTORC1/2: mTOR complex 1/2
MYC: c-Myc transcription factor
NADPH: Nicotinamide adenine dinucleotide phosphate
NAP1: Nck-associated protein 1
NCF1/2/4: Neutrophil cytosolic factor 1/2/4
NF1: Neurofibromin 1
NF2: Neurofibromin 2; Merlin
NFAT1: Nuclear factor of activated T-cells 1
NFSM: Non-fat skim milk
NF-κB: Nuclear factor κ-light-chain-enhancer of activated B-cells
NLS: Nuclear localization signal
NO: Nitric oxide
NOS2: Nitric oxide synthase-2
NRAS: N-ras GTPase
p-: Phosphorylated; “phospho-”
pAb: Polyclonal antibody
PAK: p21-activated kinase
PBD: p21-binding domain

PBR: Polybasic region
PD-1: Programmed cell death protein 1
PD-L1/2: Programmed cell death ligand 1/2
PEI: Polyethylenimine
PH: Pleckstrin homology
PI3K: Phosphoinositide 3-kinase
PIAS3: Protein inhibitor of activated STAT3
PIP_2: Phosphatidylinositol (4,5)-biphosphate
PIP_3: Phosphatidylinositol (3,4,5)-triphosphate
PKC: Protein kinase C
P-loop: Phosphate-binding loop
pMEL-BRAF: pMEL-BRAF V600E immortalized melanocytes (HMEL)
pMEL-NRAS: pMEL-NRAS Q61L immortalized melanocytes
P-REX: Phosphatidylinositol (3,4,5)-triphosphate-dependent Rac exchanger
PTEN: Phosphatase and tensin homolog
PTM: Post-translational modification
RAC1: Ras-related C3 botulinum toxin substrate 1
RAS: "Rat sarcoma" family GTPases
Rho: Ras homology
RHOA: Ras homolog family member A
RHOGAP: GAP acting on Rho family GTPases
RHOGDI: Guanine nucleotide dissociation inhibitor acting on Rho family GTPases
RHOGDI1: ARHGDIα
RHOGDI2: ARHGDIβ
RHOGDI3: ARHGDIγ
RHOGEF: GEF acting on Rho family GTPases
ROCK: Rho-associated coiled-coil-forming kinase
RT: Room temperature
ROS: Reactive oxygen species
SDS-PAGE: Sodium dodecyl sulphate-polyacrylamide gel electrophoresis
SH3: Src homology 3
SNAI1: Snail family transcriptional repressor 1
SNV: Single nucleotide variant
SRA1: Specifically Rac1-associated protein-1
SRC: Src non-receptor tyrosine kinase
SRF: Serum response factor
SSH1: Slingshot-1
STAT3: Signal transducer and activator of transcription 3
STEF: Sif and TIAM1-like exchange factor
SUMO: Small ubiquitin-like modifier
SYK: Spleen associated tyrosine kinase
SYNJ2: Synaptojanin 2
TBC1D4: TBC1 domain family member 4
TCF: T-cell factor
TCGA: The Cancer Genome Atlas
TIAM1: T-cell lymphoma invasion and metastasis-inducing protein 1
TMB: Tumour mutational burden

TNF: Tumour necrosis factor

Trp53: Transformation-related protein 53

UV: Ultraviolet

UVB: Ultraviolet type B

VAV1: Vav guanine nucleotide exchange factor 1

WASP: Wiskott-Aldrich syndrome protein

WAVE: WASP family verprolin-homologous

WES: Whole-exome sequencing

WNT: Wingless-related integration site

WRC: WAVE regulatory complex

WRE: WNT-responsive elements

WT: Wild-type

β-PIX: PAK-interacting exchange factor-β

1 | Introduction

1.1 Literature review

I. Cutaneous melanoma

I.1 *Overview*

Cutaneous melanoma is a malignant neoplastic outgrowth of the melanocytes situated in the basal epidermis. Melanocytes are mesenchymal cells of neural crest lineage whose primary function within the epidermis is the secretion of eumelanin and pheomelanin, which are pigmented molecules that protect underlying tissue from ultraviolet (UV) radiation. Although melanocytes are not limited to the epidermis, the function of melanocytes at alternative organ sites is poorly understood and they give rise to melanomas that possess vastly different mutational landscapes and progression trajectories, which fall beyond the scope of this thesis. Cutaneous melanoma most frequently develops on sun-exposed regions and is characterized by having among the highest tumour mutational burden (TMB) of any cancer type[1,2]. UV exposure is a known environmental risk factor for melanomagenesis. Melanomas that arise on sun-exposed skin have a distinct enrichment of cystine to thymine (C>T) transitions at dipyrimidine sites, which is a hallmark of UV type B (UVB) mutagenesis[3,4]. Despite the vast mutational landscape of melanoma, only select recurrent mutation events result in oncogene gain-of-function (GoF) or tumour-suppressor loss-of-function (LoF) that confer a significant growth advantage. Among these mutations are those considered to be the predominant driver events of melanoma initiation and they serve as the genetic basis for cutaneous melanoma classification.

Cutaneous melanoma is classified into four genetic subgroups, dependent upon the Mitogen-activated protein kinase (MAPK) pathway component affected by a single-nucleotide variant (SNV) in its coding region: BRAF-mutant (50 %), RAS-mutant (30 %), NF1-mutant (15 %), and Triple-wild-type (Triple-WT; **Fig. 1**)[5]. BRAF driver mutations most often occur at the V600 locus, which is considered the most frequent somatic mutation hotspot in melanoma[6]. V600E is the most prominent BRAF mutation in melanomas of the trunk and extremities, which develop in patients 30-60 years of age. The BRAF V600K mutant is more prevalent in melanomas of chronically sun-exposed skin, developing in patients who are 70 years and older. In the case of the

RAS-mutant subgroup, RAS proteins are small GTPases with crucial and extensive roles in cellular signaling. RAS GoF driver events typically result in constitutive activation of the protein. NRAS is the RAS species most commonly implicated in melanoma. Oncogenic SNVs most commonly produce substitutions at the Q61 locus, which is the second leading somatic mutation

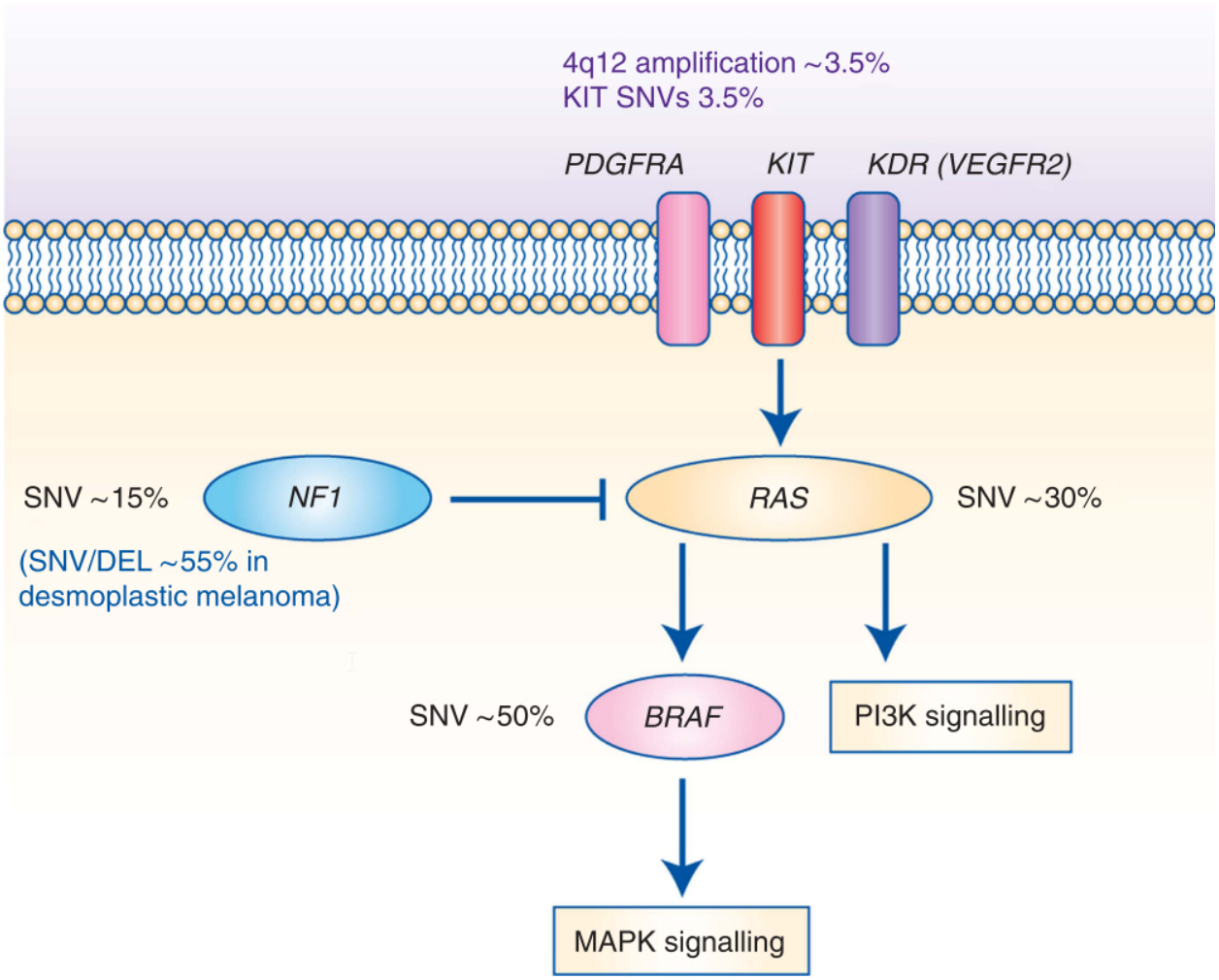

Figure 1 | Predominant driver events in melanomagenesis. Single nucleotide variants (SNVs) within MAPK pathway genes are well-established driver events in melanoma development that define the four genetic subgroups of melanoma: BRAF-mutant, RAS-mutant, NF1-mutant, and Triple-WT. In melanomas of the TCGA-SKCM cohort, 50 % harboured SNVs contributing to BRAF gain-of-function (GoF); these mutations were mutually exclusive with SNVs that led to RAS GoF, which were present in 30 % of melanomas. Loss-of-function (LoF) SNVs in *NF1*, a RAS suppressor, were identified in 15 % of melanomas. NF1 LoF is anti-correlated with BRAF GoF and has a low rate of co-occurrence with RAS GoF. Melanomas lacking SNVs in *BRAF*, *RAS*, or *NF1* were classified as Triple-WT and demonstrated a higher proportion of gene amplifications, including amplification of *KIT* amplicon 4q12. Reproduced from ref. [7] under CC BY-NC-SA 4.0.

hotspot in melanoma. These mutations are prevalent in melanomas of chronically sun-exposed areas, such as the skin of the head, neck, and distal limbs, that develop in individuals of 70 years and older[6]. BRAF V600 and NRAS driver events are mutually exclusive, which may be due in part to the distinct age groups and body regions where each is prevalent. The third genetic subgroup involves LoF of the tumour suppressor gene *NF1*, which is a GTPase activating protein (GAP) responsible for the negative regulation of RAS signaling. NF1 LoF occurs in approximately 15 % of melanoma samples analyzed by whole-exome sequencing (WES), and it is the most significantly mutated gene in desmoplastic melanomas of the head and neck[5]. NF1 LoF is significantly anticorrelated with concurrent BRAF V600 hotspot coding mutations, but not NRAS hotspot mutations, although co-occurrence is infrequent. The lack of anti-correlation with NRAS driver mutations could be a consequence of the shared sites and demographics affected by these melanomas. The three subgroups discussed above each bear a signature of UVB mutagenesis in >90 % of samples. However, as the fourth and final genetic subgroup of melanoma, Triple-WT melanomas lack a mutation in any of the three significantly mutated genes listed above, and only 30 % of samples display a strong UVB signature[7]. This subgroup is not unified by a predominant driver mutation, but these melanomas tend to have a higher proportion of gene amplifications, particularly of amplicons including *KIT* such as 4q12[5].

I.2 *Clinical treatment paradigms*

Melanoma is the deadliest form of skin cancer. Although it is only responsible for an estimated 1 % of skin cancer cases, it has a disproportionately high mortality rate. Incidence of this cancer has been on the rise for the past 30 years; between 1984 and 2015, incidence of melanoma has increased annually by 2.2 % and 2.0 % for men and women, respectively[8]. For cutaneous melanoma diagnosed in the US between 2009 and 2015, the 5-year survival rate of patients was 92 %[9]. In contrast, keratinocyte carcinomas (*i.e.* basal cell carcinoma and squamous cell carcinoma), which comprise the remaining 99 % of skin cancer cases, had 5-year survival rates ranging from 95-100 % depending on the stratum of origin[9,10]. The generalized melanoma survival statistics appear similarly high, but the stage of melanoma at diagnosis greatly influences the severity of prognosis. If melanoma is detected in the earliest stages of malignancy while it remains confined to its site of origin (*i.e.* localized; stage 0/I/II), it can be surgically resected very successfully and 5-year patient survival is 99 %[11,12]. Once it has become regionally invasive or

involves the regional lymph nodes (*i.e.* stage III), 5-year survival decreases to 65 %. As for melanoma that is highly metastatic and has invaded tissues of the lung, brain, liver, bone, or intestine (*i.e.* stage IV), 5-year survival plummets to 25 %[13]. Thus, despite the low mortality of cutaneous melanoma that is detected early and treated appropriately, late-stage disease can have very poor prognosis. Thus, the highest priority in melanoma research is the discovery of therapeutic strategies to improve management of advanced disease.

Historically, standard-of-care treatments for metastatic melanoma were primarily dacarbazine and interleukin-2 (IL-2). Dacarbazine, an alkylating agent, was approved by the Food and Drug Administration (FDA) in 1975 as a chemotherapeutic agent for treatment of advanced-stage melanoma. Systemic treatment with dacarbazine alone led to partial response in 15-28 % of cases and complete response in 3-5 % of cases, although <2 % of these responses sustained long-term remission beyond 6-8 months (reviewed in [14]). Now, as new therapies enter clinical trials, its longstanding status as a frontline treatment makes dacarbazine a common control arm within these studies. Another former frontline treatment of advanced melanoma is high-dose IL-2. Immunotherapies such as IL-2 are intended to prime the patient's immune system to improve antitumoural immune response. IL-2 itself is a T-cell growth factor that was approved by the FDA for treatment of metastatic melanoma in 1998[15]. As reviewed by Petrella *et al.*, high-dose IL-2 elicited objective responses in 5-27 % of patients, although only 0-4 % of these were complete responses[16]. Despite their rarity, only complete responses were durable—median response for complete responders was 27 months. Despite achieving durable responses in <5 % of patients, IL-2 treatment has been associated with very high toxicity. In a clinical trial pre-dating FDA-approval, toxicity profiles were reported for 270 patients treated with IL-2[17]. As per the National Cancer Institute common toxicity criteria, adverse events of severity grades 3 or 4 (*e.g.* hypotension, vomiting, diarrhea, and oliguria) occurred in 32-45 % of patients. An additional 2 % of patients died due to adverse toxic effects. Overall, these therapies were widely associated with severe toxicity and successful in only a small subset of patients, leading to an urgent demand for more efficacious therapies that would be less detrimental to patients' quality of life.

Clinical strategies for the treatment of metastatic melanoma have been revolutionized over the past decade with the emergence of precision medicine. In melanoma, such targeted approaches primarily involve inhibition of nodes along the frequently mutated MAPK pathway. Approved by

the FDA in 2011, vemurafenib is an inhibitor of BRAF that shows selectivity for BRAF V600 mutants over wild-type, and it was the pioneer drug in the evolving landscape of targeted therapies against melanoma. In a clinical study of patients with BRAF V600E/K melanomas, vemurafenib elicited an objective response rate of 48 %, in stark contrast with the 5 % objective response rate of the dacarbazine control arm[18]. Furthermore, median progressive-free and overall survival were each boosted by nearly 4 months (to 5.3 months and 13.6 months, respectively) with vemurafenib treatment relative to dacarbazine. Another BRAF mutant-selective inhibitor, dabrafenib, was approved by the FDA in 2013. Phase III trials demonstrated that dabrafenib elicited high overall response rates relative to dacarbazine (50 % vs. 7 %), and patients receiving this drug seldom experienced toxic events exceeding grade 2[19]. Additional trials demonstrated that dabrafenib also decreased or eliminated brain metastases, and it was widely effective in treating BRAF V600-mutant melanoma beyond only BRAF V600E[20]. Despite greater and more rapid overall responses upon BRAF inhibition in BRAF-mutant melanoma, resistance developed readily against these monotherapies, leading to eventual relapse. As an alternative to BRAF inhibition, MEK inhibitors such as trametinib have also been demonstrated to elicit higher response rates and improved survival relative to chemotherapy[21]. In fact, unlike BRAF inhibition, MEK inhibitors may be useful in genetic subgroups beyond BRAF-mutant melanoma; a phase III trial of MEK inhibitor binimetinib in NRAS-mutant melanoma has shown promising results where patient response rates and survival are improved relative to chemotherapy[22,23]. In BRAF-mutant melanoma, dual BRAF/MEK inhibition (*e.g.* vemurafenib plus cobimetinib or dabrafenib plus trametinib) has been implemented to target multiple nodes along the MAPK pathway to curb the onset of kinase inhibitor resistance. Administration of these inhibitors in combination boosts overall response by 20 % relative to BRAF monotherapy and significantly prolongs the duration of the response[24,25]. Despite the advantages of combination therapy, disadvantages such as increased toxicity and a higher incidence of grade 3 and 4 toxic events have also been reported.

Another key player to join the frontlines of late-stage melanoma therapy in the last decade has been immune checkpoint blockade (ICB), a new form of immunotherapy with potential pan-cancer applicability. The guiding principle of ICB leverages our understanding of tumour-mediated immune suppression via T-cell attenuation to prime a host's immune system to mount a more effective response against cancer cells. T-cells bear certain membrane receptors known as immune checkpoints that enable T-cell activity to be quickly attenuated for the prevention of

autoimmunity; however, tumours may exploit this innate machinery by expressing the cognate ligands to these receptors on the cancer cell surface. The recognition of these ligands by T-cells stimulates inhibitory signals that attenuate T-cell response and allow tumour cells to avoid detection and elimination[26]. The most well-studied immune checkpoints are cytotoxic T-lymphocyte protein 4 (CTLA-4), whose cognate ligands include CD80 and CD86, and programmed cell death protein 1 (PD-1), whose cognate ligands include programmed cell death ligand 1 (PD-L1) and PD-L2[27]. Monoclonal antibodies (mAb) against CTLA-4 (*e.g.* ipilimumab) and PD-L1 (*e.g.* nivolumab and pembrolizumab) have been approved by the FDA for the treatment of metastatic melanoma. The high mutational burden of melanoma across all four genetic subgroups makes it an ideal candidate for immune checkpoint therapy, as these neoplastic melanocytes are more likely to present neoantigens for T-cell recognition and subsequent elimination[28]. Indeed, when metastatic melanoma responds to ipilimumab treatment, patient 3-year survival rates can be boosted from 12.2 % to 20 %[29,30]. However, further investigations have demonstrated the superiority of pembrolizumab to ipilimumab as a frontline monotherapy, as they achieve 68-74 % survival and 58 % survival at 1 year, respectively[31]. Nivolumab has also emerged as a superior monotherapy to ipilimumab, achieving a 1-year survival rate of 42 % compared to 18 % with ipilimumab; however, administration of ipilimumab and nivolumab in combination further boosts 1-year survival to 49%, but it is associated with significantly higher toxicity[32]. Where combination therapy is considered, it will be critical to understand which genetic subgroups and mutational profiles of melanoma are most susceptible to such treatment to maximize benefit while minimizing risk.

I.3 *Identification of putative driver RAC1 P29S*

Even as promising new therapies shift clinical paradigms of metastatic melanoma and demonstrate remarkable improvements to patient survival, research continues unabated into additional pathways and targets that may be exploited by the next generation of therapies to further improve patient outcomes. Interestingly, the three predominant driver events used to stratify melanoma do not bear a UV signature themselves, despite the high TMB of cutaneous melanoma that is largely attributable to UV mutagenesis. Two research groups saw this disparity as an opportunity to identify novel driver events in melanoma—particularly those with SNVs consistent with UV irradiation. Historically, this had been very challenging on account of the abundance of

passenger mutations that heavily obscure which mutations, if any, positively contribute to the survival and fitness of the cancer. To search for new putative driver events that arise as a direct result of UV mutagenesis, Hodis *et al.* and Krauthammer *et al.* independently performed WES on 121 and 147 melanoma exomes, respectively, and each developed algorithms to accommodate the high TMB, which they used to discover many novel significantly mutated genes[33,34]. Among these, *RAC1* was revealed to harbour the third most frequent recurrent coding mutation hotspot following those in *BRAF* and *NRAS.* RAC activation assays confirmed that the c.85C>T hotspot mutation pattern produced a hyperactive RAC1 mutant with a proline to serine substitution at codon 29 (RAC1 p.P29S). Additional studies have indicated that this mutation is present in 5-10 % of melanoma and that it occurs across all four genetic subgroups, although there is a slight enrichment within the NRAS-mutant subgroup[33–35]. Further research efforts into RAC1 P29S-mediated melanomagenesis may reveal new actionable targets, which may in turn inform new therapeutic approaches that will be broadly applicable across genetic subgroups where RAC1 P29S is present.

II. RAC1 GTPase

II.1 *Ras superfamily of GTPases*

Small GTPases of the Ras superfamily, also known as monomeric G-proteins, function as binary molecular switches of receptor-mediated signal transduction (reviewed in [36]). As indicated by their name, these proteins are characterized by their ability to catalyze GTP hydrolysis; when bound to a GTP nucleotide, GTPases adopt their active conformation and are switched “on, enabling them to bind and activate downstream effectors to propagate a signal. When GTP is hydrolyzed to GDP, GTPases are switched “off” to an inactive state. The accompanying conformational change is incompatible with effector activation, thus terminating their capacity to stimulate signaling networks.

As GTPases are powerful tools for intracellular signal propagation, their cycling between active and inactive states is tightly regulated by three main classes of proteins: guanine nucleotide exchange factors (GEFs), GTPase-activating proteins (GAPs), and guanine nucleotide dissociation inhibitors (GDIs). GEFs bind their cognate GTPase to facilitate the exchange of GDP for GTP within the nucleotide-binding pocket of the GTPase. As such, GEFs are regulators that favour the active state. In contrast, GAPs promote GTP hydrolysis, converting GTP to GDP and thereby

inactivating the GTPase to attenuate signal transduction. Although GTPases possess some intrinsic catalytic ability, the presence of a GAP reduces the energy of activation required for the hydrolysis reaction to proceed, and thus shifts equilibrium to favour the GTPase inactive state. GDIs constitute another class of negative GTPase regulators and only affect a subset of Ras superfamily G-proteins[37,38]. Rather than causing the GTPase to cycle between active and inactive states, GDIs bind GTPases to prevent nucleotide hydrolysis and exchange, while simultaneously sequestering the GTPase in the cytosol. For signal transduction, GTPases must localize to the plasma membrane to be in proximity with their activators and downstream effectors. This localization is facilitated by post-translational lipid modifications to the C-terminus: specifically, prenylation of the CAAX tetrapeptide motif, and occasionally palmitoylation. To dissociate a lipid-modified GTPase from the plasma membrane, a GDI binds to the GTPase, then causes the C-terminal prenyl group of the GTPase to shift from its position in the plasma membrane into a hydrophobic pocket available within the GDI, thereby releasing the GTPase-GDI complex into the cytosol[37].

The Ras superfamily of GTPases is named for its founding members HRAS, KRAS, and NRAS, which have been extensively studied as oncoproteins[36]. Now, more than 150 related proteins have been identified and, consequently, the superfamily has been divided into 5 subfamilies: Ras, Rho, Ran, Rab, and Arf[36]. As the subfamily most pertinent to this thesis, the Ras homology (Rho) family includes 20 different genes, with *RAC1* (*Ras-related C3 botulinum toxin substrate 1*), *CDC42* (*Cell division cycle 42*), and *RHOA* among the most extensively characterized. Rho GTPases are broadly involved in cytoskeletal remodeling, cell polarity, vesicle transport, cell cycle progression, and gene transcription[39]. Due to their role in vesicle transport, they are prime targets for bacterial toxins; through covalent modification, they can be inactivated to prevent phagocytosis of pathogenic bacteria[40]. Indeed, RAC1 was originally discovered in 1989 and named for its susceptibility to ADP-ribosylation at residue N41 by botulinum toxin C3[41,42]. Rho GTPases are highly homologous proteins with cooperative functions within the cell, particularly with respect to the cytoskeleton. In the context of actin remodeling at the cell periphery, RAC1 is responsible for the formation of sheet-like lamellipodia and membrane ruffles, CDC42 coordinates thin filopodial protrusions, and RHOA organizes contractile actomyosin stress fibers and focal adhesion complexes[43,44].

The structural core of all Ras GTPases is the G domain, which is comprised of a six-stranded ß-sheet accompanied by five α-helices. This structure provides the framework for five conserved loop-associated motifs that align with the nucleotide-binding pocket, referred to as G boxes and labelled G1-G5, which are involved in guanine nucleotide exchange, hydrolysis, and GTP-induced conformational change[45,46]. However, Rho family GTPases uniquely share a 13 amino acid helical insert region between ß-sheet 5 and α-helix 4 that distinguishes them from other subfamilies[47]. This region often functions to strengthen and confer additional specificity to interactions between Rho proteins and certain binding partners, such as GEF and GDI regulatory proteins and IQ motif-containing GTPase-activating protein 1 (IQGAP1) and IQGAP2 actin cytoskeleton coordinators[48–50]. Other times, the insert region does not greatly influence effector binding but is essential for the activation of downstream effectors; such is the case for NADPH oxidase and Rho-associated coiled-coil-forming kinase (ROCK)[51,52]. The focus of this thesis will be RAC1, which is a member of the Rho family as part of the Rac subfamily, alongside other members RAC2, RAC3, and RHOG.

II.2 *RAC1 protein structure*

RAC1 possesses the G domain that is characteristic of Ras superfamily GTPases, as well as the Rho family-specific insert region that elongates the G domain by 13 amino acids and a C-terminal polybasic region (PBR). The G1 motif of the G domain, also known as the P-loop or phosphate-binding loop, is located N-terminally and includes residues 10-17[45,47]. This motif engages with the α- and ß-phosphates of a guanyl nucleotide to stabilize purine binding. The G2 and G3 motifs span residues 32-40 and 53-60, respectively. G2 constitutes a large portion of the effector binding interface, whereas G3 is crucial for stabilizing the nucleotide-associated Mg^{2+} ion—an important cofactor in GTP hydrolysis[45,46,53]. Next, the G4 motif spans residues 111-118 and immediately precedes the insert region, while the G5 motif covers residues 158-160[45,47].

The structure of RAC1 includes two switch regions that are crucial for interacting with binding partners: switch I spans residues 25-39, while switch II spans residues 57-75[54]. These regions are termed as such because the switch-like behaviour of GTPases depends upon the conformational changes of these regions when bound to GTP or GDP. Switch I and II have considerable overlap with G boxes G2 and G3, respectively[55]. The switch regions are critical for interaction with effectors through hydrogen bonding, electrostatic and pi-stacking forces, and they

may interdigitate with the pleckstrin homology (PH) domain of an effector[56]. These switches are also crucial for the binding and action of regulatory proteins[54,57].

As mentioned previously, Rho family GTPases share a helical insert region that distinguishes them from other subfamilies. In the RAC1 polypeptide sequence, this region spans residues 123-135[58]. In other Rho family members, this insert region has been necessary for cellular transformation and downstream effector activation. In the case of RAC1, mutants lacking the insert region maintained their transformative capacity, although they lost the ability to coordinate membrane ruffling and lamellipodia formation by the Serum response factor (SRF) signaling axis[58,59].

Finally, the C-terminal PBR of RAC1 (^{183}KKRKRK) is involved in subcellular localization and association with RAC1 effectors and regulators. The RAC1 CAAX box motif immediately follows the PBR and it is a substrate for geranylgeranyl lipid modification to anchor RAC1 to the plasma membrane in the absence of a dedicated membrane-associated domain. The RAC1 C-terminus additionally contains a proline-rich stretch that is compatible for interaction by the Src homology 3 (SH3) domain of RAC1 regulators, such as PAK-interacting exchange factor-β (β-PIX), a GEF of RAC1[60]. The PBR itself stabilizes membrane localization through dipole-dipole interactions with negatively charged membrane lipids such as phosphatidyl inositol (4,5) biphosphate (PIP_2) and PI(3,4,5)-triphosphate (PIP_3)[61]. Unlike other Rho GTPases, the RAC1 PBR also houses a nuclear localization signal (NLS) for interaction with nuclear shuttling proteins to promote its nuclear translocation, where it is involved in transcriptional regulation and cell cycle progression[62].

II.3 *Biological effects of RAC1*

As a ubiquitously expressed small GTPase, RAC1 signaling is integrated into many diverse pathways within the cell. RAC1 has been most extensively studied for its influence on actin dynamics and cell motility by enhancing actin nucleation, stabilizing actin filaments, and strengthening cell junctions. However, the signals propagated by RAC1 are not limited to cytoskeletal programs. For instance, RAC1 directly binds and activates p21-activated kinases (PAKs), which not only stimulate a signaling cascade that stabilizes actin filaments, but they also promote MAPK signaling through activation of RAF, MEK, and ERK, in addition to activation of

AKT signaling, both of which converge to stimulate cellular proliferation and survival[63–66]. Additionally, RAC1 can translocate to the nucleus, where it is involved in cell cycle regulation and contributes to transcription of WNT-dependent genes[67–70]. RAC1 also facilitates cellular glucose uptake to drive adenosine triphosphate (ATP) production, and it engages with enzymes that generate reactive oxygen species (ROS) to promote local inflammation and immune response, as well as intracellular redox and NF-κB signaling[71].

II.3.1 Cytoskeletal rearrangement

One of the primary functions of RAC1 is to stimulate reorganization of the actin cytoskeleton. This itself is an intermediary process necessary to drive many different cellular functions, and thus it can elicit a wide array of diverse outcomes such as the formation of lamellipodia, cellular migration, establishment of cellular junctions, and vesicle trafficking. Early studies of RAC1 function applied purified wild-type RAC1 and constitutively active mutant RAC1 G12V to 3T3 fibroblasts, which almost immediately prompted formation of lamellipodia[44]. Lamellipodia are actin-rich cytoplasmic extensions for cell locomotion and membrane ruffling—a phenomenon where rapidly polymerizing actin filaments accumulate at the plasma membrane. Furthermore, RAC1-driven actin polymerization strengthens adherens junctions by co-localization with E-cadherin at sites of cell-cell contact[73].

II.3.1.1 *Mechanisms of actin remodeling by RAC1*

Two predominant mechanisms have emerged for RAC1-driven actin remodeling. In the first mechanism, active RAC1 engages downstream components responsible for the nucleation of actin filaments, a critical step in the assembly of polymerized filamentous actin (F-actin) from monomeric globular actin (G-actin). To this effect, active RAC1 must bind the WAVE regulatory complex (WRC), which is a heteropentamer consisting of a Wiskott-Aldrich syndrome protein (WASP)-family verprolin-homologous (WAVE) protein, along with proteins Specifically Rac1-associated protein-1 (SRA1), Nck-associated protein 1 (NAP1), Abl interactor 2 (ABI2), and Haematopoietic stem/progenitor cell protein 300 (HSPC300)[74,75]. WAVE family proteins possess domains for simultaneous binding to a G-actin monomer and the Actin-related proteins 2/3 (ARP2/3) complex—a major nucleator of branched actin—and thus facilitate polymerization of actin filaments in conjunction with ARP2/3 nucleation[76]. WAVE exists in an inhibited

conformation within the WRC until activated by an appropriate stimulus; cryo-electron microscopy of crystallized WRC-RAC1 has revealed two distinct binding sites for active RAC1 within the complex, and simultaneous binding of RAC1 at both sites may stimulate higher WRC activation than when binding occurs at just one site[75]. Thus, RAC1 stimulates increased branched actin polymerization in a concentration-dependent manner through engagement with the WRC and ARP2/3.

The second mechanism by which RAC1 influences actin remodeling is through the relief of F-actin inhibition, enabling the accumulation of actin filaments. Specifically, active RAC1 first stimulates its immediate effector PAK. PAK serine/threonine kinases, in turn, phosphorylate LIM kinases (LIMK), which directly phospho-inactivate cofilin[77]. Cofilin is responsible for rapid actin de-polymerization, the conversion of F-actin to G-actin subunits to replenish the pool of G-actin needed to sustain dynamic actin remodeling. By inactivating cofilin, the inhibitory effect on F-actin polymers is relieved and F-actin may accumulate more easily. Taken together, these two mechanisms allow active RAC1 to regulate the actin cytoskeleton by stimulating rapid actin polymerization and halting factors that would otherwise counter this action.

II.3.1.2 *Migration*

RAC1 and other Rho GTPases are key components of cellular migration machinery. Mesenchymal migration relies on the cooperation of two distinct processes: the RAC1- and CDC42-driven manifestation of actin-rich protrusions at the leading edge of the cell in tandem with actomyosin contractility to drive translocation of the rear of the cell as governed by RHOA. As RAC1 and CDC42 work synergistically to coordinate forward movement, most literature suggests that the lamellipodia formed by RAC1 via ARP2/3 activity are the primary driver of directionally persistent movement, while CDC42 localizes to the periphery of the leading edge and is involved in directional sensing, using its ARP2/3-independent filopodia to fine-tune the directional path of the cell[79]. There is conflicting evidence from select model systems as to whether the migration driven by each RAC1 or CDC42 is primarily random or persistent, and as such this may vary based on cell type[80]. However, the significance of RAC1 in mesenchymal migration is underscored by the observation that dominant-negative mutant RAC1 T17N severely reduces migration rate, whereas cells expressing a dominant-negative CDC42 mutant continued to migrate at elevated speeds but lost the ability to chemotax along a gradient[81].

To establish polarity, migratory cells require recruitment of microtubules to the leading edge of the cell, which occurs as RAC1 and CDC42 recruit the IQGAP1 scaffold to front of the cell. There, IQGAP1 in complex with microtubule elements Cytoplasmic linker protein of 170kDa (CLIP170) and Adenomatous polyposis coli (APC) assists in the capture of microtubule plus ends to orient the cytoskeleton and cellular organelles along the polarized axis of a migrating cell[82].

Extensive negative feedback loops and crosstalk between RAC1 and RHOA facilitate the separation of their disparate spatiotemporal activities[78]. A series of positive feedback loops at the leading edge drive RAC1 activation to stimulate the elongation and branching of actin at the cell front, which correlate with fast and persistent migration, respectively[83]. These are accompanied by negative feedback loops that conversely inhibit RAC1 or the ARP2/3 complex at the cell rear to allow dynamic actin retraction and de-polymerization to keep pace with the forward movement of the cell. These antagonistic feedback mechanisms allow migration to proceed in an oscillatory manner; in the case of excess active RAC1, this regulation becomes interrupted and aberrant RAC1 signaling can shift a cell's intrinsic migratory mode from directionally persistent to a random walk, accompanied by a slight increase in velocity[84].

Many fundamental principles of single-cell migration are also appliable to collective cellular migration, a similar migratory process where sheets of cells migrate as a cohesive unit for tissue development and wound healing (reviewed in [85,86]). Cells within these collectively migrating sheets fall into one of two categories: they can be leader cells, which are prominent at the forefront of the collective and behave similarly to single cells engaged mesenchymal migration, possessing the same front-rear polarity and spatiotemporally regulated Rho GTPase activity; or they can be follower cells, which maintain strong intercellular junctions between themselves and other cells in the collective sheet as they are pulled forward by the leader cell. Leader cells are also responsible for interaction with and degradation of the extracellular matrix (ECM) as necessary, as well as reception of extracellular signals to modulate directional sensing and orientation along a gradient of stimulus. Additionally, in select cases, follower cells can contribute to chemotaxis by establishing a localized gradient. For instance, in melanoma, melanocytes are able to generate their own gradient to drive positive chemotaxis in an otherwise homogeneous solution; they are able to break down lysophosphatidic acid (LPA), an active component in serum, to decrease its relative proximal concentration and thus establish a chemoattractant gradient[87]. Furthermore, specialized

cytoplasmic structures may mediate leader-follower contacts in certain cell types. It has been demonstrated in endothelial cells that "cadherin fingers" (*i.e.* thin membrane protrusions rich in VE-cadherin) extend behind a leader cell and are engulfed within the cytoplasm of the follower cell[88]. Insertion of these cadherin fingers greatly increases the surface area available for adherens junctions between leader and follower cells, and it improves the capacity of leader cell rear contractility to pull follower cells along. Collective migration is generally slower than single-cell migration, but it confers improved directionality; as many leader cells must cooperate to move along the gradient, the influence of lamellipodia that protrude out of alignment with the gradient is dampened and the predominant direction of locomotion at any moment in time is more likely to be carefully directed along the gradient.

In addition to its role in coordinating actin polymerization at the front of single and collectively migrating cells, RAC1 is able to stimulate actin reorganization at the nuclear envelope to induce reorientation of the nucleus during migration. A contractile structure known as the actin cap is a cytoskeletal organelle responsible for regulating nuclear morphology and mechanotransduction in coordination with cell polarization and migration. Sif and TIAM1-like exchange factor (STEF) is a GEF that is recruited to the perinuclear envelope, where it mediates RAC1 activity. MEFs with *STEF* knockout exhibit fewer perinuclear actin cables, a phenotype that is partially rescued by re-induction of STEF expression or a constitutively active RAC1 G12V construct with an introduced KASHext domain to direct perinuclear localization[89]. As such, RAC1 recruitment and activation at the nuclear envelop maintains and adjusts nuclear morphology for efficient migration.

II.3.1.3 *Adherens junctions*

Live-imaging of recombinant RAC1-GFP protein in MDCK cells has revealed that upon collision of single migratory cells *in vitro*, RAC1-GFP localizes to the site of cell-cell contact and drives an increase in lamellipodia formation at that site, coupled with rapid polymerization of cortical actin[72]. Indeed, RAC1-driven actin polymerization strengthens adherens junctions by co-localizing with E-cadherin to cell-cell contacts, thus increasing the relative abundance of active RAC1 available at the plasma membrane to stimulate the WRC and ARP2/3 complexes for actin nucleation[73]. RAC1 also promotes adherens junctions by preventing IQGAP1 from destabilizing their intracellular assembly. IQGAP1 is a multi-domain scaffold protein and a known interactor of

GTP-bound RAC1. Although IQGAP family proteins possess a Ras GAP-related domain (GRD), it is inert as a GAP and instead stabilizes Rho GTPases RAC1 and CDC42 in their GTP-loaded forms[90]. In the context of cadherin-mediated adherens junctions, IQGAP1 localizes to the plasma membrane and interacts with β-catenin at these sites. β-catenin is an integral component of the intracellular assembly of adherens junctions through its function as an adapter between cadherin proteins and α-catenin, which itself is a link between the cadherin complex and the actin cytoskeleton to strengthen the intercellular junction[91]. Through interaction with β-catenin, IQGAP1 promotes its dissociation from α-catenin, effectively downregulating cadherin-mediated cell-cell junctions. However, when active RAC1 is present, it binds IQGAP1 and precludes interaction of the scaffold with β-catenin, allowing adherens junctions to evade this form of suppression[92]. The RAC1-IQGAP1 interaction further enhances cadherin-based junctions as their interaction leads to IQGAP1-mediated actin-crosslinking at the site to inhibit clathrin-dependent endocytosis of E-cadherin that would otherwise recycle it from the plasma membrane[93–95].

II.3.1.4 *Crosstalk between Rho GTPase cytoskeletal reorganization*

Despite the insights gained into RAC1's function as a coordinator actin remodeling, it has also been shown to coordinate certain actomyosin activity that would typically be associated with other Rho family members. For example, when microinjected into MDCK cells, RAC1 G12V stimulated an increase in stress fibers and focal adhesions[40]. Use of dominant-negative mutant RAC1 T17N revealed that this occurred by RAC1-mediated stimulation of a RHO isoform, which is recognized for its role in actomyosin contractility. By experimenting with diverse stimuli, researchers observed that RAC1 was a critical intermediary for mediating such stress fiber accumulation upon stimulation by growth factors or bombesin, whereas stress fiber formation following LPA stimulation occurred by a RAC1-independent mechanism[43]. These observations suggest a degree of crosstalk and interdependency between Rho family GTPases, despite their apparently distinct roles pertaining to cytoskeletal dynamics within the cell.

II.3.1.5 *Vesicle Trafficking*

RAC1-driven actin polymerization has been implicated in a number of endo- and exocytotic pathways (reviewed in [96]). For instance, early research into this topic revealed that microinjection of hyperactive RAC1 G12V into Rat2 cells stimulated membrane ruffling coupled

with internalization of extracellular fluid by macropinocytosis[44]. Macropinocytosis is a predominant mechanism governing the uptake of extracellular vesicles; biomedical engineers have taken a recent interest in this mechanism for its promise as a new delivery vehicle for therapeutics[97]. RAC1 has also been implicated in phagocytosis, where it contributes to the formation of the phagocytic cup. Incidentally, it also contributes to ROS-mediated killing of engulfed microorganisms within the phagosome (reviewed in section II.3.4)[98]. RAC1 is also involved in clathrin-independent endocytosis to mediate the internalization of signaling proteins, such as IL-2 receptor beta, at the plasma-membrane[99]. Furthermore, RAC1 inhibits clathrin-mediated endocytosis, a common mode of endocytosis that relies upon the organization of clathrin triskelions in a cage-like formation around budding vesicles. Such clathrin assembly is dependent upon PIP_2 at the plasma membrane; this is disrupted when active RAC1 recruits its direct effector Synaptojanin 2 (SYNJ2)—a phosphatase of PIP_2—to the plasma membrane[100]. In terms of exocytotic pathways, RAC1-driven actin polymerization drives translocation of glucose transporter (GLUT) storage vesicles to the plasma membrane in fat and muscle tissue (reviewed in section II.3.5), as well as the secretion of Tumour necrosis factor (TNF) in macrophages to stimulate an inflammatory response, among other functions[101]. Furthermore, the RAC1 interactor IQGAP1 has been demonstrated to localize to sites of secretory vesicle fusion[102]. As this scaffold has domains for direct binding to F-actin and is indirectly linked to the microtubule network through the CLIP170 adaptor, it seems to mediate a cooperative engagement of both cytoskeletal frameworks during exocytosis. The researchers involved in this discovery suggest that IQGAP1 itself is likely recruited to these sites by a factor other than actin—quite possibly, then, active RAC1 facilitates its localization to these sites.

II.3.2 Effector signaling in proliferation, survival, and the cell cycle

Many proliferative pathways are mediated by RAC1 activity and its subsequent engagement of kinase signaling cascades, its nuclear translocation and direct interaction with transcription machinery, and its indirect regulation through actin cytoskeletal dynamics.

A predominant class of RAC1 effector kinases are PAKs, which are subdivided into two groups. PAKs share three common domains: a p21-binding domain (PBD), an auto-inhibitory domain (AID), and a kinase domain. Inactive group I PAKs (*i.e.* PAK1-3) form trans-autoinhibited homodimers. Binding to RAC1 stimulates a conformational change that induces PAK trans-

autophosphorylation and reorients the AID, restoring the catalytic function of the kinase domain[103]. To enhance RAC1 recruitment and activation, group I PAKs have a conserved region for binding to β-PIX, a RAC1-specific GEF. Group II PAKs (*i.e.* PAK4-6) are thought to exhibit constitutive kinase activity, although their AID-like regions may form a pseudosubstrate to impair kinase catalytic function until they are bound by an activating GTPase, particularly CDC42[103].

PAKs stimulate many signaling cascades within the cell, such as those involved in actin cytoskeletal dynamics, motility, and invasion, but they also communicate with proliferative, survival, and cell cycle pathways (summarized in **Fig. 2**). For instance, the PAK/LIMK/p-cofilin signaling axis discussed previously in section II.3.1.1 also acts to inhibit MYC. MYC (or c-Myc) is a transcription factor that can promote proliferation or terminal differentiation, depending on the cellular context[104]. LIMK/p-cofilin signaling leads to a decrease in phosphorylation of Signal transducer and activator of transcription 3 (STAT3)—a regulator of MYC—thus inhibiting MYC expression[105]. PAKs can also activate members of MAPK pathways to drive downstream activation of genes for cell cycle entry and survival. PAK1 and PAK3 directly phosphorylate C-RAF and MEK1/2 of the RAF/MEK/ERK pathway, while PAK1 additionally enhances phospho-activation of MEK1/2 and ERK signaling by a kinase-independent mechanism[106–108]. In a separate MAPK pathway, RAC1 can mediate activation of MAP3K11 and downstream activation of p38MAPK to upregulate inflammatory genes with and without PAK cooperation[109–111].

In terms of cell cycle regulation, RAC1 and PAKs play important roles in the coordination of mitotic entry. In the late G2 phase, RAC1 mobilizes to the centrosomes, where it recruits PAKs to phosphorylate Aurora kinase A (AURKA) and promote centrosome maturation[112,113]. Furthermore, PAK4 organizes mitotic spindles for chromosome alignment and segregation into daughter cells[114]. Nuclear entry of RAC1 itself is also coordinated with cell cycle progression. Beginning in early G1 phase, RAC1 is excluded from the nucleus, persisting up until the late G2 phase. Michaelson *et al*. have demonstrated that RAC1 nuclear cycling is necessary for mitotic entry; when constitutively active RAC1 was expressed without its NLS, it was limited to the cytoplasmic compartment and the mitotic index of NIH/3T3 cells was reduced. In contrast, expression of constitutively active RAC1 with boosted nuclear import significantly increased the rate of mitosis[68].

Many PAKs possess one or more NLS for translocation to the nucleus, where they affect chromatin remodeling and can act as co-activator or co-repressor in response to hormone and growth factor signaling (reviewed in [115]). For example, PAK1 can phosphorylate Snail family transcriptional repressor 1 (SNAI1), a transcription factor that represses E-cadherin expression and mediates epithelial-to-mesenchymal transition (EMT), thereby increasing SNAI1 nuclear accumulation and repressive function[116]. EMT is an important developmental mechanism, but spatiotemporally inappropriate EMT pathway activation (*i.e.* by hyperactive PAK1) can promote oncogenesis. Additionally, PAK1 can interact with the promoter and coding sequences of the *Nuclear factor of activated T-cells 1* (*NFAT1*) gene, repressing its transcript; in contrast, RAC1

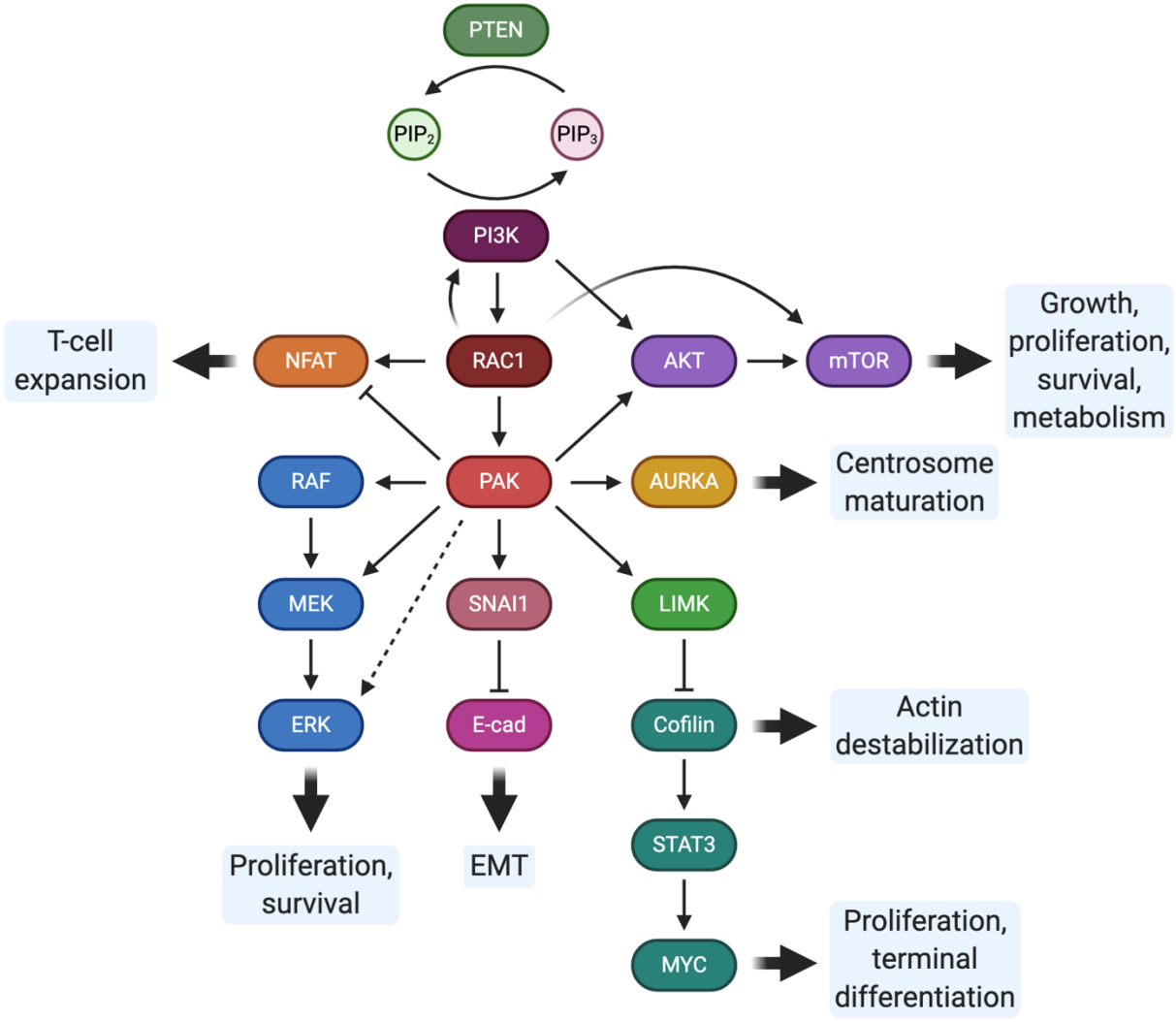

Figure 2 | An overview of the RAC1/PAK signaling axis. RAC1 is known to stimulate effector PAKs to propagate downstream signaling to modulate diverse outcomes such as proliferation, survival, EMT, differentiation, and actin dynamics. Schematic created using BioRender.com.

mediates the subcellular localization of NFAT family transcription factors to the nucleus and stimulates transcription of their regulon—by this process, RAC1 can stimulate T-cell clonal expansion[117]. These opposing mechanisms are suggestive of inhibitory crosstalk between RAC1 signaling pathways to maintain tight regulation of key proliferative programs.

A common activating stimulus for RAC1 signaling is Phosphoinositide 3-kinase (PI3K), which catalyzes PIP_2 phosphorylation to PIP_3 in response to an extracellular signal. Phosphatase and tensin homolog (PTEN), a tumour suppressor, is a phosphatase of PIP_3 that works in opposition to PI3K by catalyzing reconversion of its lipid substrate to PIP_2[118]. Two arms of PI3K signaling include the recruitment of protein kinase AKT to the plasma membrane for activation, which proceeds to stimulate Mammalian target of rapamycin (mTOR) signaling for growth, proliferation, survival, and insulin-dependent metabolism[119]; and PIP_3-mediated recruitment of RAC1 and associated GEFs to activate RAC1 signaling. But there is a considerable amount of crosstalk and redundancy between PI3K/AKT and RAC1 signaling. For example, RAC1/PAK signaling can activate AKT by a separate mechanism to further potentiate AKT signaling. Additionally, regardless of the RAC1 active state, RAC1 can drive activation of mTOR signaling independently from AKT through direct interactions with mTOR complex 1 (mTORC1) and mTORC2 that aid the localization of these components[120]. Interesting, it has also been suggested that Rho GTPases can act upstream of PI3K in a positive feedback loop. Indeed, Rho GTPases RAC1 and RHOG of the Rac subfamily cooperate with CDC42 to indirectly drive PI3K activation[121]. This occurs by a mechanism distinct from the well-characterized RAS-driven PI3K activation, where RAS isoforms would activate the p110 catalytic subunit of PI3K independently from the p85 regulatory subunit[122]. In addition, Fritsch and colleagues have demonstrated that GTP-bound RAC1 can also directly bind and activate the p110β catalytic subunit of the PI3Kβ heterodimer as another mechanism to promote PI3K/AKT/mTOR signaling[123].

In summary, RAC1 acts upstream of a vast and interconnected signaling network to regulate proliferative and mitotic signal transduction pathways. Many additional signaling pathways leverage RAC1 signaling to achieve diverse outcomes. These pathways will be discussed in greater depth within the following sections.

II.3.3 Development

RAC1 plays an indispensable role in embryological development and morphogenesis, and its inactivation causes embryonic lethality in mice[124]. Specifically, embryos fail because RAC1-driven convergent extension through adhesion dynamics and lamellipodial protrusion is necessary for establishment of the three germ layers during gastrulation; otherwise, cells of the mesodermal layer arrest development. Vertebrate gastrulation is considered to be under the control of WNT signal transduction, named for the homologous *Wingless* (*wg*) gene in *Drosophila* in combination with the gene's original name of *Integration-1* (*INT-1*)[125]. RAC1 participates in canonical WNT signaling and thus contributes to cell fate determination and limb outgrowth in early embryogenesis[126,127], although the underlying mechanisms require further investigation. This section of the thesis describes current efforts and models for RAC1 involvement in canonical WNT signaling. This is followed by discussion of RAC1 in noncanonical WNT signaling, which governs cell polarity and migration to drive morphogenic processes such as gastrulation[127].

WNT family proteins are secreted growth factors that modulate a series of pathways governing embryological development, proliferation, differentiation, and adult tissue homeostasis[128,129]. Aberrant activation of WNT pathways can contribute to the development of many different cancers[130,131]. WNT pathways are broadly characterized into two branches: canonical WNT/β-catenin signaling and non-canonical WNT signaling. In canonical WNT signaling, WNT ligand recognition stimulates transcriptional changes by enhancing nuclear accumulation of β-catenin (reviewed in [132,133]). In the absence of a WNT ligand, cytosolic β-catenin is readily degraded. It is captured by a destruction complex composed of scaffold proteins Adenomatous polyposis coli (APC) and Axis inhibitor (AXIN), as well as protein kinases Glycogen synthase kinase-3 (GSK3) and Casein kinase 1α (CK1α), which ultimately targets β-catenin for polyubiquitination and subsequent proteasomal degradation. However, when a WNT ligand binds to heterodimerized co-receptors Frizzled (FZD) and Low-density lipoprotein receptor-related protein 5 or 6 (LRP5/6), the activated co-receptors recruit Dishevelled (DVL) for binding to LRP5/6. Then, DVL binds AXIN and mediates recruitment of the destruction complex to LRP5/6 to attenuate β-catenin degradation. Thus, β-catenin becomes available for two of its primary localizations: the plasma membrane, where it stabilizes cell junctions, and—most importantly for WNT-signaling—the nucleus, where it serves as a co-repressor and co-activator

to T-Cell Factor/Lymphoid Enhancer Factor (TCF/LEF) transcription factors at WNT-responsive elements (WREs) to modulate expression of WNT-responsive genes.

Although WNT/β-catenin signaling has been studied extensively, the mechanisms behind β-catenin translocation to the nucleus have remained a mystery. β-catenin itself lacks an NLS for nuclear entry and no single protein has been presented as a compelling adaptor. In an effort to address this uncertainty, researchers noted the ability of constitutively active RAC1 G12V to increase TCF-activated transcription, whereas dominant-negative RAC1 T17N inhibited TCF-activated transcription[134]. They demonstrated that active RAC1 accumulates in the nucleus where it associates with both β-catenin and TCF, and that RAC1 hyperactivity and β-catenin overexpression operate synergistically to promote TCF-activated transcription[134]. This synergy was reliant on the intact C-terminal PBR of RAC1, which houses its NLS[62]. Thus, a hypothesis emerged that phosphorylated β-catenin is shuttled into the nucleus in a complex with RAC1, which is supported by evidence that RAC1 undergoes nuclear import in complexes with proteins that, like β-catenin, possess an armadillo domain[62]. More recently, conflicting evidence has been presented by Jamieson *et al.*, who reported that although RAC1 hyperactivity could drive WNT-dependent gene expression in the presence or absence of a WNT stimulus, it had only a modest effect on β-catenin localization in the presence or absence of WNT pathway activation, likely because β-catenin can mediate its own nuclear shuttling by direct interaction with the nuclear pore complex[67,135].

Another team proposed an alternate mechanism involving RAC1 for nuclear transport of β-catenin. They observed that active RAC1 formed a cytosolic complex with β-catenin, c-Jun N-terminal kinase 1 (JNK1) and JNK2, wherein upon activation by a WNT ligand, JNK2 became phosphorylated within the complex[126]. Phospho-JNK2 then phosphorylated residues S191 and S605 of β-catenin, which enhanced its nuclear localization through an unknown mechanism. This, too, has been countered by Jamieson *et al.*, who mutated the alleged β-catenin phospho-sites and reported no effect on the localization or import rate of β-catenin[67]. However, the latter research group did not consider the phospho-site mutations in tandem with WNT signal induction, so the possibility remains that p-JNK2 may enhance β-catenin nuclear import by a mechanism dependent on WNT signaling. The mechanism of localization notwithstanding, conservation of the phospho-

sites enhanced the β-catenin-LEF interaction necessary for canonical WNT-dependent gene transactivation[67].

Another component of RAC1 signaling that may modulate canonical WNT signaling is T-cell lymphoma invasion and metastasis-inducing protein 1 (TIAM-1), a GEF of RAC1. TIAM1 and β-catenin interact strongly, and both accumulate in the nucleus following WNT pathway stimulation[136]. In fact, TIAM1 possesses a bipartite NLS that may contribute to their joint translocation[137]. Meanwhile, in the nucleus, RAC1 and TCF/LEF transcription factors associate with WREs at baseline, but only activate WNT-responsive gene expression upon recruitment of TIAM1 and β-catenin[136]. This has led to a new model where RAC1 acts as a molecular switch to enhance WNT response at WREs following WNT-induced translocation of its activator TIAM1.

Furthermore, RAC1 also participates in noncanonical WNT signaling. These pathways are diverse and more poorly understood than the canonical pathway, but they are unified by their autonomy from β-catenin-TCF/LEF-dependent transcription. Examples of pathways governed by noncanonical WNT signaling include the planar cell polarity pathway, which promotes polarity within tissue to spatially coordinate growth and division, and convergent extension movements such as those that provide the driving force behind morphogenic events such as gastrulation[138]. In these pathways, DVL is necessary for the activation of RAC1, which may then directly mediate actin cytoskeletal rearrangement or activation of JNK to phosphorylate transcription factor JUN (also called c-JUN) to modulate transcription of genes regulated by the activator protein-1 (AP-1) complex[139,140]. Noncanonical WNT activation of RAC1 has been studied and validated in vertebrate gastrulation, neurite outgrowth, and dendritic spine branching for excitatory synapse development[138,139,141,142].

II.3.4 Superoxide production

Beyond its roles in cytoskeletal rearrangement and signaling, RAC1 is also involved in the production of reactive oxygen species (ROS), which promote inflammation, immune response, and wound healing. Through its participation in superoxide production and tolerance, RAC1 mediates host immunity and redox signaling, thereby expanding the repertoire of signaling programs under its influence and revealing another mechanism for its involvement in cellular migration machinery.

An early function of RAC1 was reported in phagocytic cells of the immune system, such as neutrophils and monocytes, where it was found to mediate the production of superoxide (O_2^-) by NADPH oxidase[143]; RAC1 also contributes to the generation of nitric oxide (NO) in macrophages through direct interaction with Nitric oxide synthase-2 (NOS2)[144]. The phagocyte NADPH oxidase complex consists of a catalytic heterodimer core at the plasma membrane formed by Cytochrome b-245 beta chain (CYBB) and alpha chain (CYBA), which associate with cytosolic proteins Neutrophil cytosolic factor 1 (NCF1), NCF2, NCF4, and RAC1 to form a functional complex upon exposure to appropriate immune-related stimuli[145,146]. ROS produced through NADPH oxidase contribute to the killing of microorganisms phagocytized by immune cells. As ROS accumulation can lead to oxidative stress and genotoxicity in the absence of enough antioxidant safeguards, NADPH oxidase is most often localized to the extracellular phagosome compartment.

NADPH oxidase has also been detected in nonphagocytic cells where it has low levels of constitutive activity to drive the generation and maintenance of intracellular superoxide, and it is responsive to growth factors and cytokines to increase ROS production[147]. In these circumstances, it is likely that superoxide functions as a second messenger as it can post-translationally modify protein thiols to modulate the activity of signaling proteins such as RAS and other MAPK pathway constituents, Src non-receptor tyrosine kinase (SRC), and Nuclear factor κ-light-chain-enhancer of activated B-cells (NF-κB). ROS stimulation of NF-κB family transcription factors is particularly interesting as ROS expression and resulting oxidative damage mediated by hyperactive RAC1 may promote apoptosis or senescence[148]; conversely, NF-κB dimers promote the expression of genes involved in survival pathways, which may help cells with elevated ROS to evade apoptosis[148,149]. Furthermore, the NF-κB pathway may contribute to positive feedback of ROS production and redox signaling as it is known to promote inflammation—a process it stimulates in part by upregulating *CYBB* expression. It also stimulates expression of antioxidant genes and additional targets that are otherwise protective against ROS to mitigate widespread oxidative stress.

Another role for superoxide within the cell lies in the regulation of actin dynamics, particularly at adhesion sites whose dynamic actin assembly and disassembly underly cell motility. Depletion of ROS by antioxidants or inhibition of NADPH oxidase reduces migration velocity by decreasing the stability of membrane protrusions and limiting the activation of Focal adhesion

kinase (FAK), which regulates focal adhesion dynamics[150]. Researchers have verified that RAC1 activity is unaffected by either treatment to ensure that these observations occur downstream of active RAC1 by a ROS-dependent pathway.

Beyond its direct involvement in cytosolic superoxide production, RAC1 can localize to the mitochondrion by a mechanism dependent upon its prenylated Cys189 residue, where it mediates additional ROS-related activities[151–153]. Mitochondria are the powerhouse of cellular ROS production. They maintain elevated concentrations of ROS that facilitate their diffusion down a gradient into the cytosol, where ROS are able to act as secondary messengers as described above[154]. When RAC1 localizes to mitochondria, it may be oxidized by cytochrome c of the electron transport chain at residue Cys178 to ultimately stimulate downstream production of mitochondrial hydrogen peroxide (H_2O_2), a non-radical variety of ROS[152]. RAC1 also contributes to the mitochondrion's tolerance of its pro-oxidant state; it interacts directly with proto-oncogene B-cell lymphoma 2 (BCL-2) to enhance BCL-2-mediated anti-apoptotic signals[155]. Thus, not only does RAC1 activity contribute to mitochondrial ROS production, it also promotes survival amid the oxidative mitochondrial environment.

II.3.5 Metabolism

RAC1 participates in glucose transport mediated by canonical insulin signaling, although it may also promote this process when stimulated by alternative mechanisms such as mechanical stress in exercising muscle tissue. In the canonical pathway, secreted insulin binds to the insulin receptors of insulin-sensitive cells to stimulate an intracellular signaling cascade wherein PI3K is recruited to increase PIP_3 levels at the plasma membrane, which leads to activation of AKT. Subsequently, vesicles containing facilitative glucose transporters (GLUT) translocate to and fuse with the plasma membrane to increase glucose uptake[156]. In skeletal muscle, the primary GLUT isoform engaged in this pathway is GLUT4. Many cell types have demonstrated a reliance on Rab GTPases for coordination of GLUT4 storage vesicle exocytosis in response to insulin signaling (reviewed in [157]). Although Rab GTPases themselves are not downstream targets of AKT, a Rab GAP—TBC1 domain family member 4 (TBC1D4)—is phosphorylated by AKT; this does not inhibit its GAP activity, but it does mediate TBC1D4 dissociation from GLUT4 storage vesicles and thus active Rab GTPases becomes liberated at those sites to mediate GLUT4 translocation in an insulin-dependent way[158]. Specifically, 14-3-3 family scaffold proteins are able to bind to

phosphorylated TBC1D4 to achieve its dissociation from GLUT4 storage vesicles[159]. Although no effects of RAC1 have been specifically detected in this branch of signaling, a recent discovery that RAC1 phosphorylated at Ser71 can directly bind with 14-3-3 family proteins raises questions about possible pathway crosstalk and merits further investigation[160].

As another effector of the insulin-PI3K pathway, RAC1 has been demonstrated to increase GLUT4 transport to the plasma membrane through an additional mechanism that occurs in parallel to the AKT-dependent pathway outlined above[161]. Following activation by PI3K, RAC1 stimulates actin reorganization by upregulating ARP2/3-dependent nucleation of actin filaments[162]. This process is coupled with enhanced de-phosphorylation of cofilin by phosphatase Slingshot-1 (SSH1); this occurs despite LIMK-mediated cofilin phospho-inactivation because the abundance of F-actin formed through ARP2/3 activity at these sites prompts a surge of SSH1 phosphatase action[163]. Consequently, cofilin is available to stimulate rapid disassembly of polymerized F-actin, leading to highly dynamic actin remodeling. Together, this rapid actin reorganization contributes to the trafficking of GLUT4 storage vesicles and is necessary for their fusion with the plasma membrane[164,165].

Although insulin signaling is the canonical pathway for glucose transport, alternative hormone-independent pathways have also been demonstrated to drive GLUT4 localization to the plasma membrane for increased glucose uptake. This is particularly true of skeletal myocytes, as these cells must upregulate glucose intake to satisfy the metabolic demands of physical exercise. Here, muscle contraction drives mechanotransduction that stimulates intracellular signaling programs to upregulate GLUT4 storage vesicle cycling to the plasma membrane, although the explicit mechanisms driving this phenomenon are unknown[166]. Even so, just as with hormone-induced glucose transport, RAC1-driven actin polymerization has been identified as a critical node within this pathway. When RAC1 or actin polymerization is inhibited in murine muscle tissue, glucose transport decreases by 30-50 %[167]. Furthermore, RAC1 hyperactivity alone has been sufficient to stimulate insulin-independent translocation of GLUT4 to the plasma membrane in myoblasts[168]. The premise that this signaling is initiated by a mechanical signal supports a key role for RAC1 involvement at the centre of the pathway, as the actin cytoskeleton drives short feedback loops to positively regulate RAC1 activity[83,169]. But how could RAC1 drive GLUT4 translocation when the canonical pathway requires cooperation with an AKT signaling arm? This may rely on

crosstalk between PAK and the PI3K-AKT signaling axis. PAKs are direct effectors of RAC1 that can stimulate AKT; it is possible that this mechanism is suitably compensatory to achieve GLUT4 transport on a smaller scale as observed upon mechanotransduction[166]. This postulation is supported by the observed phosphorylation of TBC1D4 upon muscle contraction, which suggests that even in a hormone-independent context, some AKT activity remains to facilitate vesicle trafficking by Rab[157].

II.4 *Regulation of RAC1*

As a molecular switch implicated in a wide array of intracellular processes, stringent regulation of RAC1 is crucial to avoid aberrant signaling that could contribute to certain pathologies. This regulation occurs by diverse post-translational modifications (PTMs) and regulatory proteins that coordinate the spatiotemporal activation of RAC1 (reviewed in [37,69,170]), which are summarized below.

II.4.1 Post-translational modifications

RAC1 is a substrate for many different PTMs, such as lipid modification, phosphorylation, ubiquitination, and SUMOylation, which regulate its localization, activity, and stability. Firstly, a series of C-terminal PTMs affect RAC1 localization. RAC1 may be irreversibly prenylated at Cys189 of its CLLL motif (*i.e.* CAAX box) to facilitate membrane-targeting, which is a PTM shared by most Ras superfamily GTPases. Although this PTM enhances RAC1 recruitment to the plasma membrane, it may negatively affect its interaction with certain effectors and scaffolds, including IQGAP1[171]. Subsequently, RAC1 may undergo palmitoylation at Cys178, which is a reversible lipid modification that reinforces RAC1 recruitment to the plasma membrane at cortical actin-rich sites to enhance cell spreading and migration[172]. Alternatively, subcellular localization of RAC1 to the nuclear compartment is upregulated upon ERK recruitment to the PBR and subsequent phosphorylation of RAC1 at Thr108 in response to growth factor signaling[173].

Phosphorylation of RAC1 can not only modulate its localization, but also its activity. When phosphorylated at Tyr64 by FAK or SRC, RAC1 activity is decreased and cell spreading is reduced[174]. This residue is also important for RHOGDI sequestration of RAC1 in the cytosol, as p-Tyr64 may further stabilize this interaction on account of its proximity to two RHOGDI lysine residues. RAC1 may also be phosphorylated at Ser71 by AKT or Protein Kinase C (PKC), which

can promote inhibitory or stimulatory outcomes. In human melanoma cell line SK-MEL28, this PTM was associated with decreased binding to GTP, which is predictive of decreased RAC1 activity and signaling[175]. However, maintenance of p-Ser71 has contributed to increased invasiveness of A431 human epidermoid carcinoma cells[176]. Rather than being singularly inhibitory, Ser71 phosphorylation may instead help to fine-tune the subset of GEFs and effectors that RAC1 can engage[170].

Finally, RAC1 is recognized and modified by E3-ligases. Specifically, it can be polyubiquitinated at Lys147 or Lys166 following recognition by HECT domain and ankyrin repeat containing E3 ubiquitin-protein ligase 1 (HACE1) and Inhibitor of apoptosis protein (IAP) family proteins, targeting RAC1 for proteasomal degradation and thereby suppressing RAC1-driven morphology, migration, and ROS production[177,178]. Meanwhile, RAC1 can also be recognized and modified by Protein inhibitor of activated STAT 3 (PIAS3), which is a small ubiquitin-like modifier (SUMO) E3-ligase that mediates RAC1 SUMOylation at lysines of the PBR. Such SUMOylation enhances GTP loading and consequently increases cell migration and invasion[179]. In summary, RAC1 is susceptible to many PTMs that yield competing outcomes, and a careful balance is necessary to maintain appropriate RAC1 signaling.

II.4.2 GTPase regulatory proteins: GAPs, GEFs, and GDIs

As described previously, Rho GTPases are governed by three classes of regulators: RHOGEFs, RHOGAPs, and RHOGDIs. Not only do these regulatory proteins modulate the RAC1 active state, but they also interpret cellular signals to control its appropriate spatiotemporal activity[180]. As the only class of GTPase regulatory protein that positively modulates the active state, RHOGEFs dramatically increase the intrinsic rate of GDP/GTP exchange. GTPases typically have a very high affinity for their bound nucleotide, which produces a very slow rate of exchange[181]. By disrupting the forces that stabilize GDP in the nucleotide-binding pocket, RHOGEFs accelerate GDP release. RHOGEFs may receive stimulatory signals transmitted through receptor tyrosine kinases, G-protein-coupled receptors (GPCRs), and integrin-mediated signaling. Classical RHOGEFs belong to the diffuse B-cell lymphoma (Dbl) family, which includes more than 70 members in humans[182]. These GEFs conserve two domains: a Dbl-homology (DH) domain, which mediates GDP/GTP exchange by inducing conformational changes in RAC1 to obstruct the Mg^{2+}-binding site and interrupt P-loop hydrogen bonding to the

GDP α-phosphate, thus facilitating GDP release; and a PH domain, which promotes membrane localization and GEF activation through binding to PIP_3[54]. Dbl-family RHOGEFs often encode additional domains to mediate specific protein interactions to bind members of the RAC1 interactome and facilitate precise RAC1 recruitment and downstream activity. Alternatively, non-classical RHOGEFs belonging to the Dedicator of cytokinesis (DOCK) family include 11 members in humans (DOCK1-11) and they have neither a DH nor a PH domain[183]. Instead, they each possess DOCK-homology region 1 (DHR1) and DHR2 domains. In this case, DHR1 binds phospholipids to target the GEF to the plasma membrane, while DHR2 catalyzes nucleotide exchange by excluding Mg^{2+} from the nucleotide-binding pocket to promote GDP release[184]. When considering the RHOGEFs of both families, at least 20 members are directly involved in activating RAC1 (reviewed in [170]).

As the antitheses to RHOGEFs, RHOGAPs catalyze GTP hydrolysis to inactivate Rho GTPases, shifting the equilibrium in the opposite direction to maintain homeostatic balance. GTPases maintain a weak intrinsic ability to catalyze GTP hydrolysis, but the rate of this reaction increases by several orders of magnitude upon RHOGAP engagement. RHOGAPs are defined by their conserved catalytic domain of approximately 150-190 amino acids termed the RhoGAP domain[37,185]. This domain interacts with switches I/II and the P-loop of Rho GTPases[186]. Within the catalytic RhoGAP domain resides the "arginine finger", an arginine residue that is instrumental in GAP-mediated catalysis. Upon binding to the GTPase, the arginine finger engages in hydrogen bonding to stabilize Glu61 of RAC1 as it coordinates the attacking water molecule, while simultaneously interacting with the GTP γ-phosphate, thereby stabilizing the nucleotide transition state and reducing the activation energy of the reaction to accelerate conversion of GTP to GDP and inorganic phosphate[187]. To highlight the importance of these interactions in the hydrolytic reaction, oncogenic RAS with constitutively activating G12 locus substitutions maintains GAP binding; however, the mutation disrupts the proper orientation of the arginine finger within the catalytic site to ablate RHOGAP acceleration of GTP hydrolysis[188]. Over 70 proteins in eukaryotes have a conserved RhoGAP domain, and as many as 66 RHOGAPs and RHOGAP-related proteins are encoded within the human genome[185,189]. A subset of these RHOGAPs are able to act on RAC1 to negatively modulate its active state and attenuate its signaling. Interestingly, Breakpoint cluster region protein (BCR) and Active breakpoint cluster region-related protein (ABR) are RHOGAPs of RAC1 that possess both RhoGAP and DH/PH domains, conserving both GAP and GEF

functionalities *in vitro*[190]. As many RAC1 regulators are involved in the careful management of the its active state, these dual-action regulators further emphasize the intricate regulatory network that underlies RAC1 signaling.

The final class of regulator affecting RAC1 does not directly influence the active state but instead functions by sequestering RAC1 away from the plasma membrane and holding it in an inactive state by the mechanism described in section II.1. In contrast to the extensive families of RHOGEFs and RHOGAPs, only three RHOGDIs have been characterized in mammals. RHOGDI1, also called ARHGDIα, is the most ubiquitously expressed isoform and it interacts with the greatest proportion of Rho family GTPases; RHOGDI2 (ARHGDIβ) is preferentially expressed in hematopoietic cells and favours binding to Rac1 subfamily members; and lastly, RHOGDI3 (ARHGDIγ) is expressed at low levels and predominantly engages only RHOB and RHOG (reviewed in [191]). Beyond their inhibitory role in RAC1 signaling, RHOGDIs also serve to protect their bound GTPases from proteasomal degradation. Prenylated Rho GTPases in the cytosol are particularly susceptible to degradation, but RHOGDIs can safely shuttle newly synthesized GTPases from the endoplasmic reticulum to the plasma membrane[192,193]. RHOGDIs are predominantly regulated through phosphorylation, which influences the assembly and dissolution of specific RHOGDI-Rho GTPase complexes. Phosphorylation of RHOGDI1 by PAK1 and SRC leads to its dissociation from RAC1—incidentally, this provides an interesting insight into PAK1 activity upstream of RAC1 to improve RAC1 availability[194,195]. Similarly, phosphorylation by FER tyrosine kinase prevents the formation of RHOGDI1-RAC1 complexes, but it does not necessarily promote the dissociation of pre-established complexes[196]. Additionally, SRC and PKCα can each phosphorylate sites on RHOGDI2, promoting dissociation of its complex with RAC1[197,198]. Thus, the regulatory function of RHOGDIs is more complex than at first glance. Although they sequester RAC1 in a state of inactivity, they also positively modulate RAC1 stability within the cytosol and they are receptive to many repressive signals that liberate RAC1 to resume function at the plasma membrane.

II.5 *Genetic alterations and associated disease*

Outside of somatic mutations in cancer, mutations to the *RAC1* gene and associated pathogenic phenotypes have rarely been reported in humans. Given the evidence that mammalian gastrulation is dependent on functional RAC1, as demonstrated in mice, it follows that missense

mutations altering RAC1 function may not be compatible with successful embryological development. The few cases of *RAC1* mutations that have been reported were discovered recently through WES of more than 4,000 families afflicted with developmental disorders, which revealed seven *de novo* heterozygous mutations in seven young boys with mental retardation[199]. This is consistent with our current knowledge of RAC1 in neural development, where it participates in dendritic spine formation, excitatory synapses and synaptic plasticity as a basis for learning and memory[200,201]. The nonrecurrent, autosomal dominant mutations identified in RAC1 were the following: C18Y near the P-loop; N39S within switch I; V51M, V51L, Y64D, and P73L within switch II; and C157 within the G5 motif. The influence of these mutations on overall RAC1 activity was gauged based on the cytoplasmic protrusion morphology and circularity of NIH/3T3 cells transfected with each mutant isoform, as RAC1 hyperactivity is associated with a higher rate of lamellipodial protrusion and enhanced cell spreading. The C18Y and N39S mutations were determined to be dominant-negative, whereas Y64D was more highly activated than WT, and the remainder of mutations seemed mildly inhibitory. Overall, RAC1 mutant activation status was poor predictor of the phenotypes associated with each mutation. The dominant-negative mutations were associated with decreased neuronal proliferation and microencephaly in the young boys, but surprisingly, other inhibitory mutations were associated with macroencephaly. A deleterious role for hyperactive RAC1 at synapses has already been established, corroborating the developmental delay observed in the individual with the activating Y64D mutation, whose brain was of normal size[202]. The seven patients displayed a variety of concomitant afflictions such as congenital cardiac anomalies, epilepsy, corpus callosum hypoplasia, eczema, and diabetes mellitus, which is accordant with the deregulation of RAC1 in many cardiac, neurological, inflammatory, and metabolic diseases (reviewed in [203]). Interestingly, mutations in RAC1 GEFs HACE1 and TRIO, as well as effector PAK3, have also been associated with neurodevelopmental disorders, substantiating the role of RAC1 as a central player in cognitive development[204–206].

In cancer, the prevalence of genetic alternations to RAC1 and related pathways has emerged following a series of large-scale sequencing efforts over the past decade. *RAC1* codon 29 has been identified as the third most frequent recurrent somatic mutation hotspot in cutaneous melanoma, with P29S as the predominant substitution at this locus. Following its recognition in melanoma, the same c.85C>T nucleotide transition responsible for the P29S missense mutation has also been reported in cancers of the breast, endometrium, thyroid, lung, and upper

aerodigestive tract, in addition to Merkel cell and squamous cell carcinomas, as archived by the COSMIC database[207]. A large-scale pan-cancer analysis of more than 10,000 patient tumours by the Memorial Sloan-Kettering Cancer Centre as part of the MSK-IMPACT clinical sequencing initiative corroborates the prevalence of P29 substitutions in melanoma, as well as in Merkel cell and squamous cell carcinomas, anaplastic thyroid cancer, and breast invasive ductal carcinoma[208–210].

While RAC1 P29S substitutions occur in 5-10 % of cutaneous melanomas, recurrent mutations in a variety of other RAC1 residues have been identified at low frequency (<1 %) in cancers other than cutaneous melanoma. For instance, one such low-frequency recurrent mutation hotspot in RAC1 is the N92 locus, where N92K, N92T, and N92I have been identified in mucosal melanoma, thyroid, and gastrointestinal cancers[210,211]. Overexpression of RAC1 N92I is associated with increased GTP-loading and is sufficient to drive transformation in NIH/3T3 and MCF10A cell lines, although it has not been verified whether N92K/T substitutions can drive similar processes[212]. Germ cell testicular cancers harbour recurrent P34R, G12R/V, and Q61K/R mutations, while Q61R mutations are also seen in prostate cancer[208–210]. Identification of RAC1 G12 and Q61 missense mutations in human cancers is highly interesting; these produce constitutively activated RAC1 isoforms that are commonly used in laboratory settings as positive controls, similarly to oncogenic RAS G12V and RAS Q61L isoforms, but they had not previously been identified in RAC1 in human tumours[208–210]. Using a new algorithm to identify mutational hotspots, Chang *et al*. identified A159V as another novel low-frequency RAC1 hotspot mutation[213,214]. This activating mutation is most frequently present in head and neck cancers, but it is also found in lung adenocarcinoma, colorectal cancer, and cervical cancer. A final hotspot for recurrent mutations in RAC1 has been proposed at C18, where RAC1 C18Y and RAC1 C18S have been identified in colon and lung adenocarcinoma, respectively, and C18Y/F have been detected in head and neck squamous cell carcinoma[208–210,214,215]. The effect of these mutations is unclear as C18Y modestly increases RAC1 GTP-loading and interaction with PAK1 *in vitro*, but also appears to suppress RAC1-associated morphological phenotypes as had been similarly observed in the developmental disorder study described above[199,215].

Additional factors beyond RAC1 missense mutations are known to affect RAC1 pathway activation across cancer types, such as *RAC1* alternative splicing, amplification, and deregulation.

The *RAC1* gene encodes seven exons and it is ubiquitously expressed across tissue types, its promoter region displaying characteristics of a housekeeping gene[216]. Typically, *RAC1* exon 3b is spliced from the processed transcript; however, when exon 3b is retained in mature mRNA, the translated peptide contains an in-frame 19-amino acid insertion following the switch II motif[217]. This alternative splicing isoform—designated as RAC1B—maintains a very high intrinsic rate of GEF-independent GDP/GTP exchange, coupled with impaired enzymatic function that is 31-fold lower than wild-type RAC1 (RAC1 WT), to ultimately produce a self-activating RAC1 splice isoform[218]. RAC1B has a narrower interactome than RAC1 and its activation is linked to limited cellular outcomes, as was first evidenced by its reduced affinity for canonical RAC1 effector PAK1[218]. Increased RAC1B expression has been linked to pathology in humans as *RAC1B* transcripts accumulate in inflamed colonic mucosa, and inflammation can facilitate the onset of tumourigenesis[219]. Aberrant expression of RAC1B has been identified in colorectal, breast, thyroid, ovarian, pancreatic, and lung cancers (reviewed in [170]). Although RAC1B does not engage the RAC1/PAK signaling axis, its ability to stimulate ROS production persists, mediating survival and anti-apoptotic signals via NF-κB in addition to promoting EMT by enhancing expression of transcription factor SNAI1[220–222]. The exact functions of RAC1B may vary somewhat between cancers, as does its value as a prognostic indicator[223].

Another prominent *RAC1* alteration that persists across cancers is gene amplification, which may drive aberrant RAC1 signaling and has been reported in 24 of 32 cancer types studied as part of the TCGA PanCancer consortium available on the cBioPortal database[208,209,224]. Alternatively, regulators of RAC1 may themselves be altered in cancer, disrupting the spatiotemporal regulation of RAC1 and consequently contributing to RAC1 hyperactivity. In brief, GEFs may be upregulated, mislocalized, or mutated to enhance or alter RAC1 activity; in contrast, GAPs often play tumour suppressive roles and it is primarily through their downregulation and the associated reduction in GTP hydrolysis that they contribute to aberrant RAC1 activity (reviewed in [225]). Even so, GAP overexpression has been occasionally associated with tumour aggressiveness, invasiveness, and poor overall prognosis, further underscoring the pervasive complexity of RAC1 regulation[226–228].

III. RAC1 P29S in oncogenesis

When RAC1 becomes hyperactivated, it may pathologically overstimulate cellular programs governing proliferation, survival, and migration. Since the discovery of RAC1 P29S as a putative driver of cutaneous melanoma eight years ago, there have been many contributions to the growing literature base for RAC1 P29S participation in melanomagenesis. These investigations have granted insight into some mechanisms behind RAC1 P29S hyperactivity, the oncogenic processes and phenotypes it mediates, and certain unique characteristics of the RAC1 P29S interactome *in vivo*. This section summarizes the outcomes of these studies.

III.1 *Biochemical basis for RAC1 P29S self-activation*

When RAC1 P29S was first identified as a recurrent mutation in melanoma, researchers conducted preliminary assays to ascertain the impact of this point mutation on protein function. Multiple studies confirmed that RAC1 P29S is activated relative to RAC1 WT, as demonstrated by the enhanced GTP-loaded fraction seen with RAC1 P29S[33,34]. By consequence, it is more available to bind downstream effectors[33,34]. Methodical investigation of the underlying biochemistry revealed that RAC1 P29S has a significantly elevated rate of nucleotide exchange under physiological [Mg^{2+}] relative to RAC1 WT[229]. Still, RAC1 P29S maintains a similar rate of intrinsic GTP-hydrolysis to RAC1 WT, indicating that the mode of hyperactivity in RAC1 P29S is not reliant on the suppression of GTP hydrolysis[212,229,230]. Together, these data suggest that RAC1 P29S is a fast-cycling GTPase whose mechanism of self-activation stems from its elevated rate of intrinsic GDP to GTP exchange.

The fast-cycling phenotype of RAC1 P29S relies on destabilization of the GDP-bound state. Toyama *et al*. were the first to observe that RAC1 WT and RAC1 P29S have different rates of dissociation from Mg^{2+}, and this led them to employ NMR techniques to reveal that each isoform exists in equilibrium between a Mg^{2+}-bound and a Mg^{2+}-unbound state[231]. The Mg^{2+}-unbound state has a much higher rate of GDP-association than the Mg^{2+}-bound state, and differences in the ratios of these populations could justify the significantly elevated GDP dissociation rate of the RAC1 P29S mutant relative to wild-type. To summarize their findings, 65 % of RAC1 WT was Mg^{2+}-bound at equilibrium; however, the RAC1 P29S mutant GTPase favours the Mg^{2+}-unbound state such that only 44 % of the population is associated with a Mg^{2+}

cation at equilibrium[231]. This equilibrium shift rationalizes the previous observation that RAC1 P29S has elevated nucleotide exchange even in the presence of unchelated Mg^{2+} [229]. It is likely that conformational changes in the secondary and tertiary structure of RAC1 P29S as a consequence of the P29S point mutation are the driving forces behind the mutant's reduced affinity for Mg^{2+}, but the specifics of altered interacting forces with Mg^{2+} have not been explored.

Structurally, hyperactivity of RAC1 P29S stems from its distinct active and inactive state conformations that directly influence its affinity for guanine nucleotides. It has a conformationally distinct active state from RAC1 WT and other hyperactive RAC1 mutants. The proline to serine substitution occurs within the switch I domain of the RAC1, which is in proximity to the bound nucleotide. Analysis of the resolved RAC1 P29S crystal structure reveals that Ser29 and Gly30 of the mutant protein both become available for hydrogen bonding to GTP in a way that is analogous to Val29 and Asp30 of activated HRAS, and thereby stabilize GTP-binding[34]. These hydrogen bonding events are absent from other RAC1 isoforms, as the wild-type Pro29 residue conserves a rigid conformation of the switch I domain, sterically hindering Asp30 from participating in hydrogen bonding stabilization. *In silico* molecular dynamics simulations predict that RAC1 P29S participates in 13 hydrogen bonds with GTP, in contrast to nine by RAC1 WT, which provides a rationale for the mutant's elevated binding affinity for GTP[232]. Alterations to intramolecular and protein-solvent bonds also account for the increased flexibility of the switch I motif in RAC1 P29S, as well as the increased rigidity of switch II. These conformational changes ultimately reduce the volume distribution of the binding pocket to mediate the proximity of key residues within the pocket to GTP, enhancing the available stabilizing interactions to improve affinity[232].

III.2 *Tumourigenicity of RAC1 P29S*

As a putative driver event, the involvement of RAC1 P29S in tumour onset has been of particular interest. This mutation was identified in 9.2 % of primary lesions and 8.6 % of metastatic tumours within the Yale melanoma cohort, suggesting that this mutation occurs early in tumour development[34]. To investigate the effect of RAC1 P29S on anchorage-independent growth, it was ectopically expressed in NIH/3T3 mouse embryonic fibroblasts and MCF10A breast epithelial cells, where it was sufficient to drive transformation of both cell lines[212]. Meanwhile, ectopic overexpression of RAC1 P29S in melan-a immortal murine melanocytes did not increase the number of colonies that formed in a soft agar growth assay, but it did increase the average size of

the colonies that formed, relative to the parental strain[233]. In contrast, another study has demonstrated that inducible expression of an Estrogen receptor (ER)-RAC1 P29S fusion system in melan-a cells greatly increased colony formation in soft agar[234]. Subsequent *in vivo* assays have demonstrated that subcutaneous injection of NIH/3T3 cells overexpressing RAC1 P29S led to tumour growth in nude mice, whereas RAC1 WT overexpression did not[212]. Mouse models engineered to express RAC1 P29S ubiquitously have demonstrated that whole-body RAC1 P29S expression did not produce melanocytic neoplasms in mice by 2 years of age; however, it did contribute to the formation of lymphomas and squamous cell tumours during this time, whereas the RAC1 WT control did not[234]. Although RAC1 P29S produces tumourigenic phenotypes, it requires additional variables to drive melanomagenesis.

Despite the preliminary evidence for the transformative potential of RAC1 P29S, it is likely insufficient to drive melanocytic neoplasia on its own. In a zebrafish model system, melanocyte-specific RAC1 G12V overexpression was unable to initiate neoplastic growth *in vivo*[235,236]. Even so, constitutively active RAC1 has accelerated malignant progression in models that were already predisposed to malignancy. RAC1 is necessary for melanocyte anchorage-independent growth in the context of oncogenic NRAS, as well as for tumour onset and malignant progression in NRAS-driven melanoma and other skin cancers[237,238]. To evaluate whether RAC1 P29S can drive melanomagenesis in a model system tailored to melanoma, recent studies of the RAC1 P29S mutant in engineered mouse models with melanocyte-specific expression have verified that RAC1 P29S expression alone does not promote melanocyte hyperplasia or neoplasia[234]. However, when introduced into a mutational landscape that is already known to drive melanocyte hyperplasia, such as BRAF V600E; BRAF V600E and *Pten*-hemizygous; BRAF V600E and *Trp53*-null; and *Nf1*-null and *Trp53*-null contexts, RAC1 P29S significantly accelerated the progression of hyperplasia to melanoma[234]. Our lab has also illustrated a role for RAC1 P29S in tumourigenesis. pMEL immortalized melanocytes expressing either BRAF V600E (pMEL-BRAF) or NRAS Q61L (pMEL-NRAS) were infected with lentivirus to stably express RAC1 WT, RAC1 P29S, or a GFP control. When injected into immunocompromised mice, more xenograft tumours formed from RAC1 P29S-expressing melanocytes, and these tumours had accelerated rates of growth compared to RAC1 WT or GFP expression[239]. Thus, RAC1 P29S cooperates with other driver events such to promote and accelerate melanomagenesis *in vivo*.

III.3 *Proliferation and survival*

The RAC1 P29S mutation contributes to proliferation, survival, and immune evasion in melanoma. The proliferative effect of RAC1 P29S was first observed in melanocytes isolated from C57BL mice and retrovirally infected with RAC1 WT or RAC1 P29S expression plasmids[34]. Expression of RAC1 P29S was associated with a greater rate of proliferation, whereas RAC1 WT only slightly increased proliferation over the parental strain. Melan-a immortalized murine melanocytes have exhibited similarly elevated proliferation with RAC1 P29S overexpression relative to RAC1 WT overexpression or the parental strain alone[233]. Inversely, knockdown of RAC1 expression in RAC1 P29S-mutant melanoma has decreased the rate of proliferation, particularly in an NF1-mutant context[240]. Histological assessment of human primary cutaneous melanoma further revealed that RAC1 P29S was associated with a higher mitotic rate than RAC1 WT ($3/mm^2$ vs. $2/mm^2$, respectively; p-value<0.03)[35].

However, further studies have suggested that RAC1 P29S does not significantly increase proliferation under standard conditions. Melanocytes isolated from engineered mouse models that were *ER*-hemizygous, *Trp53*-null, and carried either hemizygous *Rac1* c.85C>T (p.P29S) or homozygous *Rac1* (WT) had no significant differences in their doubling time in tissue culture, although endogenous RAC1 P29S was protective against apoptosis under low-adhesion and low-serum conditions[234]. Similarly, isogenic melanoma cell lines with RAC1 WT or RAC1 P29S expression maintained similar proportions of actively proliferating cells[241]. The specific melanoma lines assayed were A375s with stable overexpression of RAC1 WT or RAC1 P29S, and IGR1s with endogenous expression of RAC1 P29S or a RAC1 WT isotype control generated by a single base-pair mutation. Surprisingly, when these same cell lines were treated with MAPK inhibitors dabrafenib or trametinib, RAC1 P29S expression was uniquely associated with sustained, elevated proliferation in both sets of isogenic cell lines[241]. Whereas inhibitor treatment decreased the proportion of actively proliferating cells by 80 % in A375 and >90 % in IGR1 melanocytes with RAC1 WT expression, RAC1 P29S exerted a protective effect such that proliferation decreased by only 30-40 % in A375 and 60-70 % in IGR1. Additionally, similar effects have been observed in MCF10A breast epithelial cells with RAC1 WT or RAC1 P29S overexpression; proliferation was similar among isogenic lines in full culture medium, but when growth factors were reduced, RAC1 P29S sustained a higher rate of proliferation than RAC1 WT or an empty-vector control[234].

Mouse studies have demonstrated a similar phenomenon *in vivo*. When the previously described A375 or IGR1 isogenic cells lines were subcutaneously injected into the flanks of nude mice, RAC1 P29S was associated with larger metastatic nodules that contained a higher proportion of mitotic nuclei; in contrast, the primary tumours were of similar size with wild-type or mutant RAC1, and the proportion of mitotic nuclei within the primary tumour did not differ significantly either[241]. So, rather than consistently enhancing baseline proliferation, RAC1 P29S appears to confer a proliferative advantage to melanoma particularly when subjected to growth-challenging conditions, such as inhibition of proliferative pathways, limited access to soluble growth factors, or localization to a distant tissue site during metastatic colonization. Discrepancies between RAC1 P29S effects on proliferation at baseline between earlier and later studies may be explained by the heterogeneous mutational burden of melanoma, which can make it challenging to compare different melanoma cells, in addition to the low frequency of RAC1 P29S in human samples which may confound the outcome of histological studies.

Some additional biochemical insight has been gained into the pathways for RAC1 P29S-driven proliferation and survival. Presumably, RAC1 P29S may hyperactivate many of the proliferative signaling pathways known to be governed by RAC1 (described in section II.3.2). Vu *et al*. have confirmed in melan-a cells that RAC1 P29S expression increases active PAK (p-T212), which is supportive of previous evidence that RAC1 P29S maintains the ability to bind the PAK1 PBD[33,34,233]. RAC1 P29S likewise maintains binding to downstream Mixed-lineage kinase 3 (MLK3), a MAP3K involved in mitogen signaling[34]. In an inducible RAC1 expression system in MCF10A cells and melan-a melanocytes, RAC1 P29S led to greater activation of p-PAK1/2 (S199) and p-AKT (S473) than RAC1 WT[234]. Endogenous RAC1 P29S additionally stimulates AKT signaling in melanoma, which is dramatically reduced when RAC1 is silenced by shRNA[234]. This AKT activation contributes to the protection against apoptosis that has been associated with RAC1 P29S[234].

Furthermore, reverse phase protein arrays using melan-a cells overexpressing RAC1 WT, RAC1 P29S, or RAC1 Q61L have been used to identify proteins regulated specifically by RAC1 P29S and not other RAC1 isoforms[233]. Upregulated proteins include cyclin B1, which promotes cell cycle progression and mitosis[242]; Ets proto-oncogene 1 (ETS1), a transcription factor typically found in immune cells that can mediate pro-oncogenic changes[243]; spleen associated tyrosine

kinase (SYK), also normally restricted to immune cells, it enhances pre-B-cell proliferation and reduces their apoptosis[244]; and lastly PD-L1, an immune checkpoint protein that attenuates T-cell response. Likewise, our lab has identified that immune response pathways, such as interferon-γ (IFN-γ) response pathways that regulate PD-L1 expression, are upregulated specifically in RAC1 P29S-mutant xenograft tumours[239]. In contrast, cellular respiration pathways are downregulated, suggesting that RAC1 P29S may favour anerobic respiration in accordance with the Warburg effect[245]. These results demonstrate that not only does RAC1 P29S upregulate genes involved in cell cycle progression, proliferation, and protection from apoptosis, but it is also strongly associated with PD-L1 expression, which may help RAC1 P29S melanoma to evade immune suppression.

RAC1 P29S has long been associated with cell-spreading phenotypes based on RAC1 involvement in lamellipodia formation and actin rearrangement, but a link has recently been proposed between this morphology and the ability of RAC1 P29S to sustain proliferation under growth challenge. Mohan *et al.* have noted that upon treatment of their A375 or IGR1 systems with dabrafenib or trametinib, P29S-expressing cells dramatically shifted their morphology to increase cell spreading, producing large lamellipodia with rapid actin-treadmilling[212]. This phenotype corresponded with increased traction strain and an increased focal adhesions, which are distributed evenly across the ventral surface of the cells[212]. Despite this, there has been no evidence to support the involvement of focal adhesion signaling in the sustained proliferation conferred by RAC1 P29S upon MAPKi treatment. Instead, this was dependent on branched actin nucleation; pharmacological inhibition and genetic perturbation of the ARP2/3 complex impaired the proliferation advantage associated with RAC1 P29S[212]. Furthermore, RAC1 P29S maintained cell cycle progression amid MAPKi by mediating cyclin D1 accumulation, despite sustaining only marginal ERK activity, suggesting that RAC1 P29S promotes proliferation by an alternate pathway[212]. Strategic inhibition and immunoblotting of known RAC1 signaling pathways has shown that MAPKi-resistant proliferation specific to RAC1 P29S does not occur by PI3K, YAP, p38MAPK, or JNK signaling[212].

Mohan *et al*. have further identified that RAC1 P29S expression under MAPKi treatment was correlated with accumulation of phospho-inactivated Neurofibromin 2 (NF2). NF2 is a tumour suppressor that downregulates cyclin D1 and arrests the cell cycle in G1 phase[246]. NF2 is known

to negatively regulate the RAC1-PAK signaling axis; conversely, group I PAKs can phosphorylate NF2 at S518, alleviating its growth suppression and its inhibition of RAC1 signaling[247,248]. Accordingly, ectopic expression of phospho-deficient NF2-S518A restored sensitivity of RAC1 P29S-expressing cells to MAPKi, as did PAK inhibition in a dose-dependent manner[241]. As both PAK and p-NF2 accumulate within the lamellipodia of RAC1 P29S-expressing cells upon MAPKi, Mohan *et al.* have hypothesized that the dynamic dendritic actin network mediated by hyperactive RAC1 P29S coordinates a microdomain wherein active PAK and NF2 co-localize to promote sequestration of phospho-inactive NF2 within the lamellipodia, alleviating tumour suppressive function and facilitating oncogenic RAC1 signaling at these sites. This argument is strengthened by independent studies that have shown the loss of NF2 to promote canonical WNT/β-catenin signaling leading to loss of contact inhibition, where RAC1 itself mediates this increased canonical WNT signaling[249,250].

III.4 *Melanocyte dedifferentiation*

Melanocyte dedifferentiation is a hallmark of melanomagenesis analogous to EMT in other cancer types; melanocytes themselves are already mesenchymal cells, but they undergo gene expression changes to restore a less differentiated phenotype that is highly plastic, ultimately promoting migration, invasion, and resistance to immune response and pharmaceutical intervention[251]. During dedifferentiation, melanocyte-inducing transcription factor (MITF) is commonly downregulated. Following gene set enrichment analysis (GSEA) using RNA-sequencing data from excised xenograft RAC1 P29S and GFP-control tumours, our lab has found RAC1 P29S overexpression to be associated with dedifferentiation pathways *in vivo*[239]. These findings are matched by GSEA of WES data from human melanoma of the TCGA-SKCM dataset[5,239]. Lionarons *et al*. have also recently identified an enrichment in dedifferentiation pathways associated with RAC1 P29S expression relative to a RAC1 WT control in three separate model systems: melan-a cells with inducible ER-RAC1 P29S fusion protein expression; melanocytes isolated from engineered heterozygous RAC1 P29S mice; and BRAF V600E-hemizygous, *PTEN*-hemizygous, RAC1 P29S-hemizygous melanoma induced *in vivo*[234]. From their unbiased approach, they discerned that several of the dedifferentiation-related transcription factors upregulated with RAC1 P29S expression—such as JUN and SNAI2—were targets of SRF.

SRF activity can be regulated in two ways: either MAPK signaling cascades can stimulate TCFs to associate with SRF and coordinate expression of the SRF regulon; or Rho GTPases can stimulate translocation of Myocardin-related transcription factor (MRTF) to the nucleus to positively regulate expression of SRF target genes[252]. MRTF is highly sensitive to G-actin, which inhibits MRTF nuclear import and actively drives its export. This inhibitory effect is alleviated by RAC1 actin remodeling as it drives F-actin accumulation and a reciprocal decrease in cytosolic G-actin. Thus, hyperactive RAC1 P29S actin remodeling could drive dedifferentiation by promoting the SRF/MRTF signaling axis.

When RAC1 P29S-endogenous melanocytes were screened with an siRNA library to identify synthetic lethal genetic dependencies, they were uniquely dependent on RAC1, AKT3, MRTF, and dendritic actin pathway components WAVE2 and ARP3, whereas RAC1 WT control melanocytes were not[234]. Interrogation with a panel of inhibitors further revealed that RAC1 P29S sensitized cells to SRF/MRTF inhibition by the largest margin, followed by inhibition of RAC1 itself, and inhibition of the ARP2/3 complex. Many of these are intermediaries of the RAC1 P29S/MRTF/SRF axis. As detailed in section II.3.1, RAC1 promotes F-actin formation by the following pathway: active RAC1 binds directly to WAVE subunits of the WRC, which then engages the ARP2/3 complex to simulate branched actin nucleation. As ARP2/3 activity increases, the relative concentration of cytoplasmic G-actin would correspondingly decrease, liberating MRTF for nuclear import and positive regulation of SRF transcriptional activity. Together, these findings strengthen the initial observation that SRF/MRTF signaling may play a significant role in RAC1 P29S melanoma.

III.5 *Migration and invasion*

Just as RAC1 is a well-known for its role in actin remodeling, the hyperactive RAC1 P29S mutant maintains the ability to coordinate cytoskeletal reorganization. However, its contribution to migratory and invasive phenotypes in melanoma has not yet been extensively characterized. The P29S mutant has demonstrated an increased binding affinity for the WRC, but whether this has a structural basis or is a consequence of increased GTP-loading in the RAC1 P29S population has not been elucidated[75]. In accordance with its enhanced ability to stimulate the WRC, many sources have noted increased lamellipodia formation and membrane ruffling during their work with RAC1 P29S, indicating that it could promote a more motile phenotype[34,212,241,253,254].

Lamellipodia promoted by RAC1 P29S are also wider than with RAC1 WT, which may favour microdomains of oncogenic signaling[234,241]. Enhanced actin polymerization by RAC1 P29S may also directly contribute to melanocyte dedifferentiation to a more plastic and oncogenic phenotype, accelerating malignant progression, suppressing apoptosis and promoting BRAF inhibitor resistanc[234]. To investigate the influence of RAC1 P29S on cell motility, Krauthammer *et al*. performed a trans-well migration assay to evaluate the effect of RAC1 P29S on chemotaxis[34]. Serum-starved melanocytes expressing RAC1 P29S migrated toward the chemoattractant remarkably more readily than the parental strain or those expressing RAC1 WT, suggestive of a highly migratory phenotype associated with RAC1 P29S. However, in fibroblasts, RAC1 P29S expression abrogated haptotaxis and slightly decreased migration velocity, suggesting that proper RAC1 regulation is necessary to mediate this process[255].

RAC1 P29S has also been demonstrated to promote the melanoma invasiveness. In human superficial spreading melanoma, RAC1 is highly immunoreactive in at least 65 % of probed samples at the border of the horizontal growth phase[35]. This suggests that even in RAC1 WT melanoma, active RAC1 coordinates the leading edge of collective cell migration to promote local invasion. If RAC1 P29S adopts a similar localization, it may exert a more prominent effect on horizontal growth than RAC1 WT. This could be in part because of enhanced RAC1 P29S-associated motility, but also through matrix metalloprotease (MMP)-mediated degradation of the ECM. PAKs are known to upregulate MMPs, and given that elevated PAK activity has been validated in melanoma models of RAC1 P29S expression, such melanomas may also have increased MMP secretion[64]. Indeed, overexpression of RAC1 P29S and not wild-type has contributed to enhanced matrix invasion, as well as macropinocytosis, in mouse embryonic fibroblasts[256]. Conversely, Revach and colleagues have presented an unexpected role for RAC1 P29S in invadopodia and ECM degradation in human melanoma cell lines[254]. Using two endogenous RAC1 P29S melanoma cell lines (83T and 104T) and two RAC1 WT lines (31T and A375), they observed that wild-type RAC1 promoted invadopodia function and formation; however, RAC1 P29S appeared to negatively regulate invadopodia formation and matrix degradation. The significance of these findings is unclear without additional studies to strengthen one case over the other or otherwise elucidate the complex signaling network underlying these seemingly contradictory outcomes seen with RAC1 P29S.

Available evidence additionally suggests that RAC1 P29S contributes to metastatic spread. For patients with RAC1 P29S melanoma, they had enhanced regional metastasis at the time of diagnosis. These patients were 3-fold more likely to have positive regional lymph nodes relative to those with non-RAC1-mutant melanoma[35]. *In vivo* mouse xenograft studies have provided some insight into the role of RAC1 P29S in distant metastases. When injected subcutaneously into immunocompromised mice, A375 cells with RAC1 P29S overexpression and IGR1 cells with endogenous RAC1 P29S each greatly increased the overall metastatic burden relative to RAC1 WT control tumours[241]. Both sets of isogenic melanoma lines with RAC1 P29S expression led to visibly more metastatic nodules on the lungs of mice, and immunohistochemical staining revealed that these nodules were also larger than those promoted by RAC1 WT. Additionally, RAC1 P29S metastatic nodules were more highly proliferative, as per observations that RAC1 P29S confers a proliferative advantage under such growth challenge as a new metastatic niche. In summary, the role of RAC1 P29S in migration and invasion remains controversial; much of the evidence suggests that RAC1 P29S promotes these processes, but isolated studies report conflicting findings. As the role of RAC1 P29S has been comprehensively investigated in neither migration nor invasion, there is an immediate need for such efforts to bring clarity to this issue.

III.6 *RAC1 P29S enriched interaction with IQGAP1*

RAC1 effectors rely on the switch I and II motifs for recognition of and interaction with RAC1; a mutation such as P29S that occurs within switch I and notably alters its configuration may have consequences for signal transduction that extend beyond its fast-cycling phenotype[257]. In an unbiased RAC1 interactome analysis that coupled native complex isolation with mass spectrometry, our lab identified that IQGAP1 was highly enriched in complex with RAC1 P29S rather than RAC1 WT[239]. IQGAP1 is binds GTP-loaded RAC1 and CDC42; however, its GRD is unable to stimulate these GTPases to hydrolyze GTP. Instead, IQGAP1 acts as a catalytically inert scaffold that localizes to the plasma membrane, where it is able to bind MAPK pathway constituents, focal adhesion complexes, and cadherin-mediated junctions[258]. Through its involvement in actin and microtubule dynamics, IQGAP1 plays a role in cytoskeletal regulation at the cell periphery. Considering the existing evidence for the cooperation of RAC1-IQGAP1 in RAC1 signaling and actin remodeling, elevated RAC1 P29S-IQGAP1 interaction may serve a pivotal role in the development of oncogenic phenotypes such as migration and drug resistance.

As recent studies suggest that morphological changes associated with RAC1 P29S may drive changes to cellular signaling and gene expression, it would be of great interest to dissect the role of IQGAP1 in the functional and transcriptomic changes that have been observed with RAC1 P29S in the growing body of literature.

IV. Pharmacological targeting of RAC1 P29S-mutant melanoma

IV.1 *Response to existing melanoma therapies*

IV.1.1 RAC1 P29S as a biomarker for BRAF and MEK intervention

As BRAF-mutant and NRAS-mutant GoF driver events account for more than 70 % of cutaneous melanoma, targeted inhibition of BRAF and/or MEK has become a frontline clinical intervention. RAC1 P29S can co-occur with either of these prevalent driver events, and it may be a predictor of early resistance to MAPK inhibition (MAPKi)[259]. Watson *et al*. performed an in-depth functional analysis of the role of RAC1 P29S in MAPK inhibitor resistance and support it as a predictive biomarker for such therapies[260]. Compared with a panel of V600E melanoma lines expressing RAC1 WT, IGR1 cells—which express endogenous BRAF V600K and RAC1 P29S—were considerably less sensitive to BRAF inhibitors vemurafenib and dabrafenib as well as MEK inhibitors (MEKi) trametinib and PD325901[260]. Similarly, WM3060—an NRAS Q61K melanoma line with endogenous RAC1 P29S—was less sensitive to MEKi when compared against a panel of NRAS Q61K-mutant melanoma[260]. Ectopic RAC1 P29S could also promote resistance in otherwise sensitive melanoma lines that did not harbour an endogenous RAC1 P29S mutant[260]. These findings support the investigations described in section III.3, where RAC1 P29S was found to sustain proliferation in A375 (ectopically) and IGR1 (endogenously) cultured melanoma lines in the presence of each dabrafenib and trametinib[241].

Functionally, Watson *et al*. have demonstrated that RAC1 P29S expression reduced apoptosis upon dabrafenib treatment and concomitantly sustained MAPK signaling under BRAF inhibition, as measured by immunoblotting for p-MEK1/2 (S217/S221)[260]. Inducible RAC1 silencing in IGR1 conversely led to a substantial decrease in p-MEK and p-ERK1/2 (T202/Y204), converging with the RAC1 P29S overexpression models to suggest that RAC1 P29S mediates MAPKi resistance by sustaining limited MAPK pathway signaling. Mouse xenograft studies have demonstrated that these findings are also relevant *in vivo*. A375 cells with stable overexpression

of GFP, RAC1 WT, or RAC1 P29S were injected into nude mice and received PLX4720 BRAF V600E inhibitor treatment starting 1 wk post-injection. Nearly 90 % of RAC1 P29S tumours progressed while on treatment, whereas <30 % of GFP tumours progressed. RAC1 P29S expression was correlated with poorer survival and faster tumour growth than GFP; by day 41 of treatment, 13/15 mice with RAC1 P29S tumours had reached endpoint tumour burden versus 9/15 with RAC1 WT and 1/15 with GFP. These data provide new insight into the mechanisms for RAC1 P29S insensitivity to MAPKi and the wider applicability of these findings.

In contrast to the results above, two studies have reported conflicting evidence for RAC1 P29S as a predictor of MAPKi response. Select RAC1 P29S melanomas of the Yale cohort have been reported to have variable BRAFi and MEKi resistance[240]. The YURIF cell line expresses BRAF V600E and RAC1 P29S, but it has intermediate sensitivity to vemurafenib and high sensitivity to MEK inhibition, seemingly in contrast to above observations of RAC1 P29S-mediated resistance. However, YUHEF (*i.e.* a patient-derived RAC1 P29S cell line of the NF1-mutant subgroup) displayed resistance to MEKi, but another NF1-mutant RAC1 P29S cell line did not. Meanwhile, when NRAS-mutant cells with ectopic expression of RAC1 WT, RAC1 P29S, or RAC1 Q61L were treated with 90 nM trametinib for 48 h, all lines displayed sensitivity[233]. They additionally obtained the YUHEF cell line and silenced RAC1 to evaluate the effect on trametinib sensitivity. Although RAC1 knockdown increased baseline apoptosis, the relative increase in apoptosis upon MEKi was not affected by RAC1 knockdown, so it did not appear that depleting RAC1 P29S increased trametinib sensitivity[233]. Unfortunately, neither of these studies reported their dose-response curves for reference. These outliers may be attributed to the diverse, heterogenous mutational landscape of melanoma that extends far beyond BRAF, NRAS, and NF1 mutation status; or they could be a consequence of study design and uninformative drug dosages. Even so, they serve as an important reminder against making broad generalizations from experiments in a limited number of model systems that may not fully represent the grander scheme, especially when RAC1 P29S occurs at a relatively low frequency in melanoma, thus limiting the availability human samples with endogenous *RAC1* c.85C>T.

In addition to sustaining MAPK signaling, RAC1 P29S appears to stimulate additional mechanisms of BRAFi and MEKi resistance. For example, Mohan *et al*. have proposed that RAC1 P29S/PAK signaling inactivates the NF2 tumour suppressor to sustain proliferation amid MAPK

inhibition, as discussed previously[241]. Further support for the RAC1 P29S/PAK signaling axis in mediating MAPKi resistance has been published where A375 cells overexpressing RAC1 P29S with PAK knockdown were treated with PLX4720[261]. PAK knockdown reduced p-ERK levels upon inhibitor treatment and effectively re-sensitized the cells to BRAFi. PAK knockdown also further sensitized A375 cells without RAC1 P29S overexpression to BRAF inhibition. AKT-mediated BRAFi resistance was also shown to be dependent on PAK—as mentioned previously, RAC1 signaling has a degree of crosstalk with AKT signaling, mediated through PAK[261]. Taken together, RAC1 downstream effector PAK plays a complex and extensive role in mediating BRAFi resistance. Synergistic co-inhibition of PAK and BRAF could be a promising strategy to improve response in BRAF-mutant/RAC1 P29S melanoma, and its usefulness would likely extend to RAC1 WT contexts as well, as high PAK1 activation has been detected in many melanoma samples without RAC1 P29S[261]. Similarly, inhibition of the SRF/MRTF signaling axis has been shown to reverse BRAFi resistance that is otherwise associated with the dedifferentiated phenotype of RAC1 P29S melanoma, and combination therapy has been successful in mouse models to sensitize tumours to inhibition. If RAC1 P29S does confer early resistance to BRAFi intervention, combination therapies present a promising option to mitigate resistance and improve treatment outcomes.

IV.1.2 Immune checkpoint blockade

As another frontline strategy for melanoma intervention, ICB is a promising option for RAC1 P29S melanoma. There has been a correlation between RAC1 P29S mutational status in human melanoma of the TCGA-SKCM cohort and PD-L1 mRNA upregulation, which is a positive prognostic marker for response to anti-PD-1 immunotherapy, suggesting that RAC1 P29S expression itself may be a predictor of response[253]. Additional studies discussed in section III.3 provide further evidence for PD-L1 upregulation by RAC1 P29S[233,239]. However, further research is needed to validate these observations as melanoma is a mutationally heterogeneous disease and this relationship may not be maintained uniformly across cases of RAC1 P29S-mutant melanoma. Even so, additional factors also contribute to the status of RAC1 P29S melanoma as a promising target for ICB. RAC1 P29S occurs in melanoma that have a significant UV-damage signature and an elevated TMB[33]. Greater TMB is thought to increase the enrichment of neoantigens available for immune recognition, and RAC1 P29S itself may act as a neoantigen as well[262]. If ICB could

be applied in these patients to suppress immune evasion, these tumours may be more highly sensitized to immune clearance[28].

IV.2 *Potential specific therapeutic targets in RAC1 P29S melanoma*

As the most evident driving force in RAC1 P29S mutant melanoma, RAC1 P29S itself is an attractive target for inhibition in affected melanomas. Many techniques for inhibition RAC1 signaling currently exist, although their applications are largely limited to a research context. Small GTPases have been notoriously challenging therapeutic targets due to their high affinity for guanine nucleotides and poor availability of deep binding pockets, but there has been some success in developing competitive RAC1 inhibitors that interfere with GTP-binding at the nucleotide-binding pocket. Some such RAC1 inhibitors have shown promise in pancreatic cancer cell culture[263,264]. RAC1 inhibitors may alternatively interrupt appropriate localization necessary for RAC1 activity. More frequently, RAC1 inhibitors are designed to interrupt GEF binding, and the discovery of Trp56 as a critical RAC1 residue for GEF selectivity was an important milestone in the guidance of such inhibitors[265]. NSC23766 was one of the frontrunners of this class, blocking selective RAC1-TIAM1 and RAC1-TRIO association and suppressing tumourigenesis in cancer models, but it had low efficacy and was deemed unsuitable for clinical settings (reviewed in [266]). EHT1864 similarly blocks RAC1-TIAM1 interaction while also displacing the bound nucleotide, but unfortunately it has reportedly been ineffective at suppressing RAC1 P29S or RAC1 WT in melanoma models[240,264]. More potent derivatives of NCS23766 have been designed, such as EHop-016, which blocks RAC1-VAV1 interaction to suppress breast cancer cell migration, but it is poorly selective for RAC1[267]. Virtual screens have identified many more like inhibitors, most notably 1A-116, which blocks RAC1-PIP_3-dependent Rac exchanger 1 (P-REX1) and has suppressed pro-tumourigenic effects of RAC1 activation *in vitro* and *in vivo* (reviewed in [264]). This year, it was reported that 1A-116 could suppress the activity of the RAC1 P29S mutant isoform *in vitro*[268]. If suitable for the clinic, a drug such as 1A-116 could be useful in RAC1 P29S melanoma and beyond; interference with P-REX binding could be widely advantageous since P-REX1 and P-REX2 are often upregulated or mutated in melanoma[269]. It is important to note that RAC1 is a ubiquitously expressed protein and its inhibition could lead to adverse effects in healthy tissue. The RAC1 P29S mutant presents a unique opportunity for exclusive selectivity toward this mutant and not the wild-type protein as RAC1 P29S adopts a highly distinctive conformation by

consequence of its switch I substitution[34]. It will be interesting to see if rational drug design will exploit these differences to develop new RAC1 P29S-specific compounds in the coming years.

Not only does intrinsic RAC1 P29S hyperactivity contribute to its oncogenicity, but direct regulators that influence RAC1 P29S activity and localization may also be responsible for aberrant RAC1 signaling. Thus, regulatory proteins present another route for intervention in RAC1 P29S melanomagenesis, though they are not ideal drug targets. Such strategies have already produced promising results *in vitro.* DOCK1 knockout has been shown to ablate RAC1 P29S-driven invasion and macropinocytosis in mouse embryonic fibroblasts with overexpression of HA-tagged RAC1 P29S[256]. Treatment with DOCK inhibitor TBOPP was similarly able to reverse the RAC1 P29S-associated oncogenic behaviour in a dose-dependent manner. When these DOCK1 inhibition experiments were performed in cancer lines with endogenous RAC1 P29S expression, such as IGR1 (melanoma) and MDA-MB-157 (breast cancer), TBOPP maintained its ability to suppress invasiveness and macropinocytosis. To date, other inhibitors of RAC1 regulators have not been tested for their efficacy in a RAC1 P29S setting.

In addition, RAC1 P29S signaling may be interrupted by targeting alternative nodes along its signaling axis. In a triple-WT melanoma setting, a xenograft model has demonstrated that RAC1 P29S-mutant tumour growth could be reduced *in vivo* by treatment with group A PAK inhibitor FRAX-1036[270]. Comparatively, vemurafenib was most effective at reducing tumour growth of RAC1 P29S melanoma in a BRAF-mutant context, while PAK inhibition elicited a lesser response. Unfortunately, although these data suggest that PAK inhibition may be a promising therapeutic strategy for RAC1 P29S-mutant melanoma, FRAX-1036 itself is unsuitable for clinical use due to its strong inhibition of hERG potassium channels and consequent toxicity, and other existing PAK inhibitors are likewise ineligible for therapeutic applications[270,271].

Since RAC1 can act directly upstream of PI3Kβ, efforts have been made in the past year to assess the sensitivity of RAC1 P29S melanoma to PI3K inhibition[123]. A study published by Uribe-Alvarez *et al*. suggested that PI3Kβ inhibitors TGX221 and GSK2636771 selectively decreased the viability of melanoma cell lines with endogenous RAC1 P29S expression[272]. They also observed that PI3K inhibition decreased wound healing rate, PAK activation, and ERK activation selectively in RAC1 P29S melanoma lines. Conversely, another study reported that RAC1 P29S melanoma cells were variably sensitive to a panel of four PI3Kβ inhibitors in a colony

formation assay, instead observing more pronounced responses following inhibition of the PI3Kα isoform[273]. Even so, RAC1 P29S lines that showed sensitivity to any PI3Kβ inhibitors maintained sensitivity across all PI3Kβ inhibitors. The variability between lines may be attributed to their different background mutations and cooperative driver events, but this cannot be readily verified as the study regrettably did not include RAC1 WT control lines to match the background of each of their RAC1 P29S lines. Immunoblotting the lysates of cells treated with PI3K inhibitors did not replicate the results of the former study, instead demonstrating inconsistent effects of PI3Kβ on the phospho-activation of downstream signaling components[273]. At this stage, the RAC1 P29S mutation has not been consistently predictive of response to PI3K intervention, and more compelling evidence will be necessary to justify PI3K inhibition in RAC1 P29S-mutant melanoma.

1.2 Research objectives

Over the past decade, extensive genomic screening of melanoma samples has revealed a new putative driver mutation in *RAC1* (c.85C>T) encoding the fast-cycling RAC1 P29S mutant[33,34,229]. Occurring in 5-10 % of cutaneous melanoma, this is the third most frequent recurrent coding hotspot mutation following those in *BRAF* and *NRAS*. Aberrant RAC1 signaling in RAC1 P29S melanoma contributes to disease severity and poor response to several existing therapies. Unbiased interactome analysis performed in our lab has revealed a strongly enriched complex between RAC1 P29S and IQGAP1[239]. Given the role for IQGAP1 in cytoskeletal dynamics, we suspect that an enrichment of RAC1 P29S-IQGAP1 complexes may serve a pivotal role in the development of migratory phenotypes associated with RAC1 P29S. As recent studies have also suggested that morphological changes caused by RAC1 P29S have consequences for cellular signaling, we are interested in uncovering the role of IQGAP1 in other functional and transcriptomic changes that have been observed in the growing body of literature. The primary focus of this thesis is to expand our understanding of the mechanism by which RAC1 P29S affects melanocyte biology, and we hypothesize that the enhanced association of RAC1 P29S with IQGAP1 is a driving force of certain phenotypic and transcriptomic changes associated with malignant progression. In this thesis, we interrogate the role of RAC1 P29S in cellular migration, proliferation, and signaling, while simultaneously exploring the dependence of these processes on interaction with IQGAP1.

2 | Methods

2.1 Cell culture

The primary cell line used in this thesis was HMEL, a partially transformed immortalized human melanocyte line (hTERT/CDK4(R24C)/p53DD) with BRAF V600E expression (pMEL-BRAF V600E). Isogenic HMEL-pHAGE (eGFP, RAC1 WT, RAC1 P29S) lines have been previously established using lentiviral infection, and further lentiviral infection (see section 2.12) was performed in this thesis to generate HMEL-pHAGE-pLKO.1-BLAST (pHAGE: eGFP, RAC1 WT, RAC1 P29S; pLKO.1-BLAST: SH016C, shIQGAP1#4, shIQGAP1#5). A complete list of HMEL-derived lines can be found in **Table 1** and shRNA oligo sequences are listed in **Table 5**. HEK293RR and HEK293FT human embryonic kidney cells were used in polyethylenimine (PEI) transfection and lentiviral production protocols, respectively. All cell lines were maintained in Dulbecco's modified Eagle's medium (DMEM) supplemented with 5 % Fetal Bovine Serum (FBS) and 1 % Penicillin-Streptomycin at 37 °C in a humidified 5 % CO_2 incubator. Cells were passaged using 0.25 % trypsin; once cells lifted; trypsin was quenched with excess complete medium and cells were re-plated. Cells were counted using a T20 Automated Cell Counter (Bio-Rad, 1450102) when necessary to ensure reproducible plating.

Table 1 | Summary of generated HMEL-derived lines with stable exogeneous expression of target genes or shRNA.

Cell line code	Expression plasmid 1	Expression plasmid 2
HMEL-GFP	pHAGE-IRES-Ef1α-eGFP	N/A
HMEL-RAC1 WT	pHAGE-IRES-Ef1α-RAC1 WT	N/A
HMEL-RAC1 P29S	pHAGE-IRES-Ef1α-RAC1 P29S	N/A
HMEL-GFP-shCtl	pHAGE-IRES-Ef1α-eGFP	pLKO.1-BLAST-SH016C
HMEL-GFP-shIQGAP1#4	pHAGE-IRES-Ef1α-eGFP	pLKO.1-BLAST-shIQGAP1#4
HMEL-GFP-shIQGAP1#5	pHAGE-IRES-Ef1α-eGFP	pLKO.1-BLAST-shIQGAP1#5
HMEL-RAC1 WT-shCtl	pHAGE-IRES-Ef1α-RAC1 WT	pLKO.1-BLAST-SH016C
HMEL-RAC1 WT-shIQGAP1#4	pHAGE-IRES-Ef1α-RAC1 WT	pLKO.1-BLAST-shIQGAP1#4
HMEL-RAC1 WT-shIQGAP1#5	pHAGE-IRES-Ef1α-RAC1 WT	pLKO.1-BLAST-shIQGAP1#5
HMEL-RAC1 P29S-shCtl	pHAGE-IRES-Ef1α-RAC1 P29S	pLKO.1-BLAST-SH016C
HMEL-RAC1 P29S-shIQGAP1#4	pHAGE-IRES-Ef1α-RAC1 P29S	pLKO.1-BLAST-shIQGAP1#4
HMEL-RAC1 P29S-shIQGAP1#5	pHAGE-IRES-Ef1α-RAC1 P29S	pLKO.1-BLAST-shIQGAP1#5

2.2 Cell lysis

Cell plates were rinsed 2x in cold D-PBS and lysed in an appropriate lysis buffer with gentle agitation for 30 m at 4 °C. For immunoprecipitation, lysates were prepared in EBC lysis buffer (120 mM NaCl, 0.5 % (v/v) IGEPAL CA-630, 0.2 mM sodium orthovanadate, 100 mM NaF, 50 mM Tris-Cl (pH 8.0), supplemented with 1X Halt protease inhibitor cocktail (Thermo Scientific, 78430)). All other lysates were prepared in RIPA lysis buffer (150 mM NaCl, 50 mM Tris (pH 8.0), 1 % (v/v) IGEPAL CA-630, 0.5 % (m/v) sodium deoxycholate, 0.1 % (m/v) SDS, supplemented with 1X Halt protease inhibitor cocktail). Lysates were centrifuged at 14,000 rpm for 10 m at 4 °C. Supernatant was kept on ice and protein concentration was quantitated using the DC protein assay (Bio-Rad, 5000116) according to manufacturer's protocol. With the exception of material intended for pulldown protocols (see sections 2.6 and 2.7), protein samples were normalized and a 1:3 volume of 4X NuPAGE LDS Sample Buffer (Invitrogen, NP0007) with 0.05 M DTT was added prior to boiling the samples at 95 °C for 5 m. Denatured protein samples were stored at -20 °C prior to gel electrophoresis.

2.3 SDS-PAGE and western blot

Polyacrylamide 8 % separating and 5 % stacking gels were cast the day of electrophoresis. A minimum of 12.5 µg protein was loaded per sample, alongside 10 µL of Precision Plus Protein Kaleidoscope Prestained Protein Standard (Bio-Rad, 1610395). Tris-glycine running buffer (25 mM Tris, 192 mM Glycine, 0.1 % SDS, pH 8.3) chilled to 4 °C was used for sodium dodecyl sulphate-polyacrylamide gel electrophoresis (SDS-PAGE). Gels were run at 100 V for 30 m, then at 120-130 V for 40-80 m, depending on the required degree of separation.

Proteins were transferred to nitrocellulose using the Trans-Blot Turbo Transfer System (Bio-Rad, 17001915) on the Mixed MW (Turbo) setting according to manufacturer's protocol. Membranes were blocked in 5 % non-fat skim milk (NFSM)-PBS-T (137 mM NaCl, 2.7 mM KCl, 8 mM Na_2HPO_4, and 2 mM KH_2PO_4 with 0.01 % (v/v) Tween-20) for 1 h at room temperature (RT), then rinsed in PBS-T and immunoblotted with primary antibodies overnight under gentle agitation at 4 °C. Primary antibodies were diluted in PBS-T (0.05) with 5 % bovine serum albumin (BSA) and 0.05 % NaN_3. Primary antibodies used: α-HSP70 at 1/1,000 (Cell Signaling Technologies, 4872); α-IQGAP1 at 1/500 (Abcam, ab86064); α-VINCULIN at 1/10,000 (Abcam,

ab18058); α-PD-L1 at 1/1,000 (Cell Signaling Technology, 13684); α-RAC1 at 1/500 (Cell Biolabs, STA-401-1, Part No. 240106); α-GAPDH at 1/2,000 (Cell Signaling Technologies, 2118); α-GFP at 1/2000 (Clontech, 632381); and α-V5-Tag at 1/2000 (Invitrogen, 46-0705). Next, membranes were rinsed 5x in PBS-T and secondary antibody was added at a 1:2,000 dilution prepared in 5 % NFSM-PBS-T and incubated at RT with agitation for 60 m. Secondary antibodies used: α-rabbit IgG, HRP-linked (Cell Signaling Technologies, 7074) and α-mouse IgG, HRP-linked (Cell Signaling Technologies, 7076). Membranes were then rinsed 5x in PBS-T, followed by addition of ECL Prime Western Blotting Detection Reagent (Sigma-Aldrich, RPN2236) and 3 m incubation at RT. Blots were captured and developed in a dark room using traditional film technique.

2.4 PEI transfection

HEK293RRs were grown to 80 % confluence in 100 mm tissue culture dishes. For each transfection, 3 μg of plasmid DNA (per plasmid) and 4:1 linear PEI were combined in Opti-MEM Reduced Serum Medium (Gibco, 31985070) to a total volume of 640 μL. The mixture was vortexed for 10 s and incubated at RT for 20 m. Meanwhile, HEK293RR plates were rinsed 2x in D-PBS and replenished with 9 mL of complete DMEM. Following incubation, 600 μL of transfection mixture was added dropwise to the plate in a concentric circle pattern. The plate was gently mixed to facilitate diffusion of the transfection mixture and then incubated at 37 °C in a humidified 5 % CO_2 incubator. At 12 – 16 h post-transfection, transfection media was aspirated and replenished with complete medium. Cells were lysed next day for use in proteomic investigative protocols. Plasmids used in transfection: pLX307-IQGAP1 (V5 tag); pcDNA3-RAC1 (GFP tag; RAC1 T17N, RAC1 WT, RAC1 P29S, RAC1 Q61L). All plasmids had been sequence-verified following midi-prep (Qiagen, 12943) to validate the gene of interest by sanger sequencing.

2.5 siRNA transfection

HMELs were seeded at 1.25E5 cells/well in a 6-well plate. The next day, cells were transfected with siRNA according to manufacturer's protocol, where 5 μL DharmaFECT reagent was used per transfection. The siRNAs applied include siGENOME IQGAP1 siRNAs #3 and #4 (Dharmacon, D-004694-03-0002 and D-004694-04-0002), siGENOME Non-Targeting Control

siRNA #1 (Dharmacon, D-001210-01-05), and ON-TARGETplus GAPD Control siRNA – Human (Dharmacon, D-001830-01-05). Transfection media was replaced with complete media after 24 h. Cells were lysed at 48 h post-transfection unless otherwise indicated.

2.6 Co-immunoprecipitation

Protein A Sepharose CL-4B beads (GE Healthcare, 17-0780-01) were prepared by reconstituting 0.375 g of beads in 20 mL of 4 % BSA-NETN (NETN: 100 mM NaCl, 20mM Tris-Cl (pH 8.0), 0.5 mM EDTA, 0.5% (v/v) Nonidet P-40) and rocking the mixture for 30 m at 4 °C, followed by centrifugation at 3000 rpm for 5 m at 4 °C and aspiration of the supernatant. Next, beads were rinsed 2x in 4 % BSA-NETN, where each rinse was followed by 5 m of rocking at 4 °C and centrifugation at 3000 rpm for 5 m at 4 °C. Finally, the beads were suspended in an equal volume of NETN and stored at 4 °C until use.

Cells were lysed in EBC lysis buffer according to the cell lysis protocol. Protein stocks were normalized to 1 µg/µL and kept on ice; 1 mL was used for each co-immunoprecipitation (co-IP), while 4X NuPAGE with 0.05 M DTT was added 1:3 to the remainder, which was boiled at 95 °C for 5 m and stored at -20 °C. To each 1 mL of protein lysate, 2 µg of IP antibody was added (GFP-IP: α-GFP rabbit pAb (Clontech, 632460); or V5-IP: α-V5 rabbit pAb (Millipore, AB3792)) and the solution was rotated end-over-end for 90 m at 4 °C. To the protein-antibody solution, 60 µL of Protein A Sepharose CL-4B beads were added and the mixture was rotated end-over-end for 30 m at 4 °C, followed by centrifugation at 13,000 rpm for 30 s at 4 °C. Supernatant was carefully aspirated and beads were rinsed 5x in 0.5 mL NETN. Following the final rinse and aspiration, 50 µL of 1X NuPAGE with 0.013 M DTT was added to co-IP products, which were boiled at 95 °C for 5 m and stored at -20 °C. When separating co-IP products by SDS-PAGE, 15 µL (30%) of co-IP product was loaded; 12 µg of input sample was loaded; and 10 µL of Precision Plus Protein Kaleidoscope Prestained Protein Standard (Bio-Rad, 1610395) was loaded. SDS-PAGE ran at 100 V for 30 m, followed by an additional 90 m at 130 V.

2.7 RAC1 activation assay

HMELs were seeded at 1.50E5 cells/well in triplicate in a 6-well format. Following siRNA transfection, cells were lysed in RIPA lysis buffer and triplicate lysates were pooled prior to quantitation. Protein was normalized and 30 µg per sample was aliquoted for immediate addition

of 4X NuPAGE with 0.05 M DTT and boiling according to cell lysis protocol for use as an input reference. The remaining 550 µg per sample was topped up to a volume of 1 mL with RIPA, 25 µL of resuspended PAK PBD Agarose bead slurry (Cell Biolabs, STA-401-1) was added to each sample, and the RAC1 pulldown assay was performed according to manufacturer's protocol with the following deviation: only 25 µL of 2X NuPAGE with 0.025 M DTT was used for final bead pellet resuspension. When running products by SDS-PAGE, 18 µg of input sample and 40 % (16 µL) of pulldown product were loaded, and gels were run at 100 V for 30 m, then at 130 V for 30 m.

2.8 IFN-γ induction

HMELs were seeded in 100 mm tissue culture plates at a density of 3.00E5 cells/plate, or in triplicate at 1.50E5 cells/well in a 6-well format when coupled with siRNA transfection. After two days of growth or at 24 h post-siRNA transfection, medium was replaced with complete medium supplemented with 0.1 µg/mL IFN-γ (PBL Assay Science, 11500-1). At 48 h post-IFN-γ addition, cells were lysed in RIPA lysis buffer according to the cell lysis protocol. When running products by SDS-PAGE, 21 µg of sample was loaded, and the 8 % polyacrylamide gels were run at 100 V for 30 m, then at 130 V for 30 m.

2.9 Time-lapse live cell-imaging

HMELs were seeded in a µ-Slide 8-well ibiTreat plate with DIC lid (ibidi, 80826 and 80055) at 7.5E3 cells/well for next day imaging. When coupled with siRNA transfection, cells were seeded for imaging at 24 h post-transfection, and time-lapse imaging occurred between 48 h and 72 h post-transfection. During image acquisition, live cell chamber conditions were maintained at 37 ˚C and 5 % CO_2 with humidification. Three representative positions were selected per well and images were captured at 10 m intervals spanning 16 h (96 frames). Due to limited equipment availability, each replicate of random migration experiments was captured under slightly different microscopy conditions, as summarized in **Table 2-4**.

Table 2 | HMEL random migration settings for each experimental replicate.

Biological replicate	n=1	n=2	n=3
Microscope	LSM 700 AxioObserver	LSM 700 AxioObserver	Axio Observer.Z1/7
Objective	20x/0.8	10x/0.45	10x/0.3
Laser (nm): power (%)	639: 1	488: 0.5	None (halogen light source)
Z-stack	3 slices (8 µm)	3 slices (8 µm)	None
Image size (pixels)	512x512	512x512	1376x1104
Scaling (µm per pixel)	1.25x1.25	2.50x2.50	0.908x0.908
Bit Depth	12-bit	12-bit	14-bit

Table 3 | HMEL with siIQGAP1-03 random migration settings for each experimental replicate.

Biological replicate	n=1	n=2	n=3
Microscope	LSM 700 AxioObserver	LSM 700 AxioObserver	Axio Observer.Z1/7
Objective/aperture	20x/0.8	10x/0.45	10x/0.3
Laser (nm): power (%)	488: 1	488: 0.5	None (halogen light source)
Z-stack	3 slices (8 µm)	3 slices (8 µm)	None
Image size (pixels)	512x512	512x512	1376x1104
Scaling (µm per pixel)	1.25x1.25	2.50x2.50	0.908x0.908
Bit Depth	12-bit	12-bit	14-bit

Table 4 | HMEL with siIQGAP1-04 random migration settings for each experimental replicate.

Biological replicate	n=1	n=2
Microscope	LSM 700 AxioObserver	LSM 700 AxioObserver
Objective	20x/0.8	10x/0.45
Laser (nm): power (%)	488: 1	488: 0.5
Z-stack	3 slices (8 µm)	3 slices (8 µm)
Image size (pixels)	1024x1024	512x512
Scaling (µm per pixel)	0.63x0.63	2.50x2.50
Bit Depth	12-bit	12-bit

2.10 Migration data processing and analysis:

Manual cell tracking was performed in Fiji using the MTrackJ plugin. All cells were tracked and only tracks spanning ≥ 3 h (18 frames) were used in analysis. In the case of cell division, a parent's track was terminated before emergence of a visible mitotic phenotype and daughter cells were each given distinct tracks once they resolve in the frames following division. Where possible, the nucleus of a cell was used for tracking; in ambiguous cases, the GFP channel

was used to guide manual tracking of the DIC channel to track the center of the cell if it could not otherwise be confidently discerned due to poor contrast. The MTrackJ point readout for each condition was formatted for compatibility with the ibidi Migration and Chemotaxis Tool plugin for Fiji to retrieve directionality plots as well as Euclidean distance and directionality metrics. The MTrackJ track readouts for each condition were compiled along with the additional metrics, and the data were analyzed in R. The "car" package was used to perform ANOVAs, and the "multcomp" package was used for post-hoc Tukey-Kramer multiple comparison tests. Graphs were produced using Prism6. Experimental replicates were evaluated independently, and representative experiments are presented; data were never pooled from temporally distinct biological replicates.

2.11 Subcloning pLKO.1-BLAST with shIQGAP1 oligos

First, pLKO.1-BLAST (empty vector) was validated by a diagnostic double digest using SphI-HF and AgeI-HF (New England Biolabs). The vector was then linearized with simultaneous EcoRI-HF and AgeI-HF endonuclease digestion (500 ng DNA, 25 µL reaction volume) performed 4x in parallel and each run on a 1 % agarose gel at 130V for 35 m. Bands were excised and purified according to kit protocol (Qiagen, 28704). The four columns were eluted sequentially using 30 µL total elution buffer to pool the purified DNA. shRNA oligos were designed and ordered through Sigma Aldrich, summarized in **Table 5**. Reconstituted oligo pairs were annealed by combining 1.125 nmol of each oligo with 10X annealing buffer (1 M NaCl, 100 mM Tris-HCl, pH 7.4), heating the mixture to 95 ˚C and allowing it to slowly cool to RT in an insulated box over a period of 5 h. The cooled mixture was diluted 1:400 in 0.5X annealing buffer and stored at -20 ˚C. Ligation of annealed pairs into the linearized plasmid backbone was performed by combining 1 µL of diluted annealed oligos with 1 µL of purified digested plasmid (10-20 ng), 1 µL of 10X ligase buffer, 1 µL of T4 DNA ligase, and 6 µL of H_2O. The mixture was incubated at RT for 3 h. On ice, 4 µL of ligation product was added to 25 µL of StBl3 *E. coli*, incubated for 30 m followed by a 45 s heat shock at 42 ˚C, then incubated on ice again for 5 m. Next 500 µL SOC medium was added and transformed bacteria were incubated at 37 ˚C for 30 m in a shaking incubator. LB agar plates with 50 µg/mL carbenicillin were warmed to 37 ˚C, plated with 200 µL of cell mixture, and incubated overnight at 37 ˚C. Single colonies were isolated, DNA-prepped and sequence-verified using pLKO shRNA fw sequencing primer.

Table 5 | Oligo and primer sequences used in sub-cloning of pLKO-BLAST-shIQGAP1.

ID	Type	Sequence
shIQGAP1#4 – T2	Oligo	CCGGGGCATCCACTTACCAGGATATACTCTCGAGAGTATATCCTGGTAAG TGGATGCCTTTTT
shIQGAP1#4 - B	Oligo	AATTAAAAAGGCATCCACTTACCAGGATATACTCTCGAGAGTATATCCTG GTAAGTGGATGCC
shIQGAP1#5 - T	Oligo	CCGGCCAGTAATCTACATTTCCATTCTCGAGAATGGAAATGTAGATTACT GGTTTTT
shIQGAP1#5 - B	Oligo	AATTAAAAACCAGTAATCTACATTTCCATTCTCGAGAATGGAAATGTAGA TTACTGG
SH016C - T	Oligo	CCGGGCGCGATAGCGCTAATAATTTCTCGAGAAATTATTAGCGCTATCGC GCTTTTT
SH016C - B	Oligo	AATTAAAAAGCGCGATAGCGCTAATAATTTCTCGAGAAATTATTAGCGCT ATCGCGC
pLKO shRNA fw sequencing primer	Primer	GGCAGGGATATTCACCATTATCGTTTCAGA

2.12 Lentivirus production and stable cell line generation

HEK293FT cells were seeded in 100 mm plates at 4.00E6 cells/plate the day before transfection. For 500 µL total volume, 2000 ng of desired expression plasmid, 500 ng of pMD2G, and 1500 ng of psPAX2 were combined in Opti-MEM Reduced Serum Medium. In the negative infection control, no expression plasmid was added. Separately, 15 µL Lipofectamine 2000 was diluted in 485 µL Opti-MEM Reduced Serum Medium, to be combined 1:1 with the DNA mixture and incubated at RT for 20 m. Next, 1 mL of combined transfection mix was added dropwise to HEK293FTs immersed in 9 mL complete DMEM and plates were transferred to a viral incubator. Media was collected and replenished at 24 h, 48 h, and 72 h post-transfection and stored at 4 ˚C. At 72 h, pooled collected media was centrifuged at 2500 rpm for 5 m and passed through a 0.45 filter. The filtered media was supplemented with 25 % (v/v) polyethylene glycol and refrigerated overnight. Finally, the solution was centrifuged for 30 m at 4000 rpm and 4 ˚C. The viral pellet was resuspended in 100 µL complete medium (with approx. 100 µL residual liquid) and aliquoted in 5 x 40 µL for storage at -80 ˚C.

2.12.1 *Lentiviral infection*

HMELs were seeded at 3.00E5 cells in a 100 mm plate the day before infection. Next day, media was replaced with 10 mL complete medium supplemented with 6 µg/mL polybrene and 20

μL viral suspension. After 24 h exposure to lentivirus, cells were rinsed 3x with D-PBS. A 24 h recovery period was allotted before selection in complete media + 10 μg/mL Blasticidin S for 6 d, with media change every 3 d. Following selection, surviving populations were expanded and verified.

2.13 Proliferation assays

An IncuCyte S3 Live-Cell Analysis System (Sartorius, 4647) was used to quantify proliferation assays. HMELs were seeded in a 96-well tissue culture plate at 2.00E3 cells/well with five replicates per treatment; there were 12 conditions in all as each of six stable cell lines was cultured in either complete medium with 5 % FBS or medium with 1 % FBS. The day following seeding, the cell plate was loaded into the IncuCyte S3 unit, maintaining temperature at 37 °C in a humidified 5 % CO_2 incubator. Phase contrast imaging began immediately and three images per well were captured every 4 h for 5.7 d; the average of each set of three images was used in analysis. IncuCyte S3 proliferation analysis was trained to the dataset using selected representative images and output was visualized using Microsoft Excel. Severe outliers were detected in three proliferation curves, so these replicates were omitted from the final graphics; as such, the mean confluency for the following conditions were based on four technical replicates instead of five: 5 % FBS, HMEL-GFP-SH016C; 5 % FBS, HMEL-RAC1 WT-SH016; and 5 % FBS, HMEL-RAC1 WT-shIQGAP1#5. Due to discrepancies in initial confluency, data were compared from approx. 40 % confluence onward.

3 | Results

3.1 The RAC1 P29 mutation hotspot in melanoma

RAC1 is a frequently mutated gene in cutaneous melanoma. Our lab has performed a meta-analysis of five discreet WES studies encompassing more than 1,000 melanoma exomes to demonstrate a representative landscape of RAC1 somatic mutations and the prevalence of P29 hotspot mutations[211]. Within this dataset, RAC1 P29S has been identified at a frequency of 4.7 % in cutaneous melanoma bearing a UV signature. Here, the predicted amino acid sequence alterations for all RAC1 somatic mutations identified within the dataset are presented in combination with RAC1 mutation data available from the TCGA-SKCM dataset (**Fig. 3**). Multiple substitutions arise at the P29 locus, but P29S is the most prevalent mutation by a substantial margin and is of particular interest for bearing a signature of UV-mutagenesis by nature of its c.85C>T transition.

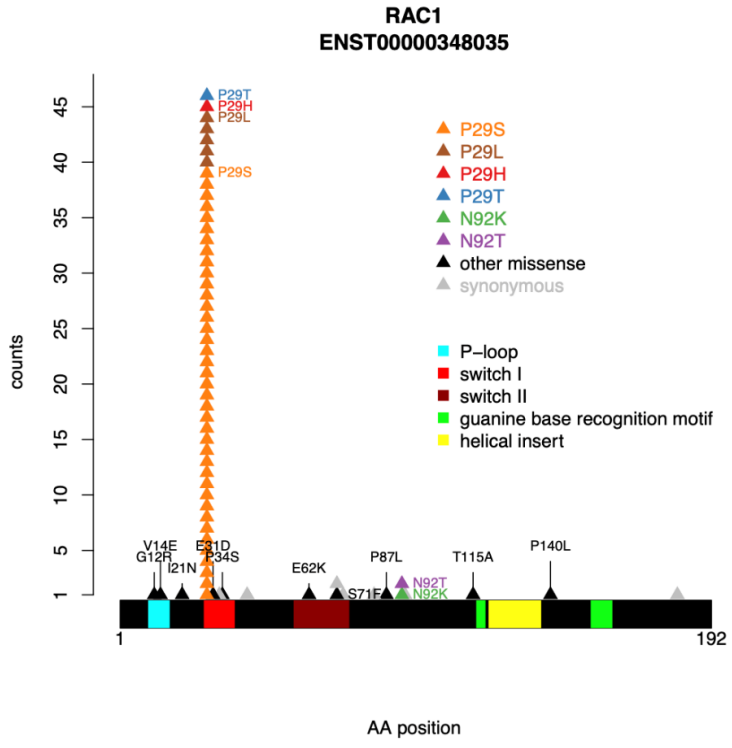

Figure 3 | Landscape of RAC1 somatic mutations in cutaneous melanoma. Publicly available WES of cutaneous melanoma from The Cancer Genome Atlas (n=479) and additional WES data curated by Alkallas *et al.* (n=1,014) were pooled[211]. Identified somatic mutations were plotted along the RAC1 amino acid sequence according to their frequency with RAC1 domains clearly annotated for reference.

3.2 RAC1 P29S enhances random migration

To understand the functional role of RAC1 P29S in the enhanced migratory and metastatic phenotypes of melanoma bearing this mutation, isogenic human immortalized melanocytes were used in a series of random migration assays to determine whether RAC1 P29S affects migration *in vitro*. First, migration of parental HMELs and HMEL-pHAGE lines was recorded using time-lapse confocal microscopy under live cell conditions. Directionality plots representing every cell track, translocated to start at origin, demonstrate similar pathing of HMEL parental cells and the HMEL-GFP control line (**Fig. 4A**). Likewise, HMELs expressing RAC1 WT or RAC1 P29S had similar tracks to one another that would terminate farther from origin than cell lines without exogenous RAC1 expression. Quantitative assessment of track mean speed (*i.e.* entire track length over time) supported these qualitative observations (**Fig. 4B**). HMEL parental and HMEL-GFP migratory speeds were statistically indistinguishable, indicating that stable expression of the pHAGE plasmid did not significantly alter migration. In contrast, overexpression of either RAC1 isoform significantly increased migration speed. While there was a slight increase in the mean migration speed of HMEL-RAC1 P29S over HMEL-RAC1 WT, their migration speeds were ultimately too similar for this relationship to be statistically significant in any biological replicates of this experimental design.

Mean migration speed is the most meaningful metric from a random migration experimental setup, but we may consider additional outcomes within the context of these mean speed observations. Track velocity (*i.e.* displacement from origin over time) is most relevant when addressing chemotaxis, but it can be informative in random migration assays for quantifying the directional persistence of movement. In this case, there were no significant differences between HMEL parental or HMEL-GFP velocities, just as there were no differences between HMEL-RAC1 WT and HMEL-RAC1 P29S velocities (**Fig. 4C**). Directionality indicates whether cells move in a straight line or take a more convoluted path, and it is defined as the displacement from origin over the entire track length. Here, directionality comparisons between isogenic lines are variable between replicates and do not indicate any remarkable trends (**Fig. 4D**). This investigation into baseline HMEL migration has revealed that RAC1 overexpression enhances migration in HMELs and that HMEL-GFP is a relevant control that will be a useful tool for subsequent experiments.

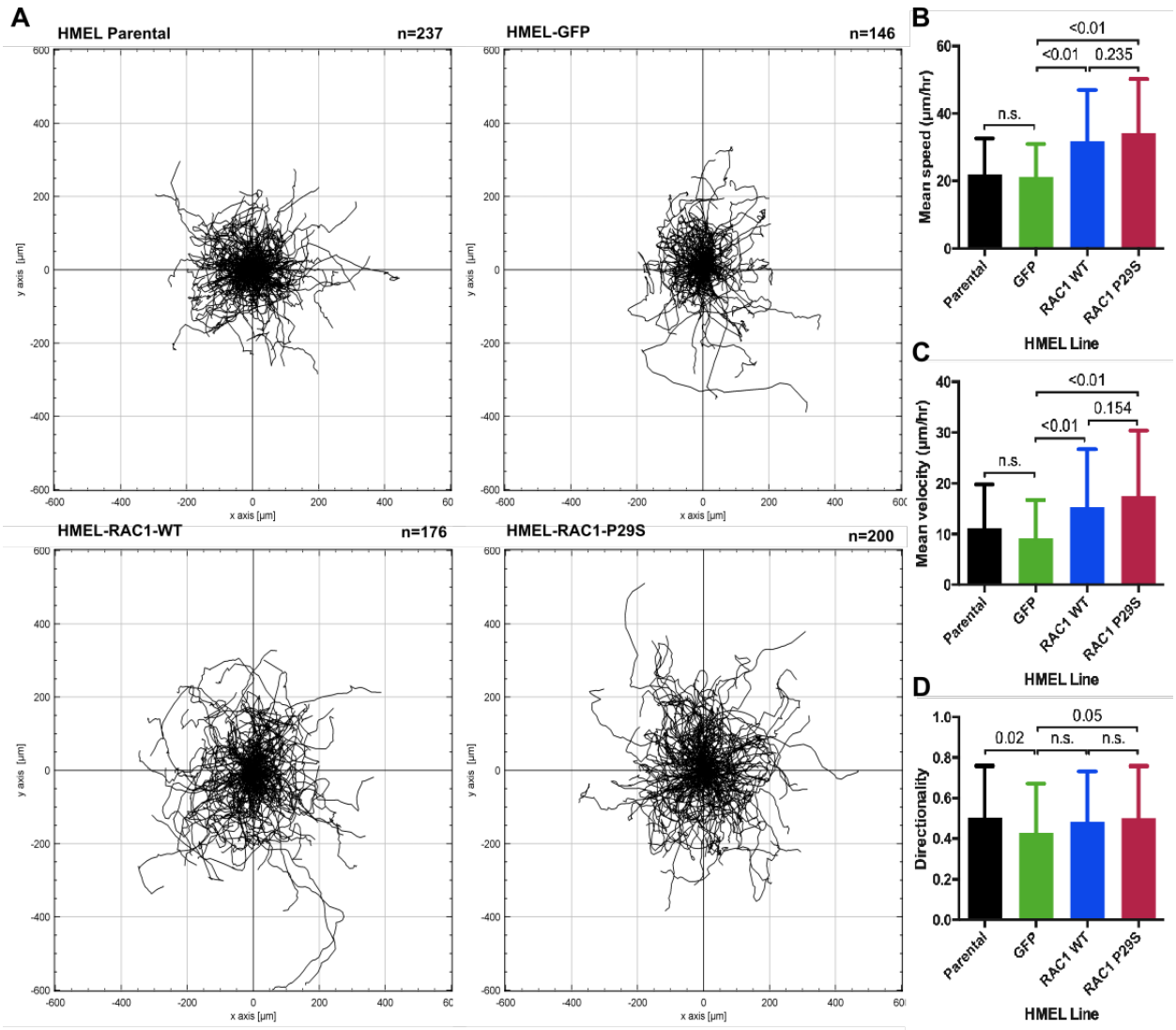

Figure 4 | RAC1 P29S enhances cellular migration in melanocytes harbouring BRAF V600E. Parental HMEL partially-transformed immortalized melanocytes (hTERT/CDK4(R24C)/p53DD and BRAF V600E) and isogenic HMEL-pHAGE lines with stable expression of GFP, RAC1 WT, or RAC1 P29S were used in time-lapse live-cell random migration assays. Each experiment had two technical replicates per cell line. For each technical replicate, three positions were imaged every 10 m for 16 h. All cells were manually tracked, and technical replicates were pooled for analysis (6 positions/cell line). Representative results from one of three biological replicates are shown. **(A)** Directionality plots of random cellular migration, where all tracks begin at origin. **(B)** Mean migration speed of HMELs, defined as total track length over time. **(C)** Mean migration velocity of HMELs, defined as Euclidean distance over time. **(D)** Directionality of random migration as the ratio between Euclidean distance and total track length, bounded between 0 and 1. Error bars represent +/- 1 SD from the mean. Statistical analyses were performed in R using ANOVA and Tukey Kramer multiple comparisons of means.

3.3 IQGAP1 is enriched in complexes with RAC1 P29S

As the RAC1 P29S mutant has previously been associated with increased IQGAP1 co-precipitation using a CapTEV pulldown system, we sought to explore this association using traditional reciprocal co-immunoprecipitation of ectopically expressed tagged constructs for reliable antibody-antigen targeting. HEK293RR cells were transfected with V5-tagged IQGAP1, a GFP-tagged RAC1 species (WT/T17N/P29S/Q61L), or a combination thereof. In the case of V5-tag pulldown, the greatest co-immunoprecipitation occurred with co-expression of RAC1 P29S, suggesting that IQGAP1 has a heightened affinity for this fast-cycling mutant over WT or Q61L (**Fig. 5A**). All RAC1 species co-precipitated with IQGAP1 to some extent; the dominant-negative T17N control was least abundant in the immunoprecipitation product, and the WT protein had an intermediate abundance between the T17N negative control and the constitutively active Q61L positive control. Pulldown of RAC1 P29S was notably pronounced over that of RAC1 Q61L, despite the constitutive activity of Q61L and the known preference of IQGAP1 for GTP-loaded

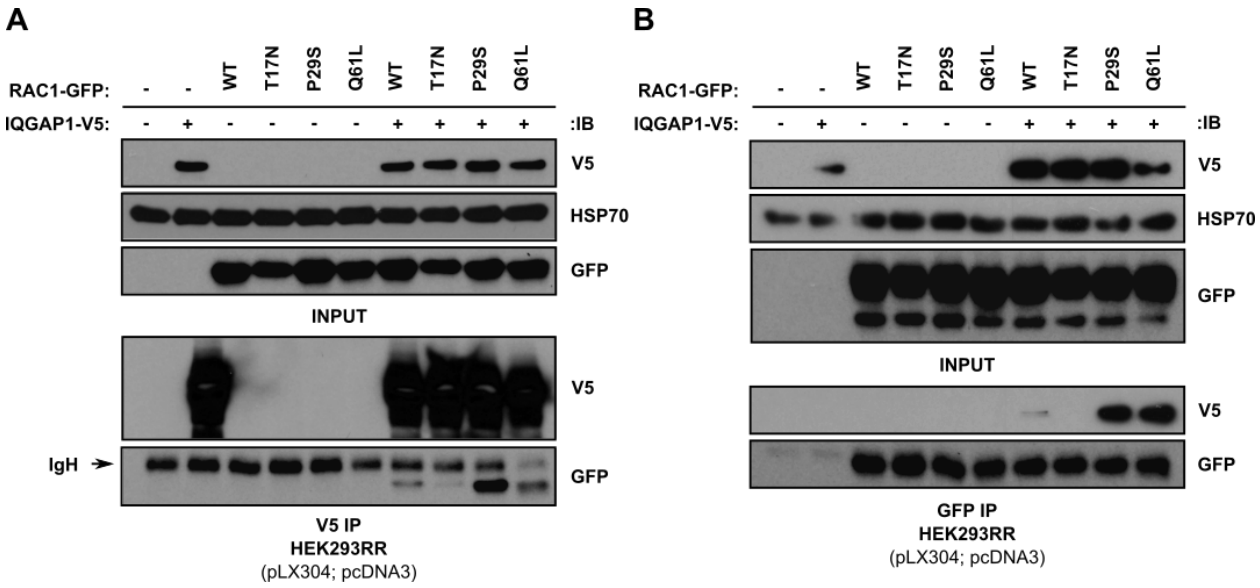

Figure 5 | IQGAP1 is enriched in RAC1 P29S complexes. HEK293RR cells were transfected with V5-tagged IQGAP1 and/or GFP-tagged RAC1 (WT/T17N/P29S/Q61L) for reciprocal co-immunoprecipitation using pAb pulldown onto Protein A Sepharose CL-4B beads. For co-IP protocol, 1 mg of protein was used per condition. SDS-PAGE 8% separating gels were loaded with 12 ug of input or 30 % of co-IP product (15 uL) and run at 100 V for 30 m, then 130 V for 90 m. Representative blots of three biological replicates are shown. **(A)** Immunoblot blot of V5-tag co-immunoprecipitation products. Presence of additional banding in GFP immunoblot is attributed to IgG heavy chain (IgH) and runs <50 kDa. **(B)** Immunoblot of GFP-tag co-immunoprecipitation products.

RAC1. This is suggestive that the unique mutant conformation of RAC1 P29S contributes to increased association with IQGAP1 beyond what would be expected from enhanced GTP-binding alone.

Reciprocal GFP pulldown also supported the notion that the immunoprecipitated RAC1 P29S complex is more strongly associated with IQGAP1 than its wild-type counterpart (**Fig. 5B**). In this experiment, co-IP products reveal once again the reliability of positive and negative control mutants as benchmarks. RAC1 WT co-precipitates with IQGAP1 considerably less than RAC1 P29S. However, here, IQGAP1 detection in the co-IP products of RAC1 P29S and RAC1 Q61L pulldown is equivalent; this may be an artifact of saturation of the beads. Even so, in both experimental setups, there is a definite role for IQGAP1 in association with all RAC1 variants, and this is considerably enriched in RAC1 P29S mutant complexes relative to RAC1 WT.

3.4 IQGAP1 sustains RAC1 P29S activity

To evaluate the role of IQGAP1 in RAC1 signaling, we employed siRNA to silence IQGAP1 expression and examine any effects on the abundance of active RAC1. First, to ensure durable IQGAP1 knockdown, we applied siRNA and validated its efficiency at 48 h and 72 h post-transfection. IQGAP1 was effectively knocked down in all cell lines for the duration (**Fig. 6A**). We then performed a pulldown of active RAC1 using beads conjugated to the PAK1 PBD, the domain of PAK1 where GTP-loaded RAC1 binds to stimulate PAK1 activation. In HMELs with exogenous RAC1 P29S expression, knockdown of IQGAP1 led to a marked reduction in GTP-loaded RAC1 (**Fig. 6B**). Thus, it seems that IQGAP1 positively regulates the RAC1 P29S active state; their enriched association could effectively impede GTP hydrolysis to sequester RAC1 P29S in the active state. Despite this prominent effect in the RAC1 P29S-expressing HMELs, lysates from GFP control cells exhibit an opposite effect, where more active RAC1 is present upon IQGAP1 knockdown. The role of IQGAP1 in modulating RAC1 activity may be relatively complex as it demonstrates the ability to either positively or negatively influence the RAC1 active state, depending on the cellular context.

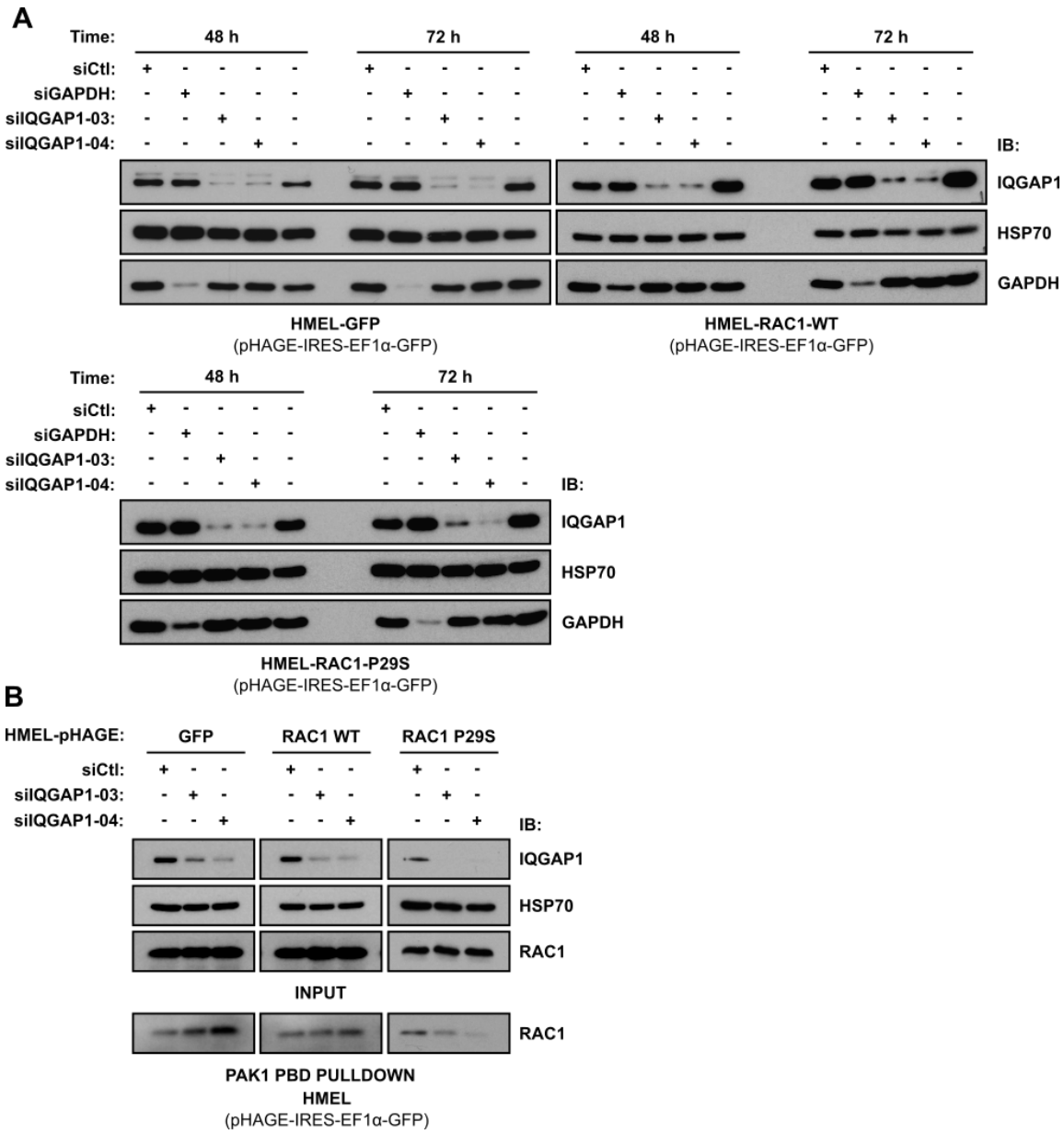

Figure 6 | The RAC1 P29S active state is positively regulated by IQGAP1. (A) HMEL-pHAGE (GFP/RAC1 WT/RAC1 P29S) were treated with non-targeting siRNA (siCtl), positive control siGAPDH, or one of two siRNAs against IQGAP1. Cells were lysed at 48 h and 72 h post-transfection to evaluate knockdown efficacy and durability. SDS-PAGE 8% separating gels were loaded with 28 ug of protein lysate and run at 100 V for 30 m, then 130 V for 50 m. **(B)** HMEL-pHAGE (GFP/RAC1 WT/RAC1 P29S) were transfected with siRNA to deplete IQGAP1 and whole cell lysates were used in PAK1 PBD pulldown to isolate GTP-loaded RAC1. For pulldown protocol, 550 μg of protein was used from each condition. SDS-PAGE 8% separating gels were loaded with 18 ug of input or 40 % of pulldown product (16 uL) and run at 100 V for 30 m, then 130 V for 30 m. Representative blots of three biological replicates are shown. Despite the appearance of similar GTP-loaded RAC1 across all cell lines in the selected exposures, there is dramatically more GTP-loaded RAC1 detected within HMEL-RAC1 P29S when like blot exposure times are compared.

3.5 IQGAP1 silencing enhances IFN-γ response of RAC1 P29S

Mouse xenograft studies have provided preliminary evidence that tumours expressing RAC1 P29S greatly upregulate interferon response pathways, including IFN-γ response. We investigated whether IQGAP1 knockdown would affect such pathways. We stimulated HMEL-RAC1 P29S with 0.1 μg/mL IFN-γ for 48 h following siRNA-mediated knockdown of IQGAP1. PD-L1 expression increased substantially in response to IFN-γ induction (**Fig. 7**). Upon silencing of IQGAP1, PD-L1 became more highly upregulated. These results indicate a possible role for IQGAP1 as a negative modulator of RAC1 P29S-mediated interferon response.

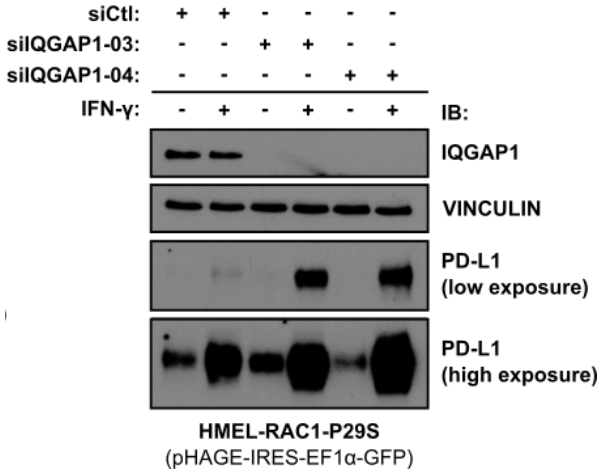

Figure 7 | IQGAP1 knockdown enhances PD-L1 expression. (B) HMEL-pHAGE-RAC1 P29S melanocytes were transfected with siRNA and treated with 0.1 μg/mL IFN-γ 24 h post-transfection. Cells were lysed following 48 h of IFN treatment. Lysates were loaded 28 ug into 8 % separating gel and SDS-PAGE was performed at 100 V for 30 m, then 130 V for 60 m. Following transfer, nitrocellulose membranes were probed for PD-L1 as a marker of IFN-γ response. Low (5 m) and high (15 m) exposures are presented to demonstrate protein abundance in the presence and absence of IFN stimulation. Representative blots of three biological replicates are shown.

3.6 RAC1 P29S slightly enhances proliferation under reduced serum

As recent studies have suggested that the RAC1 P29S mutation confers a proliferative advantage under stressed conditions such as MAPK inhibition or reduced growth factor culture medium, we investigated the effect of reduced serum on the proliferation of HMEL-pHAGE-pLKO cell lines that stable expression of shRNA against IQGAP1 or a nontargeting control. We validated the stable knockdown of IQGAP1 protein expression and observed reliable knockdown with shIQGAP1#5 only, so shIQGAP1#4-expressing cells were not used in subsequent experiments (**Fig. 8A**). Meanwhile, expression of the non-targeting control SH016C sustained IQGAP1 expression.

Next, we performed a proliferation assay using the IncuCyte system to explore any combinatorial effects of IQGAP1 knockdown with low serum on cellular proliferation. In the normal (5 % FBS) serum condition, overexpression of either RAC1 isoform led to an increased proliferative rate relative to the GFP control; however, proliferation was unaffected by IQGAP1 expression status (**Fig. 8B**). IQGAP1 knockdown only decreased proliferation in the GFP-expressing line, but the difference was subtle. Comparatively, the proliferation of all cell lines was reduced in low (1 % FBS) serum conditions, and a pattern emerged where RAC1 P29S overexpression was associated with the highest rate of proliferation, followed by RAC1 WT, and lastly GFP (**Fig. 8C**). Under reduced serum, IQGAP1 knockdown did not greatly affect proliferation in any cell line; IQGAP1 expression status was not predictive of a proliferative differential for RAC1 P29S-expressing cells under normal or reduced serum conditions (**Suppl. Fig. S1**). Instead, exogenous RAC1 expression was more strongly correlated with proliferative rate. During growth at normal serum levels, overexpression of either RAC1 protein elevated proliferation, but RAC1 P29S uniquely sustained slightly higher proliferation than RAC1 WT when cultured at a lower serum concentration.

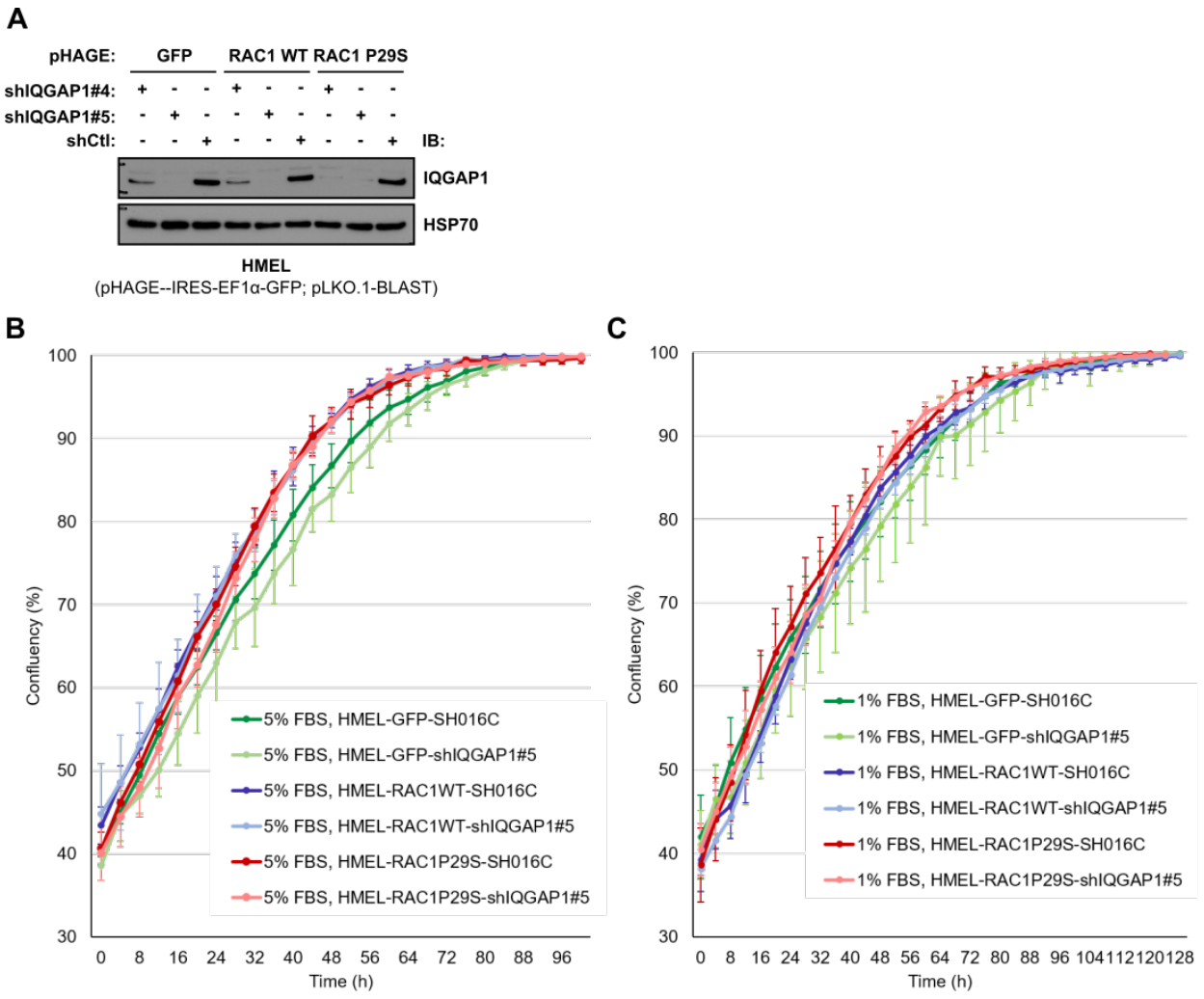

Figure 8 | RAC1 P29S slightly enhances proliferation under low serum. (A) Isogenic HMEL-pHAGE lines with stable IQGAP1 knockdown were generated by lentiviral infection with pLKO.1-BLAST (shIQGAP1#4/shIQGAP1#5 or SH016C nontargeting control). Lysates were prepared in RIPA buffer and immunoblotted to verify knockdown. Separating 8 % gels were loaded with 20 µg protein lysates and separated by SDS-PAGE for 30 m at 100 V, then 40 m at 130 V. **(B-C)** HMEL-pHAGE (GFP/RAC1 WT/RAC1 P29S)-pLKO.1 with stable knockdown of IQGAP1 (shIQGAP1#5) or a nontargeting control (SH016C) were used in an IncuCyte proliferation protocol at 5 % and 1 % FBS with five technical replicates per treatment, or four replicates due to omission of an outlier for the three following conditions: 5 % FBS, HMEL-GFP-SH016C; 5 % FBS, HMEL-RAC1 WT-SH016; and 5 % FBS, HMEL-RAC1 WT-shIQGAP1#5. Error bars represent +/- 1 SD from the mean. **(B)** Proliferation of all cells at 5 % FBS. **(C)** Proliferation of all cells at 1 % FBS.

3.7 IQGAP1 siRNA knockdown consistently reduces RAC1 P29S migratory phenotype *in vitro*

As IQGAP1 is a known coordinator of actin polymerization and RAC1 stimulates actin polymerization for migration at the leading edge, we were interested in the relationship between these two proteins in driving the mesenchymal migration of single melanocytes. Given the enhanced association of IQGAP1 with the RAC1 P29S mutant and our finding that IQGAP1 positively modulates the RAC1 P29S active state, we next performed a series of random migration assays in HMEL-pHAGE isogenic cell lines coupled with siRNA-mediated silencing of IQGAP1. We had previously confirmed the durability of the knockdown over the post-transfection period during which the time-lapse imaging would occur and both siRNAs appeared effective, although siIQGAP1-03 may be marginally less reliable than siIQGAP1-04 over time (**Fig. 9A**).

In the first series of knockdown experiments, directionality plots qualitatively suggest a sequential increase in track length from HMEL-GFP to HMEL-RAC1 WT to HMEL-RAC1 P29S (**Suppl. Fig. S2**). Treatment with siIQGAP1-04 did not seem to affect cell trajectory except in HMEL-RAC1 P29S, where tracks became less expansive and more focused around the origin. These observations were congruent with quantitative the migration outcomes; HMEL-RAC1 P29S treated with non-targeting control siRNA had the greatest migration speed of all cell lines, which was significantly higher than GFP or RAC1 WT lines. Furthermore, HMEL-RAC1 P29S was the only line to experience a reduction in migratory rate upon siIQGAP1-04 treatment (**Fig. 9A**). HMEL-RAC1 P29S with siCtl treatment also had the greatest velocity and was the only line to exhibit a statistically significant decrease in velocity upon IQGAP1 knockdown, which mirrored its reduction in migration speed (**Fig. 9B)**. As the ratio of mean velocity to mean speed was maintained, there was no significant effect on directionality (**Suppl. Fig. S3A)**. To note, the significant decline in HMEL-GFP directionality following IQGAP1 knockdown shown in this dataset was not reproducible and thus was not considered further.

In a series of similar experiments using another siRNA against IQGAP1 (siIQGAP1-03), IQGAP1 knockdown similarly decreased the mean speed and mean velocity of the HMEL-RAC1 P29S line (**Fig. 9C,D & Suppl. Fig. S4**). However, these effects were not specific to this HMEL line; all HMELs experienced some degree of significant reduction in migration speed following IQGAP1 knockdown with this siRNA. This could be a consequence of poorer specificity of this

siRNA leading to off-target effects. Even so, these experiments also support that RAC1 P29S expression contributes to a significantly elevated migration speed relative to GFP or RAC1 WT at baseline. As for directionality, there were no consistent trends of significance upon siIQGAP1-03 addition (**Suppl. Fig. S3B**).

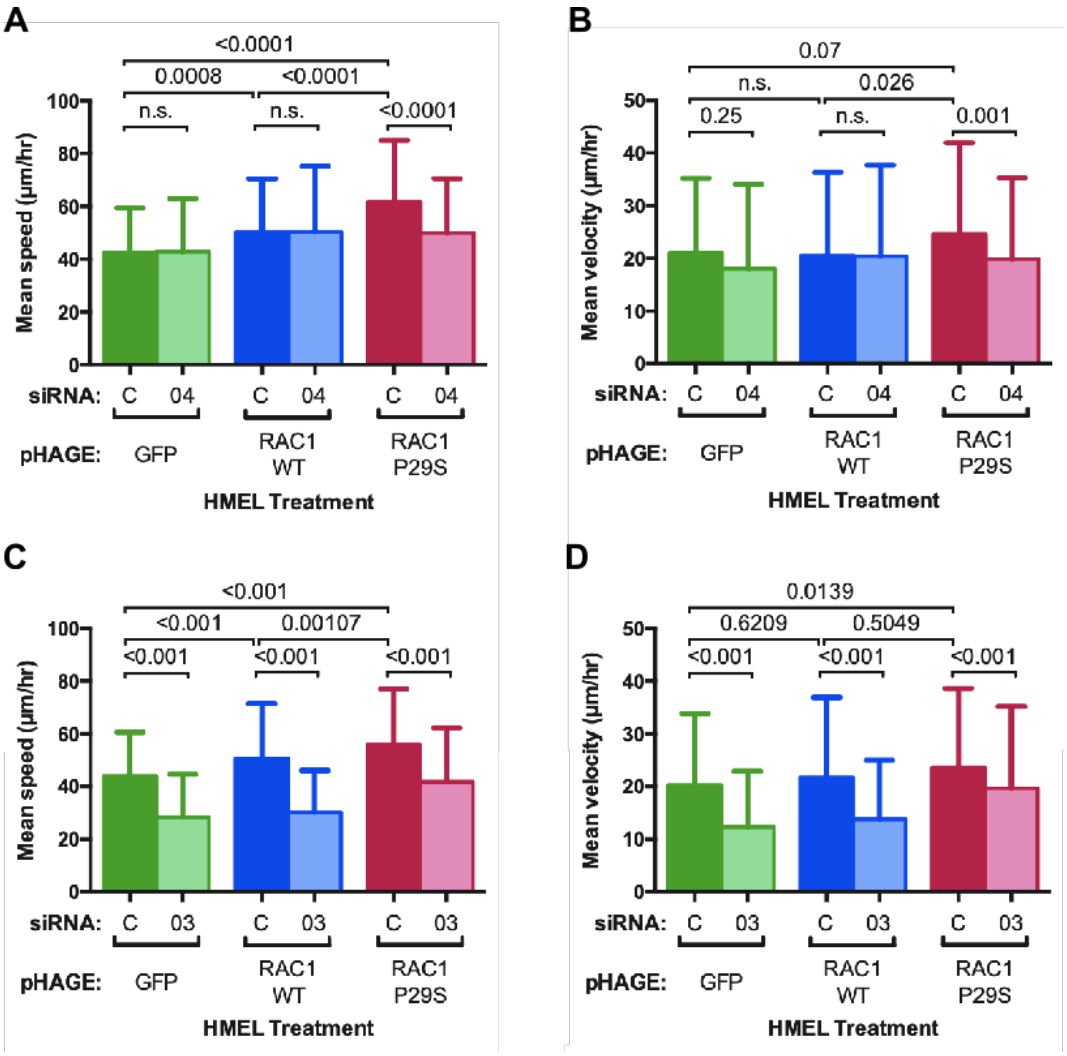

Figure 9 | IQGAP1 knockdown abrogates RAC1 P29S migration. Isogenic HMEL-pHAGE (GFP/RAC1 WT/RAC1 P29S) melanocytes were treated with an siRNA against IQGAP1 or a non-targeting control (siCtl) and used in time-lapse live-cell random migration assays. Three positions were imaged every 10 m for 16 h. All cells were manually tracked, and positions were pooled for analysis. **(A-B)** IQGAP1 knockdown was achieved using siIQGAP1-04 (04). Representative results from one of three biological replicates are shown. **(C-D)** IQGAP1 knockdown was achieved using siIQGAP1-03 (03). Representative results from one of two biological replicates are shown. **(A/C)** Mean migration speed of HMELs, defined as total track length over time. **(B/D)** Mean migration velocity of HMELs, defined as Euclidean distance over time. Statistical analyses were performed in R using ANOVA and Tukey Kramer multiple comparisons of means.

4 | Discussion

Our research group has reevaluated the RAC1 mutational landscape in cutaneous melanoma through meta-analysis of recent melanoma WES studies to demonstrate the enduring relevance of the RAC1 P29S mutation that was first identified in cutaneous melanoma in 2012, which occurs at a frequency of 4.7 % in cutaneous melanoma bearing a signature of UV-mutagenesis (**Fig. 3**)[33,34]. We have validated the association between IQGAP1 and RAC1 P29S by reciprocal co-immunoprecipitation, and we have found the strongest enrichment of IQGAP1 in complex with the P29S mutant isoform (**Fig. 5**). In fact, IQGAP1 was more highly associated with RAC1 P29S than with the constitutively active RAC1 Q61L mutant. This suggests that the basis for the enrichment of RAC1 P29S-IQGAP1complexes extends beyond the inherent hyperactivity of RAC1 P29S, as the Q61L mutation is more highly activating and favours the GTPase active state more strongly; instead, the unique mutant conformation of RAC1 P29S may specifically contribute to its enriched association with IQGAP1 to confer an advantage to this mutant isoform over constitutively activated RAC1 mutants[34].

Additionally, we report that IQGAP1 positively modulates the RAC1 P29S active state (**Fig. 6**). By nature of its enriched association with IQGAP1, RAC1 P29S may be sequestered in the active state to impede GTP hydrolysis and promote signaling. Such a relationship has been previously established between IQGAP1 and CDC42, but has not been thoroughly explored for RAC1[274]. However, the rationale for IQGAP1 knockdown having an opposite effect in the HMEL-GFP control line remains unclear. In rare cases, studies have reported RAC1 P29S and RAC1 WT to have opposing roles in regulating oncogenic processes, supposedly on the basis of having their own distinct mechanisms of regulation and GAP involvement[254]. Perhaps our observation is of a similar vein, where IQGAP1 may promote GTP hydrolysis through recruitment of GAPs to negatively regulate endogenous RAC1 WT but not the P29S mutant. Past studies have demonstrated the ability of IQGAP1 to recruit RACGAP1 to negatively regulate RAC1 activity and membrane dynamics[275]. Additional studies comparing the active states of endogenous RAC1 variants in the absence of IQGAP1 and the identification of GAPs that associate with specific RAC1-IQGAP1 complexes may further clarify the significance of this proposed selective regulation.

Recent studies have demonstrated that RAC1 P29S is associated with elevated immune pathway activation and PD-L1 expression *in vitro* and *in vivo*[239,253]. In this thesis, we present the first investigation into the influence of IQGAP1 on this signaling pathway. Upon knockdown of IQGAP1 in RAC1 P29S-overexpressing melanocytes, PD-L1 became more highly upregulated in response to IFN-γ stimulation (**Fig. 7**). This may seem counterintuitive when considering our evidence that IQGAP1 positively modulates the RAC1 P29S active state; however, IQGAP1 also influences the localization of RAC1, enhancing RAC1 recruitment to the plasma membrane to drive remodeling of cortical actin[69]. Thus, while the RAC1 P29S-IQGAP1complex is maintained, RAC1 P29S may be unable to stimulate certain signaling pathways that are incompatible with this compartmentalization, even if it is more highly present in the active state. Upon knockdown of IQGAP1, RAC1 P29S may be liberated from localizations mediated by this scaffold to become more available to stimulate IFN-γ response and other pathways requiring distinct spatial activation.

Next, we investigated the effect of IQGAP1 on proliferation. As studies have presented a model for enhanced proliferation conferred by RAC1 P29S that is reliant on cortical actin remodeling and only prevalent under stressed conditions, we designed an experiment to dissect the role of IQGAP1 in this mode of proliferation using low serum conditions. Ultimately, we found that RAC1 P29S conferred the greatest rate of proliferation under reduced-serum conditions by a very narrow margin, while stable knockdown of IQGAP1 had no effect on RAC1 P29S-mediated proliferation at 5 % FBS or 1 % FBS (**Fig. 8** & **Suppl. Fig. S1**). Even so, the proliferative advantage offered by RAC1 P29S was muted in comparison to other studies. In the model of dendritic actin-driven proliferation proposed by Mohan and colleagues, they had applied dabrafenib and trametinib MAPK inhibitors as their growth challenge; we believed that low-serum would recapitulate a similar effect because a subsequent study published that RAC1 P29S similarly conferred a proliferative advantage under reduced growth factor conditions[234,241]. Even so, it was not validated previously that low serum would elicit a proliferative advantage by the same dendritic actin-dependent mechanism as BRAF and MEK inhibition. It would be worthwhile to repeat this experiment using MAPK inhibition as our growth-challenging factor to more closely simulate the conditions under which the model was originally described.

In this thesis, we present for the first time the effect of RAC1 P29S on the random mesenchymal migration of single cells. We have found that RAC1 P29S overexpression

significantly enhanced the migration of immortalized melanocytes without affecting directional persistence (**Fig. 4** & **Fig. 9**). In the set of migration experiments presented in **Figure 4**, RAC1 P29S consistently promoted migration at slightly higher speeds than RAC1 WT, in contrast to the stark difference between the two isoforms in mouse melanocyte chemotaxis[34]. An activating effect of exogenous RAC1 WT expression was to be expected since a larger intracellular wild-type pool will produce a greater amount of GTP-loaded RAC1 WT than would be present in an endogenous population. Replication of this experimental setup and similar experiments with a non-targeting control siRNA reproduced an intermediate migratory phenotype for HMEL-RAC1 WT (**Fig. 9**). Additionally, larger sample sizes revealed that exogenous RAC1 P29S expression corresponds with a consistently elevated rate of migration, which has been significantly higher than migration speeds elicited by either RAC1 WT or GFP.

We have shown that induction of IQGAP1 knockdown with siIQGAP1-04 significantly decreased migration associated with RAC1 P29S (**Fig. 9** & **Suppl. Fig. S2**). This effect was specific to melanocytes overexpressing RAC1 P29S, which experienced a decrease in mean migration speed and mean velocity, while the migration of other cells lines was not significantly altered. Meanwhile, directional persistence was unchanged, suggesting that IQGAP1 enhances lamellipodia-based motility but is not necessary for cell steering[83]. Additionally, upon IQGAP1 knockdown, HMEL-RAC1 P29S mean migration speed was reduced to the same value as HMEL-RAC1 WT. Thus, ectopic RAC1 P29S hyperactivity alone produces migratory behaviour that is similar to ectopic RAC1 WT, but in the presence of endogenous IQGAP1, the enriched association of RAC1 P29S with IQGAP1 and the subsequent cooperation of this complex in cortical actin remodeling confers a specific advantage to RAC1 P29S over RAC1 WT in mesenchymal migration. Treatment with a second siRNA against IQGAP1 decreased migration rates of melanocytes with RAC1 P29S overexpression, but in this case, the effects extended across all isogenic melanocyte lines (**Fig. 9** & **Suppl. Fig. S4)**. Further migration experiments are currently underway implementing additional siIQGAP1 sequences to validate the specific migratory outcomes that are most representative of IQGAP1 disruption in RAC1 P29S melanoma.

4.1 Limitations and future direction

In this thesis, we have presented the effects of IQGAP1 knockdown following a series of preliminary investigations in one immortalized melanocyte line. Future studies in our lab will use

additional cell lines to validate these outcomes across diverse mutational backgrounds in representative models of melanoma. First, to dissect the significance of cooperating driver mutations with RAC1 P29S in a simplified melanocyte model, HMEL (BRAF V600E) and pMEL-NRAS (NRAS G12D) immortalized melanocytes lines could be compared using these assays to evaluate the extent to which the IQGAP1-dependence of RAC1 P29S is affected by co-occurring MAPK driver mutations within a simplified model. Then, a panel of human melanoma lines with endogenous RAC1 P29S matched to RAC1 WT lines with similar mutational landscapes could be compared to observe the effects of RAC1 P29S and IQGAP1 cooperation in cell lines that are more representative of human melanoma signaling and behaviour. Additionally, we will consider generating isogenic RAC1 WT controls from RAC1 P29S melanoma lines using targeted gene editing tools to revert the point mutation at c.85 as Mohan and colleagues have done successfully in IGR1[241].

As we explored the RAC1-IQGAP1 axis, we demonstrated the reciprocal co-immunoprecipitation of RAC1 P29S and IQGAP1 in a system of overexpression. Future work to strengthen these findings will require additional pulldowns under alternative conditions, such as endogenous or semi-endogenous protein expression. To date, we have generated HMELs with stable expression of V5-tagged RAC1 WT/T17N/P29S/Q61L to perform semi-endogenous V5-tag co-IP. Further optimization of the semi-endogenous co-IP conditions are necessary as endogenous IQGAP1 has not been readily detected in semi-endogenous co-IPs performed under similar conditions to those presented in **Figure 5**. To compensate for the reduced IQGAP1 protein content of endogenous rather than exogenous expression and detect any associations, variables to optimize include the amount of protein material in the co-IP, the amount Protein A Sepharose CL-4B beads used, and the buffer system.

In our random migration assays, we have consistently observed that depleting IQGAP1 significantly decreases the migration of cells with RAC1 P29S expression. However, it is unclear whether this effect is specific to RAC1 P29S-expressing cells as the two siRNAs we have implemented against IQGAP1 have elicited varied effects in the isogenic control lines. A third siRNA against IQGAP1 is currently being applied in another series of migration assays to address this discrepancy and clarify which outcome is most representative of specific IQGAP1 knockdown. Once this baseline behaviour has been established, additional variables can be

incorporated into the experimental design for the assays to become more informative. For instance, reducing serum or glucose levels could expose the effects of RAC1 P29S-driven enhanced dendritic actin networks on cell migration in the presence or absence of IQGAP1[241]. It would also be desirable to observe the consequences of such growth challenge not only on migration, but also invasion (*i.e.* the migration of the cells through a matrix such as Matrigel).

This thesis has presented extensive migration data from random migration assays. Future studies will include an assortment of diverse migration assays to strengthen these findings by validating whether different techniques produce convergent results. For example, trans-well migration assays are a relatively simple and informative option. Such assays have already been conducted for RAC1 P29S-expressing murine melanocytes, and these past experiments could be used as a benchmark for expected results in additional cell lines in preparation for the addition of more variables such as IQGAP1 knockdown[34]. Another option is a scratch wound assay, similarly for which existing studies could be used as a reference for RAC1 P29S-driven behaviour in melanoma lines[270]. In fact, we have attempted to use the IncuCyte system and WoundMaker pin block to perform high-throughput scratch wound assays to dissect the roles of RAC1 P29S and IQGAP1 in wound healing under varied serum conditions, but technical difficulties have rendered the results uninformative and inadmissible. Many biological replicates have been performed, but issues with inconsistent wounding by the pin block, erroneous camera auto-focusing, and other imaging anomalies suspected to be due to accidental interference by other users have culminated in results that are nonsensical and unreproducible, and so they have been omitted from this report. Our lab will work to optimize these assays in future for their addition to our repertoire of RAC1 P29S migration assays.

Finally, although the preliminary proliferation assays produced very interesting results, they would most notably have been strengthened by additional replication. However, due to sudden research ramp-down measures in response to the global pandemic, this was not possible under the circumstances. As the situation stabilizes and research priorities permit, it will be of great importance to verify the reproducibility of these results. In addition, subsequent experiments may benefit from certain changes to the protocol to accentuate existing differences between treatment groups. For instance, we may be able to exacerbate differences between normal and low serum conditions by more closely adhering to the protocol established by Lionarons *et al*. where viability

of cells with ectopic expression of RAC1 isoforms was compared between populations grown in 10 % FBS or 1 % serum and significant differences were evident[234].

4.2 Significance

Not only has this project validated enriched complexing between RAC1 P29S and IQGAP1, it has also demonstrated that this complex stabilizes the RAC1 P29S active state, drives the migratory phenotype associated with the P29S mutant, and may regulate the compartmentalization of RAC1 P29S signaling. RAC1 is responsible for driving a vast network of signaling pathways, including the regulation of cytoskeletal rearrangement, proliferation, survival, development, superoxide production, and cellular metabolism (reviewed in Literature review section II.3). Given our evidence that IQGAP1 promotes the RAC1 P29S active state, it may amplify RAC1 P29S signaling to many of its downstream effectors to initiate any or all of these signaling pathways, particularly if those effectors co-localize to the plasma membrane at cortical actin sites. For instance, this highlights the possibility of increased PAK signaling, which has an array of downstream effects ranging from MAPK pathway activation and proliferation to anti-apoptotic and dedifferentiation pathways[276,277]. RAC1 is necessary for transformation, survival, and migration in RAS-driven cancers and past studies have demonstrated the significance of RAC1/PAK1 signaling in RAS-driven skin cancer development[115,278]. In addition, aberrant AKT pathway activity is linked to many cancers[118,279]. PI3K/AKT signaling initiates at the plasma membrane; not only can PAKs potentiate AKT signaling to stimulate survival and anti-apoptosis, but RAC1 can also directly bind and activate the PI3Kβ isoform to increase downstream activation of AKT. Indeed, the dependency of RAC1 P29S-expressing melanocytes on AKT has been identified in a recent publication[234]. RAC1 P29S, by nature of its hyperactivity and the compartmentalization of its signaling by IQGAP1, possibly appropriates these pathways to contribute to melanomagenesis.

Just as RAC1 has proven necessary for RAS-driven skin cancer, a similar role for IQGAP1 in RAS- and MAPK-driven tumours has been reported[280]. IQGAP1 is known to act as a scaffold for MAPK signaling, binding to pathway constituents and holding them in close proximity with the correct orientation to enhance signaling down the kinase cascade[281]. Through its involvement in MAPK signaling, IQGAP1 has become a target of interest in many cancers with frequent MAPK pathway alterations or IQGAP1 overexpression. Silencing IQGAP1 has been shown to decrease

tumourigenesis, migration and invasion in thyroid cancer and ovarian carcinoma[282,283]. IQGAP1 has also been identified as an oncogenic target in canine melanoma, where it promotes proliferation and ERK activity by some unexplored mechanism; the canine IQGAP1 homologue is highly similar to the human form, and it maintains similar expression patterns in both canine and human melanoma[284]. While the focus of these studies has been MAPK signaling, the dependencies of these diverse cancer types on IQGAP1 are also consistent with RAC1-mediated outcomes. A RAC1 P29S-IQGAP1 complex would facilitate the action of PAK on MEK and ERK activation if held in proximity by IQGAP1 to increase their local concentration, intensifying the proliferative effects of RAC1. Accordingly, IQAGP1 silencing in glioma inhibits proliferation, migration, and invasion, while also reducing expression of MMPs and EMT-related transcription factors, whose upregulation is often associated with PAK signaling[276,285]. Involvement of RAC1 in IQGAP1-mediated tumourigenic MAPK signaling has been confirmed in colorectal cancer, where metastasis is dependent upon IQGAP1-mediated RAC1-ERK crosstalk[286].

Migratory and invasive phenotypes precipitated by IQGAP1 in cancer are especially likely to necessitate some RAC1 involvement, as RAC1 drives the predominant mode of cell locomotion in malignant cell migration[287]. Breast cancer models have specifically demonstrated that IQGAP1 promotes proliferation, tumourigenesis and invasion by a mechanism that depends upon actin, RAC1, and MAPK signaling[288]. What is most striking about these findings is the evidence for co-dependency of IQGAP1 on both RAC1 and actin, which is highly reminiscent of recent studies that have proposed RAC1 P29S-driven actin remodeling to propagate oncogenic signaling and tumour suppressor inactivation[241]. From these data, it is highly possible that this mechanism of actin-dependent regulation of gene expression could have a dependency on IQGAP1 as well[289]. This inference is further supported by additional evidence from breast cancer models, where IQGAP1 depletion inhibits the growth of metastases but not the primary tumour, reinforcing a role for IQGAP1 in sustained proliferation associated with RAC1 P29S under growth challenge[241,290]. Although the cooperation of IQGAP1 with RAC1 and actin has only been verified in breast cancer, these findings set a precedent for an indispensable role of IQGAP1 in the same oncogenic pathways that RAC1 P29S has been shown to leverage.

In addition to its involvement in tumourigenesis of the cancers described above, IQGAP1 has also been implicated in the self-renewal of multiple myeloma, suggesting that it may be more

widely involved in EMT-like pathways in cancer[291]. RAC1 is known to be involved in WNT signaling during development, which plays a role in renewal and cell fate determination. WNT/β-catenin signaling is highly activated in cancer, and IQGAP1 has been found to drive EMT in pancreatic cancer through activation of this pathway[130,292]. Specifically, IQGAP1 promotes DVL2 expression and β-catenin-dependent transcriptional activity. This highlights two potential niches for cooperation with RAC1 or RAC1 P29S in WNT signaling. On one hand, IQGAP1 maintenance of RAC1 P29S at the plasma membrane may improve its availability to assist in β-catenin nuclear transport for canonical signaling[67]. Alternatively, DVL proteins potentiate RAC1 activation of noncanonical WNT signaling through a DVL/RAC1/JNK pathway, which may cooperate with IQGAP1-mediated WNT/β-catenin signaling to amplify signaling changes and accelerate WNT-mediated dedifferentiation[140]. In addition, the Leucine-rich repeat-containing G-protein coupled receptor 5 (LGR5) receptor of the WNT pathway has been shown to promote the interaction between IQGAP1 and RAC1. It is a stem cell marker that decreases IQGAP1 phosphorylation at Ser1441 and Ser1443, thereby enhancing binding of this scaffold to RAC1 and increasing cortical actin polymerization[293]. As this enhanced RAC1-IQGAP1 interaction increases F-actin accumulation and decreases G-actin abundance, perhaps the enrichment RAC1 P29S-IQGAP1 in complex could upregulate the MRTF/SRF signaling axis, contributing to melanocyte dedifferentiation[67,234]. It would be of great interest to investigate the dependency of RAC1 P29S-driven cellular transformation on IQGAP1 by WNT or MRTF/SRF signaling, but time regrettably did not permit the performance of these assays in stably generated isogenic lines for inclusion in this thesis. Our lab is pressing onward with these studies and any co-dependency will soon be revealed.

4.3 Conclusion

Future studies into the pathways required for RAC1 P29S to drive melanomagenesis will be highly beneficial in identifying critical mediators through which RAC1 P29S promotes malignant progression. We propose that IQGAP1 may be a critical mediator of RAC1 P29S oncogenic signaling. Studies performed by our lab were initially guided by an unbiased proteomic approach that identified an enrichment of IQGAP1 interaction specifically with RAC1 P29S, and the work presented here is a step forward in our understanding of the role of IQGAP1 in RAC1 P29S-driven melanomagenesis. A thorough understanding of IQGAP1 and additional mediators

may guide the development of tools to disrupt RAC1 P29S-driven melanomagenesis and identify new actionable targets for the development of therapies against RAC1 P29S melanoma.

Literature Cited

1. Büttner, R. *et al.* Implementing TMB measurement in clinical practice: Considerations on assay requirements. *ESMO Open* **4**, (2019).
2. Pleasance, E. D. *et al.* A comprehensive catalogue of somatic mutations from a human cancer genome. *Nature* **463**, 191–196 (2010).
3. Hennessey, R. *et al.* UVA and UVB elicit distinct mutational signatures in melanoma. (2019). doi:10.1101/778449
4. Pfeifer, G. P., You, Y. H. & Besaratinia, A. Mutations induced by ultraviolet light. *Mutat. Res.* **571**, 19–31 (2005).
5. Akbani, R. *et al.* Genomic Classification of Cutaneous Melanoma. *Cell* **161**, 1681–1696 (2015).
6. Bastian, B. C. The Molecular Pathology of Melanoma: An Integrated Taxonomy of Melanocytic Neoplasia. *Annu. Rev. of Pathol.* **9**, (2014).
7. Rajkumar, S. & Watson, I. R. Molecular characterisation of cutaneous melanoma: Creating a framework for targeted and immune therapies. *Br. J. Cancer* **115**, 145–155 (2016).
8. Canadian Cancer Statistics Advisory Committee. *Canadian Cancer Statistics 2019*. (2019).
9. American Cancer Society. *Cancer Facts & Figures 2020*. (2020).
10. Canadian Cancer Statistics Advisory Committee. *Canadian Cancer Statistics 2014*. (2014).
11. Ross, M. I. & Gershenwald, J. E. Evidence-based treatment of early-stage melanoma. *J. Surg. Oncol.* **104**, 341–353 (2011).
12. Burns, D. *et al.* The Pathogenesis and Clinical Management of Cutaneous Melanoma: An Evidence-Based Review. *J. Med. Imaging. Radiat. Sci.* **50**, 460-469.e1 (2019).
13. Balch, C. M. *et al.* A new American Joint Committee on Cancer staging system for cutaneous melanoma. *Cancer* **88**, 1484–1491 (2000).
14. Crosby, T., Fish, R., Coles, B. & Mason, M. Systemic treatments for metastatic cutaneous melanoma. *Cochrane Database Syst. Rev.* **2**, (2018).
15. Jiang, T., Zhou, C. & Ren, S. Role of IL-2 in cancer immunotherapy. *OncoImmunology* **5**, (2016).
16. Petrella, T. *et al.* Single-agent interleukin-2 in the treatment of metastatic melanoma. *Curr. Oncol.* **14**, 21–26 (2007).
17. Atkins, M. B. *et al.* High-dose recombinant interleukin 2 therapy for patients with metastatic melanoma: Analysis of 270 patients treated between 1985 and 1993. *J. Clin. Oncol.* **17**, 2105–2116 (1999).
18. Chapman, P. B. *et al.* Improved survival with vemurafenib in melanoma with BRAF V600E

mutation. *N. Engl. J. Med.* **364**, 2507–2516 (2011).

19. Hauschild, A. *et al.* Dabrafenib in BRAF-mutated metastatic melanoma: A multicentre, open-label, phase 3 randomised controlled trial. *Lancet* **380**, 358–365 (2012).

20. Falchook, G. S. *et al.* Dabrafenib in patients with melanoma, untreated brain metastases, and other solid tumours: A phase 1 dose-escalation trial. *Lancet* **379**, 1893–1901 (2012).

21. Flaherty, K. T. *et al.* Improved survival with MEK inhibition in BRAF-mutated melanoma. *N. Engl. J. Med.* **367**, 107–114 (2012).

22. Dummer, R. *et al.* Binimetinib versus dacarbazine in patients with advanced NRAS-mutant melanoma (NEMO): a multicentre, open-label, randomised, phase 3 trial. *Lancet Oncol.* **18**, 435–445 (2017).

23. Muñoz-Couselo, E., Adelantado, E. Z., Ortiz, C., García, J. S. & Perez-Garcia, J. NRAS-mutant melanoma: Current challenges and future prospect. *OncoTargets Ther.* **10**, 3941–3947 (2017).

24. Flaherty, K. T. *et al.* Combined BRAF and MEK Inhibition in Melanoma with BRAF V600 Mutations. *N. Engl. J. Med.* **367**, 1694–1703 (2012).

25. Ascierto, P. A. *et al.* coBRIM: a phase 3, double-blind, placebo-controlled study of vemurafenib versus vemurafenib + cobimetinib in previously untreated BRAFV600 mutation–positive patients with unresectable locally advanced or metastatic melanoma (NCT01689519). *J. Transl. Med.* **13**, O4 (2015).

26. Pardoll, D. M. The blockade of immune checkpoints in cancer immunotherapy. *Nat. Rev. Cancer* **12**, 252–264 (2012).

27. Li, X., Shao, C., Shi, Y. & Han, W. Lessons learned from the blockade of immune checkpoints in cancer immunotherapy. *J. Hematol. Oncol.* **11**, (2018).

28. Luke, J. J., Flaherty, K. T., Ribas, A. & Long, G. V. Targeted agents and immunotherapies: Optimizing outcomes in melanoma. *Nat. Rev. Clin. Oncol.* **14**, 463–482 (2017).

29. Schadendorf, D. *et al.* Pooled analysis of long-term survival data from phase II and phase III trials of ipilimumab in unresectable or metastatic melanoma. *J. Clin. Oncol.* **33**, 1889–1894 (2015).

30. Robert, C. *et al.* Ipilimumab plus dacarbazine for previously untreated metastatic melanoma. *N. Engl. J. Med.* **364**, 2517–2526 (2011).

31. Robert, C. *et al.* Pembrolizumab versus Ipilimumab in Advanced Melanoma. *N. Engl. J. Med.* **372**, 2521–2532 (2015).

32. Larkin, J. *et al.* Combined nivolumab and ipilimumab or monotherapy in untreated Melanoma. *N. Engl. J. Med.* **373**, 23–34 (2015).

33. Hodis, E. *et al.* A landscape of driver mutations in melanoma. *Cell* **150**, 251–263 (2012).

34. Krauthammer, M. *et al.* Exome sequencing identifies recurrent somatic RAC1 mutations in melanoma. *Nat. Genet.* **44**, 1006–1014 (2012).

35. Mar, V. J. *et al.* Clinical and pathological associations of the activating RAC1 P29S mutation in primary cutaneous melanoma. *Pigment Cell Melanoma Res.* **27**, 1117–1125 (2014).

36. Wennerberg, K., Rossman, K. L. & Der, C. J. The Ras superfamily at a glance. *J. Cell Sci.* **118**, 843–846 (2005).

37. Hodge, R. G. & Ridley, A. J. Regulating Rho GTPases and their regulators. *Nat. Rev. Mol. Cell Biol.* **17**, 496–510 (2016).

38. Garcia-Mata, R., Boulter, E. & Burridge, K. The 'invisible hand': Regulation of RHO GTPases by RHOGDIs. *Nat. Rev. Mol. Cell Biol.* **12**, 493–504 (2011).

39. Jaffe, A. B. & Hall, A. Rho GTPases: Biochemistry and biology. *Annu. Rev. Cell Dev. Biol.* **21**, 247–269 (2005).

40. Etienne-Manneville, S. & Hall, A. Rho GTPases in cell biology. *Nature* **420**, 629–635 (2002).

41. Didsbury, J., Weber, R. F., Bokoch, G. M., Evans, T. & Snyderman, R. Rac, a Novel Ras-Related Family of Proteins That Are Botulinum Toxin Substrates. *J. Biol. Chem.* **264**, 16378–16382 (1989).

42. Sekine, A., Fujiwara, M. & Narumiya, S. Asparagine residue in the rho gene product is the modification site for botulinum ADP-ribosyltransferase. *J. Biol. Chem.* **264**, 8602–8605 (1989).

43. Ridley, A. J. & Hall, A. The small GTP-binding protein rho regulates the assembly of focal adhesions and actin stress fibers in response to growth factors. *Cell* **70**, 389–399 (1992).

44. Ridley, A. J., Paterson, H. F., Johnston, C. L., Diekmann, D. & Hall, A. The small GTP-binding protein rac regulates growth factor-induced membrane ruffling. *Cell* **70**, 401–410 (1992).

45. Bourne, H. R., Sanders, D. A. & McCormick, F. The GTPase superfamily: conserved structure and molecular mechanism. *Nature* **349**, 117–127 (1991).

46. Goitre, L., Trapani, E., Trabalzini, L. & Retta, S. F. The ras superfamily of small GTPases: The unlocked secrets. *Methods Mol. Biol.* **1120**, 1–18 (2014).

47. Schaefer, A., Reinhard, N. R. & Hordijk, P. L. Toward understanding RhoGTPase specificity: Structure, function and local activation. *Small GTPases* **5**, (2014).

48. Thomas, C., Fricke, I., Scrima, A., Berken, A. & Wittinghofer, A. Structural Evidence for a Common Intermediate in Small G Protein-GEF Reactions. *Mol. Cell* **25**, 141–149 (2007).

49. McCallum, S. J., Wu, W. J. & Cerione, R. A. Identification of a putative effector for Cdc42Hs with high sequence similarity to the RasGAP-related protein IQGAP1 and a Cdc42Hs binding partner with similarity to IQGAP2. *J. Biol. Chem.* **271**, 21732–21737 (1996).

50. Wu, W. J., Leonard, D. A., Cerione, R. A. & Manor, D. Interaction between Cdc42Hs and RhoGDI is mediated through the Rho insert region. *J. Biol. Chem.* **272**, 26153–26158

(1997).

51. Nisimoto, Y., Freeman, J. L. R., Motalebi, S. A., Hirshberg, M. & Lambeth, J. D. Rac binding to p67(phox). Structural basis for interactions of the Rac1 effector region and insert region with components of the respiratory burst oxidase. *J. Biol. Chem.* **272**, 18834–18841 (1997).

52. Zong, H., Kaibuchi, K. & Quilliam, L. A. The Insert Region of RhoA Is Essential for Rho Kinase Activation and Cellular Transformation. *Mol. Cell. Biol.* **21**, 5287–5298 (2001).

53. Rudack, T., Xia, F., Schlitter, J., Kötting, C. & Gerwert, K. The role of magnesium for geometry and charge in GTP hydrolysis, revealed by quantum mechanics/Molecular mechanics simulations. *Biophys. J.* **103**, 293–302 (2012).

54. Worthylake, D. K., Rossman, K. L. & Sondek, J. Crystal structure of Rac1 in complex with the guanine nucleotide exchange region of Tiam1. *Nature* **408**, 682–688 (2000).

55. Dvorsky, R. & Ahmadian, M. R. Always look on the bright site of Rho: structural implications for a conserved intermolecular interface. *EMBO Rep.* **5**, 1130–1136 (2004).

56. Jezyk, M. R. *et al.* Crystal structure of Rac1 bound to its effector phospholipase C-β2. *Nat. Struct. Mol. Biol.* **13**, 1135–1140 (2006).

57. Grizot, S. *et al.* Crystal structure of the Rac1 - RhoGDI complex involved in NADPH oxidase activation. *Biochemistry* **40**, 10007–10013 (2001).

58. Karnoub, A. E., Der, C. J. & Campbell, S. L. The Insert Region of Rac1 Is Essential for Membrane Ruffling but Not Cellular Transformation. *Mol. Cell. Biol.* **21**, 2847–2857 (2001).

59. Thapar, R., Karnoub, A. E. & Campbell, S. L. Articles Structural and Biophysical Insights into the Role of the Insert Region in Rac1 Function †. *Biochemistry* **41**, 11 (2002).

60. Lam, B. D. & Hordijk, P. L. The Rac1 hyper variable region in targeting and signaling-a tail of many stories. *Small GTPases* **4**, 78 (2013).

61. Won, D. H. *et al.* PI(3,4,5)P3 and PI(4,5)P2 lipids target proteins with polybasic clusters to the plasma membrane. *Science* **314**, 1458–1461 (2006).

62. Lanning, C. C., Ruiz-Velasco, R. & Williams, C. L. Novel mechanism of the co-regulation of nuclear transport of SmgGDS and Rac1. *J. Biol. Chem.* **278**, 12495–12506 (2003).

63. He, H. & Huynh, N. p21-activated kinase family: promising new drug targets. *Res. Reports Biochem.* **5**, 119 (2015).

64. Kumara, R., Sanawar, R., Li, X. & Li, F. Structure, biochemistry, and biology of PAK kinases. *Gene* **605**, 20–31 (2017).

65. McDaniel, A. S. *et al.* Pak1 regulates multiple c-Kit mediated Ras-MAPK gain-in-function phenotypes in Nf1+/- mast cells. *Blood* **112**, 4646–54 (2008).

66. Menges, C. W. *et al.* Group I p21-activated kinases (PAKs) promote tumor cell proliferation and survival through the AKT1 and Raf-MAPK pathways. *Mol. Cancer. Res.* **10**, 1179–

1188 (2012).

67. Jamieson, C., Lui, C., Brocardo, M. G., Martino-Echarri, E. & Henderson, B. R. Rac1 augments Wnt signaling by stimulating β-catenin–lymphoid enhancer factor-1 complex assembly independent of β-catenin nuclear import. *J. Cell Sci.* **128**, 3933–3946 (2015).

68. Michaelson, D. *et al.* Rac1 accumulates in the nucleus during the G2 phase of the cell cycle and promotes cell division. *J. Cell Biol.* **181**, 485–496 (2008).

69. Payapilly, A. & Malliri, A. Compartmentalisation of RAC1 signalling. *Curr. Opin. Cell Biol.* **54**, 50–56 (2018).

70. Yao, C. *et al.* Breast cancer-associated gene 3 interacts with rac1 and augments nf-kappab signaling in vitro, but has no effect on rankl-induced bone resorption in vivo. *Int. J. Mol. Med.* **40**, 1067–1077 (2017).

71. Chong, S. J. F., Lai, J. X. H., Eu, J. Q., Bellot, G. L. & Pervaiz, S. Reactive oxygen species and oncoprotein signaling-a dangerous liaison. *Antioxid. Redox Signal.* **29**, 1553–1588 (2018).

72. Ehrlich, J. S., Hansen, M. D. H. & Nelson, W. J. Spatio-temporal regulation of Rac1 localization and lamellipodia dynamics during epithelial cell-cell adhesion. *Dev. Cell* **3**, 259–270 (2002).

73. Nakagawa, M., Fukata, M., Yamaga, M., Itoh, N. & Kaibuchi, K. Recruitment and activation of Rac1 by the formation of E-cadherin-mediated cell-cell adhesion sites. *J. Cell Sci.* **114**, 1829–1838 (2001).

74. Chen, Z. *et al.* Structure and control of the actin regulatory WAVE complex. *Nature* **468**, 533–538 (2010).

75. Chen, B. *et al.* Rac1 GTPase activates the WAVE regulatory complex through two distinct binding sites. *elife* **6**, (2017).

76. Kurisu, S. & Takenawa, T. The WASP and WAVE family proteins. *Genome biology* **10**, 226 (2009).

77. Bokoch, G. M., Edwards, D. C., Sanders, L. C. & Gill, G. N. Activation of LIM-kinase by Pak1 couples Rac/Cdc42 GTPase signalling to actin cytoskeletal dynamics. *Nat. Cell Biol.* **1**, 253–259 (1999).

78. Duman, J. G., Mulherkar, S., Tu, Y. K., X. Cheng, J. & Tolias, K. F. Mechanisms for spatiotemporal regulation of Rho-GTPase signaling at synapses. *Neuroscience Letters* **601**, 4–10 (2015).

79. Ridley, A. J. Rho GTPase signalling in cell migration. *Curr. Opin. Cell Biol.* **36**, 103–112 (2015).

80. Ishii, S. *et al.* Distinct predictive performance of Rac1 and Cdc42 in cell migration. *Sci. Rep.* **5**, 17527 (2015).

81. Allen, W. E., Zicha, D., Ridley, A. J. & Jones, G. E. A role for Cdc42 in macrophage chemotaxis. *J. Cell Biol.* **141**, 1147–1157 (1998).

82. Fukata, M. *et al.* Rac1 and Cdc42 capture microtubules through IQGAP1 and CLIP-170. *Cell* **109**, 873–885 (2002).

83. Krause, M. & Gautreau, A. Steering cell migration: Lamellipodium dynamics and the regulation of directional persistence. *Nat. Rev. Mol. Cell Biol.* **15**, 577–590 (2014).

84. Pankov, R. *et al.* A Rac switch regulates random versus directionally persistent cell migration. *J. Cell Biol.* **170**, 793–802 (2005).

85. Zegers, M. M. & Friedl, P. Rho GTPases in collective cell migration. *Small GTPases* **5**, (2014).

86. Mayor, R. & Etienne-Manneville, S. The front and rear of collective cell migration. *Nat. Rev. Mol. Cell Biol.* **17**, 97–109 (2016).

87. Muinonen-Martin, A. J. *et al.* Melanoma Cells Break Down LPA to Establish Local Gradients That Drive Chemotactic Dispersal. *PLOS Biol.* **12**, (2014).

88. Hayer, A. *et al.* Engulfed cadherin fingers are polarized junctional structures between collectively migrating endothelial cells. *Nat. Cell Biol.* **18**, 1311–1323 (2016).

89. Woroniuk, A. *et al.* STEF/TIAM2-mediated Rac1 activity at the nuclear envelope regulates the perinuclear actin cap. *Nat. Commun.* **9**, 1–15 (2018).

90. Hart, M. J., Callow, M. G., Souza, B. & Polakis, P. IQGAP1, a calmodulin-binding protein with a rasGAP-related domain, is a potential effector for cdc42Hs. *EMBO J.* **15**, 2997–3005 (1996).

91. Kuroda, S. *et al.* Role of IQGAP1, a target of the small GTPases Cdc42 and Rac1, in regulation of E-Cadherin-mediated cell-cell adhesion. *Science* **281**, 832–835 (1998).

92. Fukata, M. *et al.* Cdc42 and Rac1 regulate the interaction of IQGAP1 with β-catenin. *J. Biol. Chem.* **274**, 26044–26050 (1999).

93. Izumi, G. *et al.* Endocytosis of E-cadherin regulated by Rac and Cdc42 small G proteins through IQGAP1 and actin filaments. *J. Cell Biol.* **166**, 237–248 (2004).

94. Müller, M. T. *et al.* Interaction of microtubules and actin during the post-fusion phase of exocytosis. *Sci. Rep.* **9**, 1555–1566 (2019).

95. Braga, V. M. M., Machesky, L. M., Hall, A. & Hotchin, N. A. The small GTPases Rho and Rac are required for the establishment of cadherin-dependent cell-cell contacts. *J. Cell Biol.* **137**, 1421–1431 (1997).

96. Chi, X., Wang, S., Huang, Y., Stamnes, M. & Chen, J. L. Roles of Rho GTPases in intracellular transport and cellular transformation. *Int. J. Mol. Sci.* **14**, 7089–7108 (2013).

97. Costa Verdera, H., Gitz-Francois, J. J., Schiffelers, R. M. & Vader, P. Cellular uptake of extracellular vesicles is mediated by clathrin-independent endocytosis and macropinocytosis. *J. Control. Release* **266**, 100–108 (2017).

98. Sayedyahossein, S. & Dagnino, L. Integrins and Small GTPases as Modulators of Phagocytosis. *Int. Rev. Cell Mol. Biol.* **302**, 321–354 (2013).

99. Grassart, A., Dujeancourt, A., Lazarow, P. B., Dautry-Varsat, A. & Sauvonnet, N. Clathrin-independent endocytosis used by the IL-2 receptor is regulated by Rac1, Pak1 and Pak2. *EMBO Rep.* **9**, 356–362 (2008).

100. Malecz, N. *et al.* Synaptojanin 2, a novel Rac1 effector that regulates clathrin-mediated endocytosis. *Curr. Biol.* **10**, 1383–1386 (2000).

101. Stanley, A. C. *et al.* The Rho GTPase Rac1 is required for recycling endosome-mediated secretion of TNF in macrophages. *Immunol. Cell Biol.* **92**, 275–286 (2014).

102. Müller, M. T. *et al.* Interaction of microtubules and actin during the post-fusion phase of exocytosis. *Sci. Rep.* **9**, 1–15 (2019).

103. Zhao, Z. & Manser, E. PAK family kinases. *Cell. Logist.* **2**, 59–68 (2012).

104. Watt, F. M., Frye, M. & Benitah, S. A. MYC in mammalian epidermis: How can an oncogene stimulate differentiation? *Nat. Rev. Cancer* **8**, 234–242 (2008).

105. Honma, M., Benitah, S. A. & Watt, F. M. Role of LIM kinases in normal and psoriatic human epidermis. *Mol. Biol. Cell* **17**, 1888–1896 (2006).

106. King, A. J. *et al.* The protein kinase Pak3 positively regulates Raf-1 activity through phosphorylation of serine 338. *Nature* **396**, 180–183 (1998).

107. Slack-Davis, J. K. *et al.* PAK1 phosphorylation of MEK1 regulates fibronectin-stimulated MAPK activation. *J. Cell Biol.* **162**, 281–291 (2003).

108. Wang, Z. *et al.* P21-activated kinase 1 (PAK1) can promote ERK activation in a kinase-independent manner. *J. Biol. Chem.* **288**, 20093–20099 (2013).

109. Pan, C. *et al.* Suppression of the RAC1/MLK3/p38 Signaling Pathway by β-Elemene Alleviates Sepsis-Associated Encephalopathy in Mice. *Front. Neurosci.* **13**, 358 (2019).

110. Westwick, J. K. *et al.* Rac regulation of transformation, gene expression, and actin organization by multiple, PAK-independent pathways. *Mol. Cell. Biol.* **17**, 1324–1335 (1997).

111. Zhang, S. *et al.* Rho family GTPases regulate p38 mitogen-activated protein kinase through the downstream mediator Pak1. *J. Biol. Chem.* **270**, 23934–23936 (1995).

112. Zhao, Z. S., Lim, J. P., Ng, Y. W., Lim, L. & Manser, E. The GIT-associated kinase PAK targets to the centrosome and regulates Aurora-A. *Mol. Cell* **20**, 237–249 (2005).

113. May, M., Schelle, I., Brakebusch, C., Rottner, K. & Genth, H. Rac1-dependent recruitment of PAK2 to G2 phase centrosomes and their roles in the regulation of mitotic entry. *Cell Cycle* **13**, 2210–2220 (2014).

114. Bompard, G. *et al.* P21-activated kinase 4 (PAK4) is required for metaphase spindle positioning and anchoring. *Oncogene* **32**, 910–919 (2013).

115. Pérez-Yépez, E. A., Saldívar-Cerón, H. I., Villamar-Cruz, O., Pérez-Plasencia, C. & Arias-Romero, L. E. p21 Activated kinase 1: Nuclear activity and its role during DNA damage repair. *DNA Repair* **65**, 42–46 (2018).

116. Yang, Z. *et al.* Pak1 phosphorylation of Snail, a master regulator of epithelial-to-mesenchyme transition, modulates Snail's subcellular localization and functions. *Cancer Res.* **65**, 3179–3184 (2005).

117. Turner, H. *et al.* Rac-1 regulates nuclear factor of activated T cells (NFAT) C1 nuclear translocation in response to Fcε receptor type 1 stimulation of mast cells. *J. Exp. Med.* **188**, 527–537 (1998).

118. Georgescu, M. M. Pten tumor suppressor network in PI3K-Akt pathway control. *Genes and Cancer* **1**, 1170–1177 (2010).

119. Zou, Z., Tao, T., Li, H. & Zhu, X. MTOR signaling pathway and mTOR inhibitors in cancer: Progress and challenges. *Cell and Biosci.* **10**, 31 (2020).

120. Saci, A., Cantley, L. C. & Carpenter, C. L. Rac1 Regulates the Activity of mTORC1 and mTORC2 and Controls Cellular Size. *Mol. Cell* **42**, 50–61 (2011).

121. Yang, H. W. *et al.* Cooperative Activation of PI3K by Ras and Rho Family Small GTPases. *Mol. Cell* **47**, 281–290 (2012).

122. Castellano, E. & Downward, J. Ras interaction with PI3K: More than just another effector pathway. *Genes and Cancer* **2**, 261–274 (2011).

123. Fritsch, R. *et al.* XRAS and RHO families of GTPases directly regulate distinct phosphoinositide 3-kinase isoforms. *Cell* **153**, 1050 (2013).

124. Sugihara, K. *et al.* Rac1 is required for the formation of three germ layers during gastrulation. *Oncogene* **17**, 3427–3433 (1998).

125. Roszko, I., Sawada, A. & Solnica-Krezel, L. Regulation of convergence and extension movements during vertebrate gastrulation by the Wnt/PCP pathway. *Semin. Cell Dev. Biol.* **20**, 986–997 (2009).

126. Wu, X. *et al.* Rac1 Activation Controls Nuclear Localization of β-catenin during Canonical Wnt Signaling. *Cell* **133**, 340–353 (2008).

127. Mezzacappa, C., Komiya, Y. & Habas, R. Activation and Function of Small GTPases Rho, Rac, and Cdc42 During Gastrulation. *Planar Cell Polarity: Methods and Protocols* **839**, 119–131 (2012).

128. Steinhart, Z. & Angers, S. Wnt signaling in development and tissue homeostasis. *Development* **145**, (2018).

129. Houschyar, K. S. *et al.* Wnt Pathway in Bone Repair and Regeneration – What Do We Know So Far. *Front. Cell Dev. Biol.* **6**, 170 (2019).

130. Jung, Y. S. & Park, J. Il. Wnt signaling in cancer: therapeutic targeting of Wnt signaling beyond β-catenin and the destruction complex. *Exp. Mol. Med.* **52**, 183–191 (2020).

131. Patel, S., Alam, A., Pant, R. & Chattopadhyay, S. Wnt Signaling and Its Significance Within the Tumor Microenvironment: Novel Therapeutic Insights. *Front. Immunol.* **10**, 2872 (2019).

132. Clevers, H. & Nusse, R. Wnt/β-catenin signaling and disease. *Cell* **149**, 1192–1205 (2012).

133. Anthony, C. C., Robbins, D. J., Ahmed, Y. & Lee, E. Nuclear regulation of Wnt/β-catenin signaling: It's a complex situation. *Genes* **11**, 1–11 (2020).

134. Esufali, S. & Bapat, B. Cross-talk between Rac1 GTPase and dysregulated Wnt signaling pathway leads to cellular redistribution of β-catenin and TCF/LEF-mediated transcriptional activation. *Oncogene* **23**, 8260–8271 (2004).

135. Jamieson, C., Sharma, M. & Henderson, B. R. Targeting the β-catenin nuclear transport pathway in cancer. *Semin. Cancer Biol.* **27**, 20–29 (2014).

136. Buongiorno, P., Pethe, V. V., Charames, G. S., Esufali, S. & Bapat, B. Rac1 GTPase and the Rac1 exchange factor Tiam1 associate with Wnt-responsive promoters to enhance beta-catenin/TCF-dependent transcription in colorectal cancer cells. *Mol. Cancer* **7**, (2008).

137. Diamantopoulou, Z. *et al.* TIAM1 Antagonizes TAZ/YAP Both in the Destruction Complex in the Cytoplasm and in the Nucleus to Inhibit Invasion of Intestinal Epithelial Cells. *Cancer Cell* **31**, 621-634.e6 (2017).

138. Schlessinger, K., Hall, A. & Tolwinski, N. Wnt signaling pathways meet Rho GTPases. *Genes Dev.* **23**, 265–277 (2009).

139. Habas, R., Dawid, I. B. & He, X. Coactivation of Rac and Rho by Wnt/Frizzled signaling is required for vertebrate gastrulation. *Genes Dev.* **17**, 295–309 (2003).

140. Fukukawa, C. *et al.* Activation of the non-canonical Dvl-Rac1-JNK pathway by Frizzled homologue 10 in human synovial sarcoma. *Oncogene* **28**, 1110–1120 (2009).

141. Rosso, S. B., Sussman, D., Wynshaw-Boris, A. & Salinas, P. C. Wnt signaling through Dishevelled, Rac and JNK regulates dendritic development. *Nat. Neurosci.* **8**, 34–42 (2005).

142. Um, K. *et al.* Dynamic Control of Excitatory Synapse Development by a Rac1 GEF/GAP Regulatory Complex. *Dev. Cell* **29**, 701–715 (2014).

143. Abo, A. *et al.* Activation of the NADPH oxidase involves the small GTP-binding protein p21rac1. *Nature* **353**, 668–670 (1991).

144. Kuncewicz, T., Balakrishnan, P., Snuggs, M. B. & Kone, B. C. Specific association of nitric oxide synthase-2 with Rac isoforms in activated murine macrophages. *Am. J. Physiol.* **281**, (2001).

145. Souabni, H., Ezzine, A., Bizouarn, T. & Baciou, L. Functional assembly of soluble and membrane recombinant proteins of mammalian NADPH oxidase complex. *Methods Mol. Biol.* **1635**, 27–43 (2017).

146. Thomas, D. C. How the phagocyte NADPH oxidase regulates innate immunity. *Free Radic. Biol. Med.* **125**, 44–52 (2018).

147. Li, J. M. & Shah, A. M. ROS generation by nonphagocytic NADPH oxidase: Potential relevance in diabetic nephropathy. *J. Am. Soc. Nephrol.* **14**, S221–S226 (2003).

148. Debidda, M., Williams, D. A. & Zheng, Y. Rac1 GTPase regulates cell genomic stability

and senescence. *J. Biol. Chem.* **281**, 38519–38528 (2006).

149. Morgan, M. J. & Liu, Z. G. Crosstalk of reactive oxygen species and NF-κB signaling. *Cell Res.* **21**, 103–115 (2011).

150. Tamborindeguy, M. T. *et al.* NADPH-oxidase-derived ROS alters cell migration by modulating adhesions dynamics. *Biol. Cell* **110**, 225–236 (2018).

151. Boivin, D. & Beliveau, R. Subcellular distribution and membrane association of Rho-related small GTP-binding proteins in kidney cortex. *Am. J. Physiol.* **269**, (1995).

152. Osborn-Heaford, H. L. *et al.* Mitochondrial Rac1 GTPase import and electron transfer from cytochrome c are required for pulmonary fibrosis. *J. Biol. Chem.* **287**, 3301–3312 (2012).

153. Phuyal, S. & Farhan, H. Multifaceted Rho GTPase Signaling at the Endomembranes. *Front. Cell Dev. Biol.* **7**, 127 (2019).

154. Chong, S. J. F., Low, I. C. C. & Pervaiz, S. Mitochondrial ROS and involvement of Bcl-2 as a mitochondrial ROS regulator. *Mitochondrion* **19**, 39–48 (2014).

155. Velaithan, R. *et al.* The small GTPase Rac1 is a novel binding partner of Bcl-2 and stabilizes its antiapoptotic activity. *Blood* **117**, 6214–6226 (2011).

156. Zaid, H., Antonescu, C. N., Randhawa, V. K. & Klip, A. Insulin action on glucose transporters through molecular switches, tracks and tethers. *Biochem. J.* **413**, 201–215 (2008).

157. Klip, A., McGraw, T. E. & James, D. E. Thirty sweet years of GLUT4. *J. Biol. Chem.* **294**, 11369–11381 (2019).

158. Mafakheri, S. *et al.* AKT and AMP-activated protein kinase regulate TBC1D1 through phosphorylation and its interaction with the cytosolic tail of insulin-regulated aminopeptidase IRAP. *J. Biol. Chem.* **293**, 17853–17862 (2018).

159. Ramm, G., Larance, M., Guilhaus, M. & James, D. E. A role for 14-3-3 in insulin-stimulated GLUT4 translocation through its interaction with the RabGAP AS160. *J. Biol. Chem.* **281**, 29174–29180 (2006).

160. Abdrabou, A., Brandwein, D., Liu, C. & Wang, Z. Rac1 S71 Mediates the Interaction between Rac1 and 14-3-3 Proteins. *Cells* **8**, 1006 (2019).

161. Sylow, L. *et al.* Akt and Rac1 signaling are jointly required for insulin-stimulated glucose uptake in skeletal muscle and downregulated in insulin resistance. *Cell. Signal.* **26**, 323–331 (2014).

162. Chiu, T. T., Patel, N., Shaw, A. E., Bamburg, J. R. & Klip, A. Arp2/3- and Cofilin-coordinated Actin Dynamics Is Required for Insulin-mediated GLUT4 Translocation to the Surface of Muscle Cells. *Mol. Biol. Cell* **21**, 3529–3539 (2010).

163. Kurita, S., Watanabe, Y., Gunji, E., Ohashi, K. & Mizuno, K. Molecular dissection of the mechanisms of substrate recognition and F-actin-mediated activation of cofilin-phosphatase slingshot-1. *J. Biol. Chem.* **283**, 32542–32552 (2008).

164. Lopez, J. A. *et al.* Identification of a distal GLUT4 trafficking event controlled by actin polymerization. *Mol. Biol. Cell* **20**, 3918–3929 (2009).

165. Boguslavsky, S. *et al.* Myo1c binding to submembrane actin mediates insulin-induced tethering of GLUT4 vesicles. *Mol. Biol. Cell* **23**, 4065–4078 (2012).

166. Douen, A. G. *et al.* Exercise induces recruitment of the 'insulin-responsive glucose transporter'. Evidence for distinct intracellular insulin- and exercise-recruitable transporter pools in skeletal muscle. *J. Biol. Chem.* **265**, 13427–13430 (1990).

167. Sylow, L., Møller, L. L. V., Kleinert, M., Richter, E. A. & Jensen, T. E. Stretch-stimulated glucose transport in skeletal muscle is regulated by Rac1. *J. Physiol.* **593**, 645–656 (2015).

168. Chiu, T. T., Sun, Y., Koshkina, A. & Klip, A. Rac-1 superactivation triggers insulin-independent glucose transporter 4 (GLUT4) translocation that bypasses signaling defects exerted by c-Jun N-terminal kinase (JNK)- and ceramide-induced insulin resistance. *J. Biol. Chem.* **288**, 17520–17531 (2013).

169. Symons, M. Rac1 activation comes full circle. *EMBO J.* **30**, 3875–3877 (2011).

170. Kotelevets, L. & Chastre, E. Rac1 signaling: From intestinal homeostasis to colorectal cancer metastasis. *Cancers* **12**, (2020).

171. Akula, M. K. *et al.* Protein prenylation restrains innate immunity by inhibiting Rac1 effector interactions. *Nat. Commun.* **10**, 1–13 (2019).

172. Navarro-Lérida, I. *et al.* A palmitoylation switch mechanism regulates Rac1 function and membrane organization. *EMBO J.* **31**, 534–551 (2012).

173. Tong, J., Li, L., Ballermann, B. & Wang, Z. Phosphorylation of Rac1 T108 by Extracellular Signal-Regulated Kinase in Response to Epidermal Growth Factor: a Novel Mechanism To Regulate Rac1 Function. *Mol. Cell. Biol.* **33**, 4538–4551 (2013).

174. Chang, F., Lemmon, C., Lietha, D., Eck, M. & Romer, L. Tyrosine Phosphorylation of Rac1: A Role in Regulation of Cell Spreading. *PLOS One* **6**, e28587 (2011).

175. Kwon, T., Kwon, D. Y., Chun, J., Kim, J. H. & Kang, S. S. Akt protein kinase inhibits Rac1-GTP binding through phosphorylation at serine 71 of Rac1. *J. Biol. Chem.* **275**, 423–428 (2000).

176. Aljagthmi, A. A. *et al.* ΔNp63α suppresses cells invasion by downregulating PKCγ/Rac1 signaling through miR-320a. *Cell Death Dis.* **10**, 1–14 (2019).

177. Oberoi-Khanuja, T. K. & Rajalingam, K. IAPs as E3 ligases of Rac1. *Small GTPases* **3**, 131–136 (2012).

178. Daugaard, M. *et al.* Hace1 controls ROS generation of vertebrate Rac1-dependent NADPH oxidase complexes. *Nat. Commun.* **4**, 1–13 (2013).

179. Castillo-Lluva, S. *et al.* SUMOylation of the GTPase Rac1 is required for optimal cell migration. *Nat. Cell Biol.* **12**, 1078–1085 (2010).

180. Müller, P. M. *et al.* Systems analysis of RhoGEF and RhoGAP regulatory proteins reveals

spatially organized RAC1 signalling from integrin adhesions. *Nat. Cell Biol.* **22**, 498–511 (2020).

181. Vetter, I. R. & Wittinghofer, A. The guanine nucleotide-binding switch in three dimensions. *Science* **294**, 1299–1304 (2001).

182. Jaiswal, M., Dvorsky, R. & Ahmadian, M. R. Deciphering the molecular and functional basis of Dbl family proteins: A novel systematic approach toward classification of selective activation of the Rho family proteins. *J. Biol. Chem.* **288**, 4486–4500 (2013).

183. Gadea, G. & Blangy, A. Dock-family exchange factors in cell migration and disease. *Eur. J. Cell Biol.* **93**, 466–477 (2014).

184. Yang, J., Zhang, Z., Mark Roe, S., Marshall, C. J. & Barford, D. Activation of Rho GTPases by DOCK exchange factors is mediated by a nucleotide sensor. *Science* **325**, 1398–1402 (2009).

185. Amin, E. *et al.* Deciphering the molecular and functional basis of RHOGAP family proteins: A systematic approach toward selective inactivation of RHO family proteins. *J. Biol. Chem.* **291**, 20353–20371 (2016).

186. Rittinger, K. *et al.* Crystal structure of a small G protein in complex with the GTPase-activating protein rhoGAP. *Nature* **388**, 693–697 (1997).

187. Bos, J. L., Rehmann, H. & Wittinghofer, A. GEFs and GAPs: Critical Elements in the Control of Small G Proteins. *Cell* **129**, 865–877 (2007).

188. Scheffzek, K. *et al.* The Ras-RasGAP complex: Structural basis for GTPase activation and its loss in oncogenic ras mutants. *Science* **277**, 333–338 (1997).

189. Tcherkezian, J. & Lamarche-Vane, N. Current knowledge of the large RhoGAP family of proteins. *Biol. Cell* **99**, 67–86 (2007).

190. Chuang, T. H. *et al.* Abr and Bcr are multifunctional regulators of the Rho GTP-binding protein family. *Proc. Natl. Acad. Sci. U. S. A. U. S. A.* **92**, 10282–10286 (1995).

191. Garcia-Mata, R., Boulter, E. & Burridge, K. The 'invisible hand': Regulation of RHO GTPases by RHOGDIs. *Nat. Rev. Mol. Cell Biol.* **12**, 493–504 (2011).

192. Boulter, E. *et al.* Regulation of Rho GTPase crosstalk, degradation and activity by RhoGDI1. *Nat. Cell Biol.* **12**, 477–483 (2010).

193. Chianale, F. *et al.* Diacylglycerol kinase α mediates HGF-induced Rac activation and membrane ruffling by regulating atypical PKC and RhoGDI. *Proc. Natl. Acad. Sci. U. S. A. U. S. A.* **107**, 4182–4187 (2010).

194. Dermardirossian, C., Schnelzer, A. & Bokoch, G. M. Phosphorylation of RhoGDI by Pak1 mediates dissociation of Rac GTPase. *Mol. Cell* **15**, 117–127 (2004).

195. DerMardirossian, C., Rocklin, G., Seo, J. Y. & Bokoch, G. M. Phosphorylation of RhoGDI by Src regulates Rho GTPase binding and cytosol-membrane cycling. *Mol. Biol. Cell* **17**, 4760–4768 (2006).

196. Fei, F. *et al.* The Fer tyrosine kinase regulates interactions of Rho GDP-Dissociation Inhibitor α with the small GTPase Rac. *BMC Biochem.* **11**, 48 (2010).

197. Wu, Y. *et al.* Src phosphorylation of RhoGDI2 regulates its metastasis suppressor function. *Proc. Natl. Acad. Sci. U. S. A.* **106**, 5807–5812 (2009).

198. Griner, E. M., Churchill, M. E. A., Brautigan, D. L. & Theodorescu, D. PKCα phosphorylation of RhoGDI2 at Ser31 disrupts interactions with Rac1 and decreases GDI activity. *Oncogene* **32**, 1010–1017 (2013).

199. Reijnders, M. R. F. *et al.* RAC1 Missense Mutations in Developmental Disorders with Diverse Phenotypes. *Am. J. Hum. Genet.* **101**, 466–477 (2017).

200. Bongmba, O. Y. N. The role of Rac1 in synaptic plasticity, learning, and memory. (Univeristy of Houston [unpublished doctoral thesis], 2012).

201. Lai, K. O. & Ip, N. Y. Structural plasticity of dendritic spines: The underlying mechanisms and its dysregulation in brain disorders. *Biochim. Biophys. Acta Mol. Basis Dis.***1832**, 2257–2263 (2013).

202. Oh, D. *et al.* Regulation of synaptic Rac1 activity, long-term potentiation maintenance, and learning and memory by BCR and ABR Rac GTPase-activating proteins. *J. Neurosci.* **30**, 14134–14144 (2010).

203. Marei, H. & Malliri, A. Rac1 in human diseases: The therapeutic potential of targeting Rac1 signaling regulatory mechanisms. *Small GTPases* **8**, 139–163 (2017).

204. Hollstein, R. *et al.* HACE1 deficiency causes an autosomal recessive neurodevelopmental syndrome. *J. Med. Genet.* **52**, 797–803 (2015).

205. Pengelly, R. J. *et al.* Mutations specific to the Rac-GEF domain of TRIO cause intellectual disability and microcephaly. *J. Med. Genet.* **53**, 735–742 (2016).

206. Allen, K. M. *et al.* PAK3 mutation in nonsyndromic X-linked mental retardation. *Nat. Genet.* **20**, 25–30 (1998).

207. Tate, J. G. *et al.* COSMIC: The Catalogue Of Somatic Mutations In Cancer. *Nucleic Acids Res.* **47**, D941–D947 (2019).

208. Cerami, E. *et al.* The cBio Cancer Genomics Portal: An open platform for exploring multidimensional cancer genomics data. *Cancer Discov.* **2**, 401–404 (2012).

209. Gao, J. *et al.* Integrative analysis of complex cancer genomics and clinical profiles using the cBioPortal. *Sci. Signal.* **6**, (2013).

210. Zehir, A. *et al.* Mutational landscape of metastatic cancer revealed from prospective clinical sequencing of 10,000 patients. *Nat. Med.* **23**, 703–713 (2017).

211. Alkallas, R. *et al.* Multi-omic analysis reveals significantly mutated genes and DDX3X as a sex-specific tumor suppressor in cutaneous melanoma. *Nat. Cancer* **1**, 635–652 (2020).

212. Kawazu, M. *et al.* Transforming mutations of RAC guanosine triphosphatases in human cancers. *Proc. Natl. Acad. Sci. U. S. A.* **110**, 3029–3034 (2013).

213. Chang, M. T. *et al.* Identifying recurrent mutations in cancer reveals widespread lineage diversity and mutational specificity. *Nat. Biotechnol.* **34**, 155–163 (2016).

214. Stransky, N. *et al.* The mutational landscape of head and neck squamous cell carcinoma. *Science* **333**, 1157–60 (2011).

215. Gao, J. *et al.* 3D clusters of somatic mutations in cancer reveal numerous rare mutations as functional targets. *Genome Med.* **9**, 4 (2017).

216. Matos, P. *et al.* Small GTPase Rac1: Structure, localization, and expression of the human gene. *Biochem. Biophys. Res. Commun.* **277**, 741–751 (2000).

217. Jordan, P., Brazão, R., Boavida, M. G., Gespach, C. & Chastre, E. Cloning of a novel human Rac1b splice variant with increased expression in colorectal tumors. *Oncogene* **18**, 6835–6839 (1999).

218. Haeusler, L. C. *et al.* Purification and biochemical properties of Rac1, 2, 3 and the splice variant Rac1b. *Meth. Enzymol.* **406**, 1–11 (2006).

219. Matos, P. *et al.* Ibuprofen inhibits colitis-induced overexpression of tumor- related Rac1b. *Neoplasia* **15**, 102–111 (2013).

220. Radisky, D. C. *et al.* Rac1b and reactive oxygen species mediate MMP-3-induced EMT and genomic instability. *Nature* **436**, 123–127 (2005).

221. Faria, M. *et al.* RAC1b overexpression stimulates proliferation and NF-κB-mediated antiapoptotic signaling in thyroid cancer cells. *PLOS One* **12**, (2017).

222. Li, G. *et al.* Rac1b enhances cell survival through activation of the JNK2/c-JUN/Cyclin-D1 and AKT2/MCL1 pathways. *Oncotarget* **7**, (2016).

223. Melzer, C., Hass, R., Lehnert, H. & Ungefroren, H. RAC1B: A Rho GTPase with Versatile Functions in Malignant Transformation and Tumor Progression. *Cells* **8**, 21 (2019).

224. Hoadley, K. A. *et al.* Cell-of-Origin Patterns Dominate the Molecular Classification of 10,000 Tumors from 33 Types of Cancer. *Cell* **173**, 291-304.e6 (2018).

225. Kazanietz, M. G. & Caloca, M. J. The Rac GTPase in cancer: From old concepts to new paradigms. *Cancer Res.* **77**, 5445–5451 (2017).

226. Mi, S. *et al.* RNA-seq identification of RACGAP1 as a metastatic driver in uterine carcinosarcoma. *Clin. Cancer Res.* **22**, 4676–4686 (2016).

227. McHenry, P. R. *et al.* P190B RhoGAP has pro-tumorigenic functions during MMTV-Neu mammary tumorigenesis and metastasis. *Breast Cancer Res.* **12**, R73 (2010).

228. He, Y. *et al.* The Cdc42/Rac1 regulator CdGAP is a novel E-cadherin transcriptional co-repressor with Zeb2 in breast cancer. *Oncogene* **36**, 3490–3503 (2017).

229. Davis, M. J. *et al.* RAC1P29S is a spontaneously activating cancer-associated GTPase. *Proc. Natl. Acad. Sci. U. S. A.* **110**, 912–917 (2013).

230. Buhrman, G., Wink, G. & Mattos, C. Transformation efficiency of RasQ61 mutants linked to structural features of the switch regions in the presence of Raf. *Structure* **15**, 1618–29

(2007).

231. Toyama, Y., Kontani, K., Katada, T. & Shimada, I. Conformational landscape alternations promote oncogenic activities of Ras-related C3 botulinum toxin substrate 1 as revealed by NMR. *Sci. Adv.* **5**, (2019).

232. Rajendran, V., Gopalakrishnan, C. & Purohit, R. Impact of point mutation P29S in RAC1 on tumorigenesis. *Tumor Biol.* **37**, 15293–15304 (2016).

233. Vu, H. L., Rosenbaum, S., Purwin, T. J., Davies, M. A. & Aplin, A. E. RAC1 P29S regulates PD-L1 expression in melanoma. *Pigment Cell Melanoma Res.* **28**, 590–598 (2015).

234. Lionarons, D. A. *et al.* RAC1P29S Induces a Mesenchymal Phenotypic Switch via Serum Response Factor to Promote Melanoma Development and Therapy Resistance. *Cancer Cell* **36**, 68-83.e9 (2019).

235. Dalton, L. E. *et al.* Constitutive rac activation is not sufficient to initiate melanocyte neoplasia but accelerates malignant progression. *J. Invest. Dermatol.* **133**, 1572–1581 (2013).

236. Frantz, W. T. & Ceol, C. J. From Tank to Treatment: Modeling Melanoma in Zebrafish. *Cells* **9**, 1289 (2020).

237. Li, A. *et al.* Activated mutant NRas Q61K drives aberrant melanocyte signaling, survival, and invasiveness via a Rac1-dependent mechanism. *J. Invest. Dermatol.* **132**, 2610–2621 (2012).

238. Wang, Z. *et al.* Rac1 is crucial for Ras-dependent skin tumor formation by controlling Pak1-Mek-Erk hyperactivation and hyperproliferation in vivo. *Oncogene* **29**, 3362–3373 (2010).

239. Nguyen, X. T. S. Uncovering the role of mutant RAC1 in cutaneous melanoma. (McGill University [unpublished master's thesis], 2017).

240. Halaban, R. RAC1 and Melanoma. *Clin. Ther.* **37**, 682–685 (2015).

241. Mohan, A. S. *et al.* Enhanced Dendritic Actin Network Formation in Extended Lamellipodia Drives Proliferation in Growth-Challenged Rac1 P29S Melanoma Cells. *Dev. Cell* **49**, 444-460.e9 (2019).

242. Baumann, K. Cell cycle: Activities of a mitotic master. *Nat. Rev. Mol. Cell Biol.* **11**, 389 (2010).

243. Garrett-Sinha, L. A. Review of Ets1 structure, function, and roles in immunity. *Cell Mol Life Sci.* **70**, 3375–3390 (2013).

244. Fueyo, J., Alonso, M. M., Kerrigan, B. C. P. & Gomez-Manzano, C. Linking inflammation and cancer: The unexpected SYK world. *Neuro. Oncol.* **20**, 582–583 (2018).

245. Hanahan, D. & Weinberg, R. A. Hallmarks of Cancer: The Next Generation. *Cell* **144**, 646–674 (2011).

246. Xiao, G.-H. *et al.* The NF2 Tumor Suppressor Gene Product, Merlin, Inhibits Cell Proliferation and Cell Cycle Progression by Repressing Cyclin D1 Expression. *Mol. Cell.*

Biol. **25**, 2384–2394 (2005).

247. Kissil, J. L., Johnson, K. C., Eckman, M. S. & Jacks, T. Merlin phosphorylation by p21-activated kinase 2 and effects of phosphorylation on merlin localization. *J. Biol. Chem.* **277**, 10394–10399 (2002).

248. Kissil, J. L. *et al.* Merlin, the product of the Nf2 tumor suppressor gene, is an inhibitor of the p21-activated kinase, Pak1. *Mol. Cell* **12**, 841–849 (2003).

249. Bosco, E. E., Nakai, Y., Hennigan, R. F., Ratner, N. & Zheng, Y. NF2-deficient cells depend on the Rac1-canonical Wnt signaling pathway to promote the loss of contact inhibition of proliferation. *Oncogene* **29**, 2540–2549 (2010).

250. Morrow, K. A. *et al.* Loss of tumor suppressor Merlin results in aberrant activation of Wnt/β-catenin signaling in cancer. *Oncotarget* **7**, 17991–18005 (2016).

251. Tsoi, J. *et al.* Multi-stage Differentiation Defines Melanoma Subtypes with Differential Vulnerability to Drug-Induced Iron-Dependent Oxidative Stress. *Cancer Cell* **33**, 890-904.e5 (2018).

252. Gau, D. & Roy, P. SRF'ing and SAP'ing - The role of MRTF proteins in cell migration. *J. Cell Sci.* **131**, 1–11 (2018).

253. Vu, H. L., Rosenbaum, S., Purwin, T. J., Davies, M. A. & Aplin, A. E. RAC1 P29S regulates PD-L1 expression in melanoma. *Pigment Cell Melanoma Res.* **28**, 590–598 (2015).

254. Revach, O. Y., Winograd-Katz, S. E., Samuels, Y. & Geiger, B. The involvement of mutant Rac1 in the formation of invadopodia in cultured melanoma cells. *Exp. Cell Res.* **343**, 82–88 (2016).

255. King, S. J. *et al.* Lamellipodia are crucial for haptotactic sensing and response. *J. Cell Sci.* **129**, 2329–2342 (2016).

256. Tomino, T. *et al.* DOCK1 inhibition suppresses cancer cell invasion and macropinocytosis induced by self-activating Rac1P29S mutation. *Biochem. Biophys. Res. Commun.* **497**, 298–304 (2018).

257. Bishop, A. L. & Hall, A. Rho GTPases and their effector proteins. *Biochem. J.* **348**, 241–255 (2000).

258. Briggs, M. W. & Sacks, D. B. IQGAP proteins are integral components of cytoskeletal regulation. *EMBO Rep.* **4**, 571–574 (2003).

259. Van Allen, E. M. *et al.* The genetic landscape of clinical resistance to RAF inhibition in metastatic melanoma. *Cancer Discov.* **4**, 94–109 (2014).

260. Watson, I. R. *et al.* The RAC1 P29S hotspot mutation in melanoma confers resistance to pharmacological inhibition of RAF. *Cancer Res.* **74**, 4845–4852 (2014).

261. Mahamat Babagana, Sydney Johnson, Hannah Slabodkin, Wiam Bshara, Carl Morrison, and E. S. K. P21-Activated Kinase 1 Regulates Resistance to BRAF Inhibition in Human Cancer Cells. *Mol. Carcinog.* **56**, 1515–1525 (2017).

262. Coelho, A. C. M. F. *et al.* NeoANT-HILL: An integrated tool for identification of potential neoantigens. *BMC Medical Genom.***13**, 30 (2020).

263. Arnst, J. L. *et al.* Discovery and characterization of small molecule Rac1 inhibitors. *Oncotarget* **8**, (2017).

264. Cardama, G. A., Gonzalez, N., Maggio, J., Menna, P. L. & Gomez, D. E. Rho GTPases as therapeutic targets in cancer (Review). *Int. J. Oncol.* **51**, 1025–1034 (2017).

265. Gray, J. L., Delft, F. & Brennan, P. E. Targeting the Small GTPase Superfamily through Their Regulatory Proteins. *Angew. Chemie Int. Ed.* **59**, 6342–6366 (2020).

266. Bid, H. K., Roberts, R. D., Manchanda, P. K. & Houghton, P. J. RAC1: An emerging therapeutic option for targeting cancer angiogenesis and metastasis. *Mol. Cancer Ther.* **12**, 1925–1934 (2013).

267. Montalvo-Ortiz, B. L. *et al.* Characterization of EHop-016, novel small molecule inhibitor of Rac GTPase. *J. Biol. Chem.* **287**, 13228–13238 (2012).

268. González, N. *et al.* Computational and in vitro Pharmacodynamics Characterization of 1A-116 Rac1 Inhibitor: Relevance of Trp56 in Its Biological Activity. *Front. Cell Dev. Biol.* **8**, 240 (2020).

269. Srijakotre, N. *et al.* P-Rex1 and P-Rex2 RacGEFs and cancer. *Biochem. Soc. Trans.* **45**, 963–977 (2017).

270. Araiza-Olivera, D. *et al.* Suppression of RAC1-driven malignant melanoma by group A PAK inhibitors. *Oncogene* **37**, 944–952 (2018).

271. Semenova, G. & Chernoff, J. Targeting PAK1. *Biochem. Soc. Trans.* **45**, 79–88 (2017).

272. Uribe-Alvarez, C. *et al.* Targeting effector pathways in RAC1P29S-driven malignant melanoma. *Small GTPases* (2020).

273. Foth, M., Parkman, G., Battistone, B. & McMahon, M. RAC1mutation is not a predictive biomarker for PI3'-kinase-β-selective pathway-targeted therapy. *Pigment Cell Melanoma Res.* **33**, 719–730 (2020).

274. Swart-Mataraza, J. M., Li, Z. & Sacks, D. B. IQGAP1 is a component of Cdc42 signaling to the cytoskeleton. *J. Biol. Chem.* **277**, 24753–63 (2002).

275. Jacquemet, G. *et al.* Rac1 is deactivated at integrin activation sites through an IQGAP1-filamin-A-RacGAP1 pathway. *J. Cell Sci.* **126**, 4121–4135 (2013).

276. Rane, C. K. & Minden, A. P21 activated kinase signaling in cancer. *Semin. Cancer Biol.* **54**, 40–49 (2019).

277. Molli, P. R., Li, D. Q., Murray, B. W., Rayala, S. K. & Kumar, R. PAK signaling in oncogenesis. *Oncogene* **28**, 2545–2555 (2009).

278. Li, A. *et al.* Activated mutant NRas Q61K drives aberrant melanocyte signaling, survival, and invasiveness via a Rac1-dependent mechanism. *J. Invest. Dermatol.* **132**, 2610–2621 (2012).

279. Nitulescu, G. M. *et al.* The Akt pathway in oncology therapy and beyond (Review). *Int. J. Oncol.* **53**, 2319–2331 (2018).

280. Sanchez-Laorden, B., Viros, A. & Marais, R. Mind the IQGAP. *Cancer Cell* **23**, 715-7 (2013).

281. White, C. D., Erdemir, H. H. & Sacks, D. B. IQGAP1 and its binding proteins control diverse biological functions. *Cell. Signal.* **24**, 826–834 (2012).

282. Dong, P. X. *et al.* Silencing of IQGAP1 by shRNA inhibits the invasion of ovarian carcinoma HO-8910PM cells in vitro. *J. Exp. Clin. Cancer Res.* **27**, 77 (2008).

283. Liu, Z. *et al.* IQGAP1 plays an important role in the invasiveness of thyroid cancer. *Clin. Cancer Res.* **16**, 6009–6018 (2010).

284. Lee, B. H., Neela, P. H., Kent, M. S. & Zehnder, A. M. IQGAP1 is an oncogenic target in canine melanoma. *PLOS One* **12**, e0176370 (2017).

285. Diao, B. *et al.* IQGAP1-siRNA inhibits proliferation and metastasis of U251 and U373 glioma cell lines. *Mol. Med. Rep.* **15**, 2074–2082 (2017).

286. Zhang, T. *et al.* Plastin 1 drives metastasis of colorectal cancer through the IQGAP1/Rac1/ERK pathway. *Cancer Sci.* **111**, 2861–2871 (2020).

287. Yilmaz, M. & Christofori, G. Mechanisms of motility in metastasizing cells. *Mol. Cancer Res.* **8**, 629–642 (2010).

288. Jadeski, L., Mataraza, J. M., Jeong, H. W., Li, Z. & Sacks, D. B. IQGAP1 stimulates proliferation and enhances tumorigenesis of human breast epithelial cells. *J. Biol. Chem.* **283**, 1008–1017 (2008).

289. Kosol, S. *et al.* Interaction between the scaffold proteins CBP by IQGAP1 provides an interface between gene expression and cytoskeletal activity. *Sci. Rep.* **10**, 1–15 (2020).

290. Hebert, J. D. *et al.* The scaffold protein IQGAP1 is crucial for extravasation and metastasis. *Sci. Rep.* **10**, 1–10 (2020).

291. Gocke, C. B. *et al.* IQGAP1 Scaffold-MAP Kinase Interactions Enhance Multiple Myeloma Clonogenic Growth and Self-Renewal. *Mol. Cancer Ther.* **15**, 2733–2739 (2016).

292. Hu, W. *et al.* IQGAP1 promotes pancreatic cancer progression and epithelial-mesenchymal transition (EMT) through Wnt/β-catenin signaling. *Sci. Rep.* **9**, (2019).

293. Carmon, K. S. *et al.* LGR5 receptor promotes cell-cell adhesion in stem cells and colon cancer cells via the IQGAP1-Rac1 pathway. *J. Biol. Chem.* **292**, 14989–15001 (2017).

Appendix A: Supplementary Figure S1

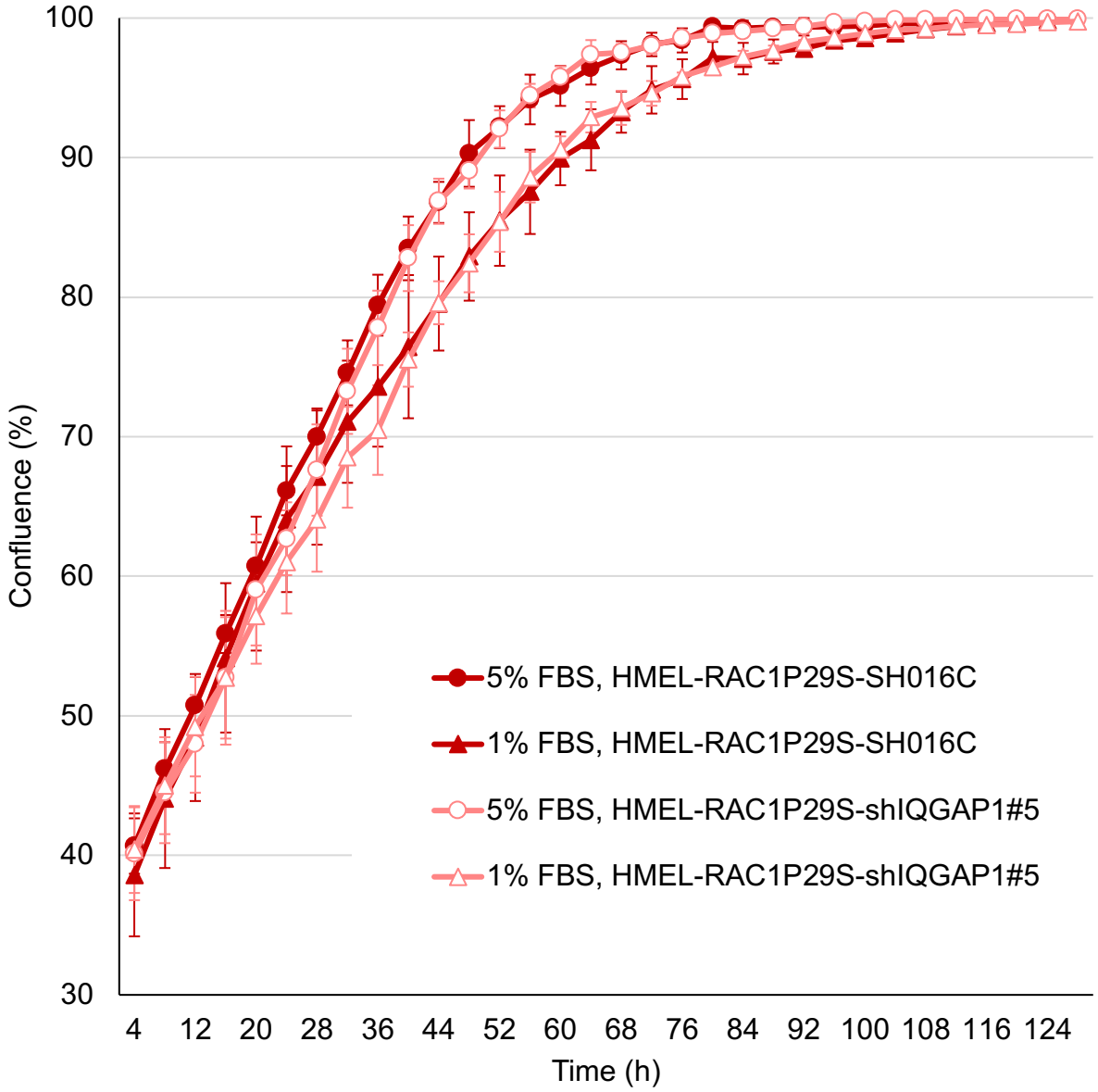

Supplementary Figure S1 | IQGAP1 does not contribute to melanocyte proliferation. HMEL-pHAGE (GFP/RAC1 WT/RAC1 P29S)-pLKO.1 with stable knockdown of IQGAP1 (shIQGAP1#5) or a nontargeting control (SH016C) were used in an IncuCyte proliferation protocol at 5 % and 1 % FBS with five technical replicates per treatment. Plotted above is the proliferation of HMEL-RAC1 P29S cells for each condition. Error bars represent +/- 1 SD from the mean.

Appendix B: Supplementary Figure S2

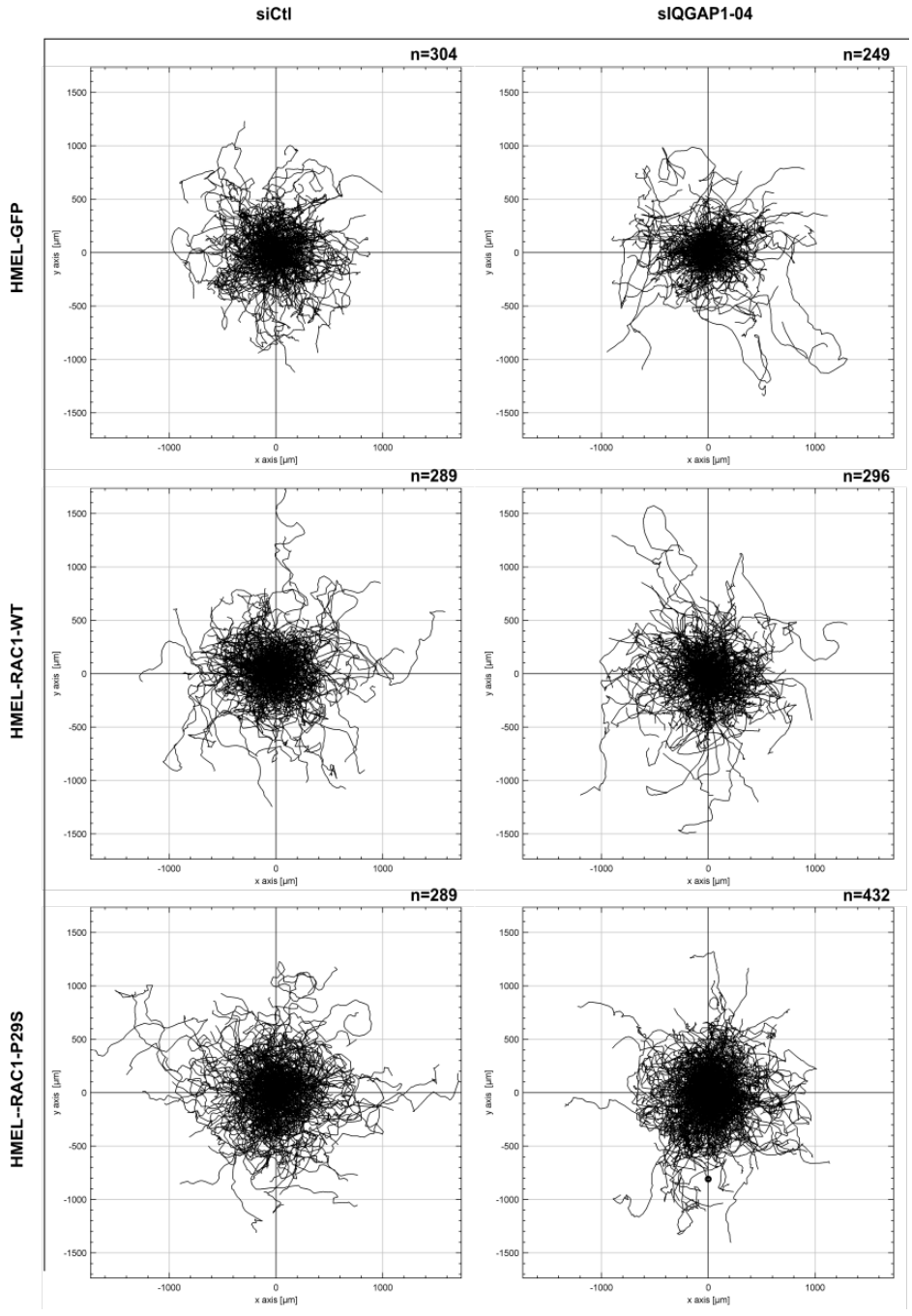

Supplementary Figure S2 | Directionality plots of HMEL-pHAGE random migration with siIQGAP1-04. Isogenic HMEL-pHAGE (GFP/RAC1 WT/RAC1 P29S) melanocytes were treated with an siRNA against IQGAP1 (siIQGAP1-04) or a non-targeting control (siCtl) and used in time-lapse live-cell random migration assays. Three positions were imaged every 10 m for 16 h. All cells were manually tracked, and positions were pooled for analysis. Number of cells tracked per treatment is reported with each directionality plot, where all tracks begin at origin.

Appendix C: Supplementary Figure S3

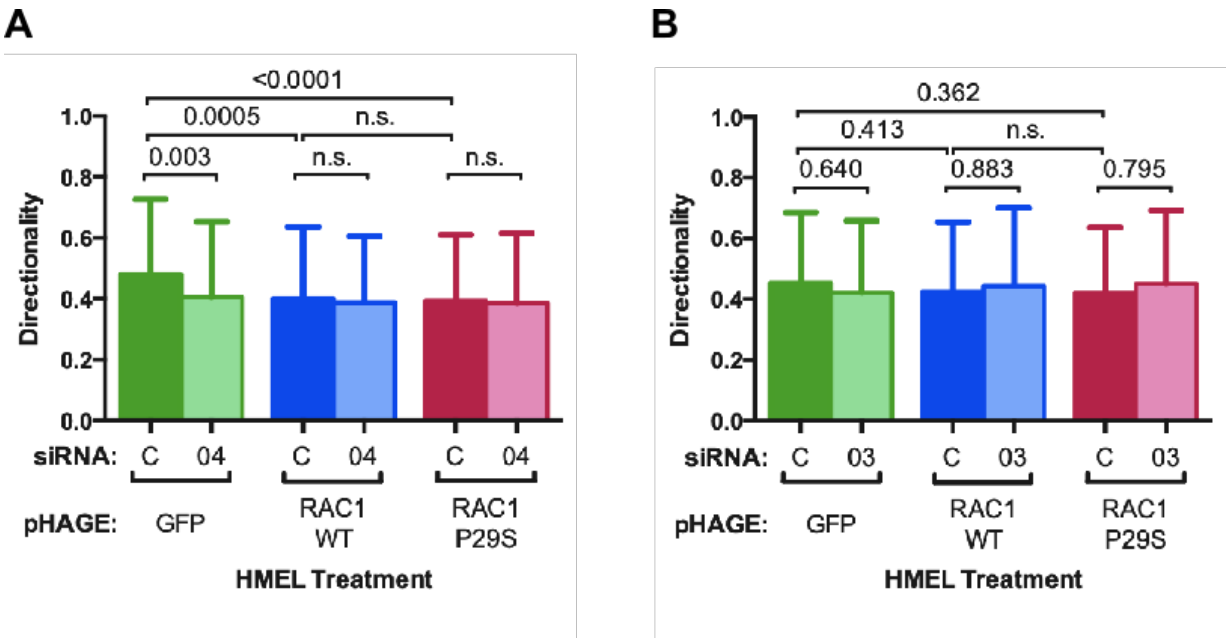

Supplementary Figure S3 | Directionality of HMEL-pHAGE migration following IQGAP1 knockdown. Isogenic HMEL-pHAGE (GFP/RAC1 WT/RAC1 P29S) melanocytes were used in time-lapse live-cell random migration assays following treatment with a non-targeting control (siCtl) or one of two siRNAs against IQGAP1: siIQGAP1-04 **(A)** or siQGAP1-03 **(B)**. Three positions were imaged every 10 m for 16 h. All cells were manually tracked, and positions were pooled for analysis. Plots represent directionality of random migration as the ratio between Euclidean distance and total track length, bounded between 0 and 1. Error bars represent +/- 1 SD from the mean. Statistical analyses were performed in R using ANOVA and Tukey Kramer multiple comparisons of means.

Appendix D: Supplementary Figure S4

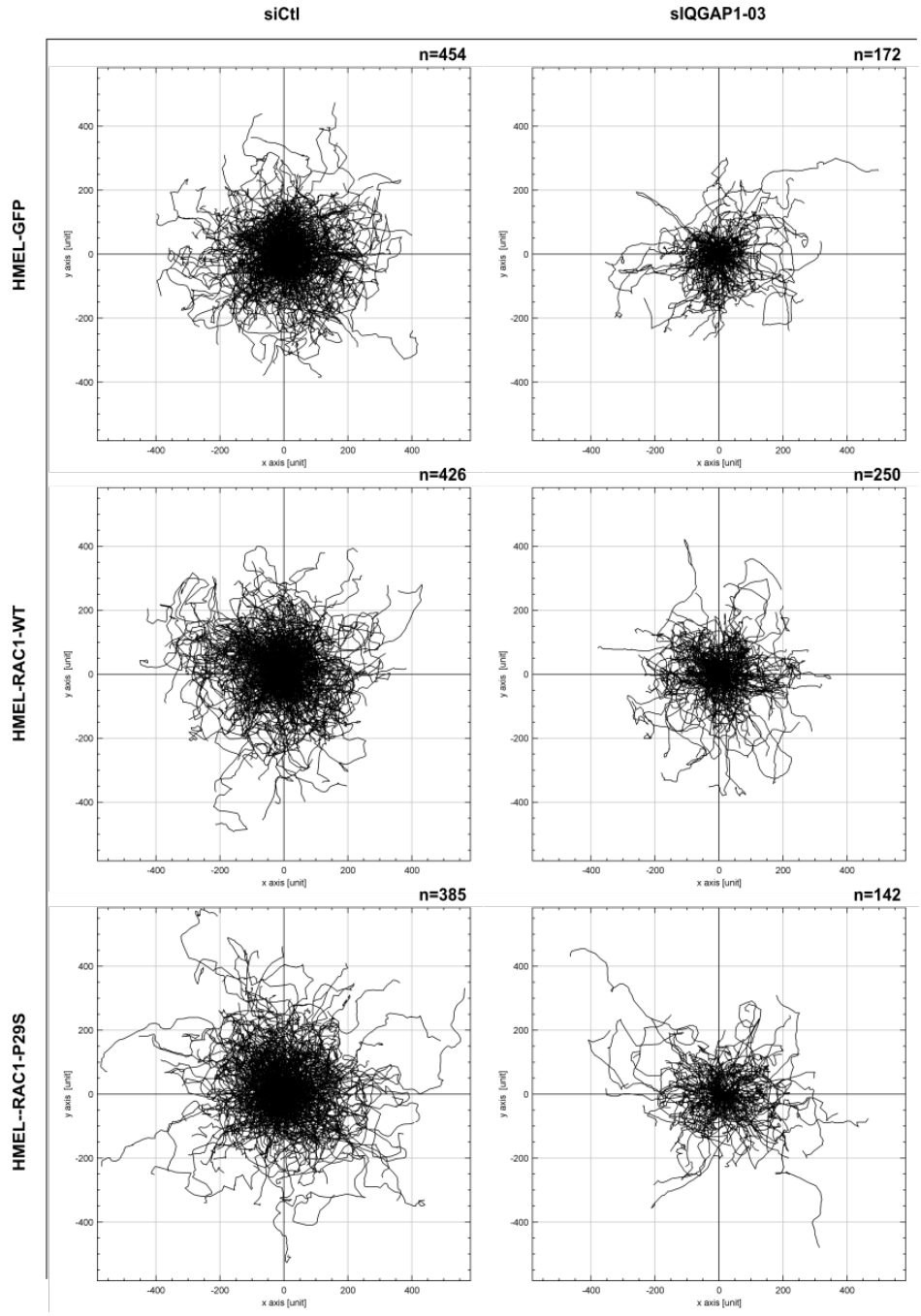

Supplementary Figure S4 | Directionality plots of HMEL-pHAGE random migration with siIQGAP1-03. Isogenic HMEL-pHAGE (GFP/RAC1 WT/RAC1 P29S) melanocytes were treated with an siRNA against IQGAP1 (siIQGAP1-03) or a non-targeting control (siCtl) and used in time-lapse live-cell random migration assays. Three positions were imaged every 10 m for 16 h. All cells were manually tracked, and positions were pooled for analysis. Number of cells tracked per treatment is reported with each directionality plot, where all tracks begin at origin.